



Publicly Accessible Penn Dissertations


2018

Distinct Temporal Requirements For Sonic Hedgehog In The Development Of The Tuberal Hypothalamus

Tanya Corman

University of Pennsylvania, tcorman@pennmedicine.upenn.edu

Follow this and additional works at: <https://repository.upenn.edu/edissertations>

 Part of the [Developmental Biology Commons](#), [Genetics Commons](#), and the [Neuroscience and Neurobiology Commons](#)

Recommended Citation

Corman, Tanya, "Distinct Temporal Requirements For Sonic Hedgehog In The Development Of The Tuberal Hypothalamus" (2018). *Publicly Accessible Penn Dissertations*. 3103.
<https://repository.upenn.edu/edissertations/3103>

This paper is posted at ScholarlyCommons. <https://repository.upenn.edu/edissertations/3103>
For more information, please contact repository@pobox.upenn.edu.

Distinct Temporal Requirements For Sonic Hedgehog In The Development Of The Tuberal Hypothalamus

Abstract

Sonic hedgehog (Shh) is a secreted morphogen that plays integral roles in the development of several brain and spinal cord regions. However, defining roles for Shh in the development of the hypothalamus has presented a challenge owing to its complex anatomy and neuronal heterogeneity. Of particular interest is the tuberal hypothalamus, a brain region with important homeostatic function. Early deletions of Shh from non-neuronal sources result in a severe brain malformation similar to a condition termed Holoprosencephaly in humans. In mouse models of this disorder, the hypothalamus fails to form. Later disruptions of Shh signaling within the hypothalamus itself implicate the hypothalamic source of Shh in proper development of the optic nerve and pituitary in addition to the hypothalamus. These phenotypes are associated with another disorder in patients termed Septo-optic dysplasia. We use conditional deletion models in mice to further define requirements for dynamic Shh activity at distinct stages of tuberal hypothalamic development. We find tuberal hypothalamic nuclei are dependent on early roles for Shh in dorsoventral patterning, neurogenesis, and restricting ventral midline area. We then utilize fate mapping techniques to demonstrate that Shh expressing and responsive progenitors contribute to distinct neuronal subtypes, accounting for some of the cellular heterogeneity in tuberal hypothalamic nuclei. Conditional deletion of the Hedgehog transducer Smoothed (Smo) at time points after dorsoventral patterning has been established reveals that Shh signaling is necessary to maintain proliferation and progenitor identity during peak periods of hypothalamic neurogenesis. We also find that mosaic disruption of Smo causes a non-cell autonomous gain in Shh signaling activity in neighboring wild type cells, suggesting a possible mechanism for the growth of hypothalamic hamartomas, a benign tumor that forms at fetal stages of hypothalamic development.

Degree Type

Dissertation

Degree Name

Doctor of Philosophy (PhD)

Graduate Group

Cell & Molecular Biology

First Advisor

Douglas J. Epstein

Keywords

Hypothalamus, Sonic hedgehog

Subject Categories

Developmental Biology | Genetics | Neuroscience and Neurobiology

This dissertation is available at ScholarlyCommons: <https://repository.upenn.edu/edissertations/3103>

DISTINCT TEMPORAL REQUIREMENTS FOR SONIC HEDGEHOG IN THE
DEVELOPMENT OF THE TUBERAL HYPOTHALAMUS

Tanya S. Corman

A DISSERTATION

in

Cell and Molecular Biology

Presented to the Faculties of the University of Pennsylvania

in

Partial Fulfillment of the Requirements for the

Degree of Doctor of Philosophy

2018

Supervisor of Dissertation

Douglas J. Epstein, Ph.D., Professor of Genetics

Graduate Group Chairperson

Daniel S. Kessler, Ph.D., Associate Professor of Cell and Developmental Biology

Dissertation Committee:

Sarah Millar, Ph.D., Albert M. Kligman Professor in Dermatology II

Michael Granato, Ph.D., Professor of Cell and Developmental Biology

Wenqin Luo, M.D., Ph.D., Associate Professor of Neuroscience

Patrick Seale, Ph.D., Associate Professor of Cell and Developmental Biology

Dedication

This work is dedicated to my family and friends. To my friends, past and present, near and far, who have been my sources of stability and strength. To my father the pragmatist for offering advice at every turn. And for never once pointing out I should have followed in his engineering footsteps. To my mother who has always been able to anticipate and offer the support I need before I've even realized I needed it. To my sister who has provided optimism, realism, or cynicism at various points of graduate school to suit my needs; who went from a supporter to a graduate student peer providing everything from external pressure not to get "lapped," literal wake up calls, and cute animal pictures at every step of the way. And finally, to my grandfather, who spent the latter part of his 99 years poking and prodding me to hurry up and graduate.

ACKNOWLEDGMENT

When you're in graduate school for the better part of a decade, there are countless people who have supported you in that journey. I would like to first thank my mentor Doug Epstein for his taking me on as a graduate student in less than ideal circumstances. He has provided an environment for me to grow in my critical thinking and helped me identify my own skills and weaknesses. I have no doubt my time in his lab has prepared me for wherever my next step takes me.

Additionally, I would like to thank my committee members for their seemingly unconditional support and positive comments throughout. I would also like to thank Dan Kessler, Sarah Millar, and Jonathan Raper for their occasional check-ins and reassurances.

I would like to acknowledge the high school and undergraduate students I had the pleasure of working with on some experiments that were included in this work, Ben Kahn and Korah Lovelace. I would like to thank all members of the Epstein lab, past and present, for their endless support. In particular, Yao Yao for her insightful discussions of data and life choices, Staci Rakowiecki for her constant positive presence and hugs, and Alex Rohacek for the hours of conversations and mutual fondness for Game of Thrones and Parks and Rec.

ABSTRACT

DISTINCT TEMPORAL REQUIREMENTS FOR SONIC HEDGEHOG IN THE DEVELOPMENT OF THE TUBERAL HYPOTHALAMUS

Tanya S. Corman

Douglas J. Epstein, Ph.D.

Sonic hedgehog (Shh) is a secreted morphogen that plays integral roles in the development of several brain and spinal cord regions. However, defining roles for Shh in the development of the hypothalamus has presented a challenge owing to its complex anatomy and neuronal heterogeneity. Of particular interest is the tuberal hypothalamus, a brain region with important homeostatic function. Early deletions of Shh from non-neuronal sources result in a severe brain malformation similar to a condition termed Holoprosencephaly in humans. In mouse models of this disorder, the hypothalamus fails to form. Later disruptions of Shh signaling within the hypothalamus itself implicate the hypothalamic source of Shh in proper development of the optic nerve and pituitary in addition to the hypothalamus. These phenotypes are associated with another disorder in patients termed Septo-optic dysplasia. We use conditional deletion models in mice to further define requirements for dynamic Shh activity at distinct stages of tuberal hypothalamic development. We find tuberal hypothalamic nuclei are dependent on early roles for Shh in dorsoventral patterning, neurogenesis, and restricting ventral midline area. We then utilize fate mapping techniques to demonstrate that Shh expressing and responsive progenitors contribute to distinct neuronal subtypes, accounting for some of the cellular heterogeneity in tuberal hypothalamic nuclei. Conditional deletion of the Hedgehog transducer Smoothed (Smo) at time points after dorsoventral patterning

iv

has been established reveals that Shh signaling is necessary to maintain proliferation and progenitor identity during peak periods of hypothalamic neurogenesis. We also find that mosaic disruption of *Smo* causes a non-cell autonomous gain in Shh signaling activity in neighboring wild type cells, suggesting a possible mechanism for the growth of hypothalamic hamartomas, a benign tumor that forms at fetal stages of hypothalamic development.

TABLE OF CONTENTS

ACKNOWLEDGMENT	III
ABSTRACT	IV
LIST OF ILLUSTRATIONS	IX
CHAPTER 1: INTRODUCTION	1
The Hypothalamus	1
The tuberal hypothalamus:	2
Sonic Hedgehog	3
Hedgehog genes:	3
Hedgehog signaling pathway:	4
Shh in the neural tube:	6
Shh in the hypothalamus:	6
Mis-regulation of Shh in the hypothalamus:.....	8
Figures	10
CHAPTER 2: PRENATAL ETHANOL EXPOSURE IN MICE PHENOCOPIES CDON MUTATION BY IMPEDING SHH FUNCTION IN THE ETIOLOGY OF OPTIC NERVE HYPOPLASIA	13
Abstract	13

Introduction.....	15
Results	19
Cdon mutation and prenatal ethanol exposure independently cause ONH.....	19
Formation of the optic disc is not disturbed in Cdon ^{-/-} and ethanol-exposed embryos.....	20
Shh-dependent proliferation of RPCs is compromised in Cdon ^{-/-} and ethanol-treated embryos	21
Precocious differentiation of RGCs in Cdon ^{-/-} and ethanol-treated embryos.....	23
Discussion	25
Ethanol and Cdon mutation impede Shh signaling in RPCs to cause ONH.....	25
Strain-dependent modifiers and timing of prenatal ethanol exposure influence Shh-related phenotypes.....	26
Effects of ethanol on Shh signaling.....	27
SOD is a multifactorial disorder	28
Materials and Methods	30
Figures	32
CHAPTER 3: DISTINCT TEMPORAL REQUIREMENTS FOR SONIC HEDGEHOG SIGNALING DEVELOPMENT OF THE TUBERAL HYPOTHALAMUS	43
Abstract.....	43
Introduction.....	45

Results	49
Shh is required for the development of tuberal hypothalamic nuclei	49
Alterations in dorsoventral patterning, neurogenesis and ventral midline formation explain the absence of tuberal hypothalamic nuclei in Shh ^{Δhyp} embryos.....	49
Descendants of Shh expressing progenitors contribute to the VMH	52
Descendants of Gli1 expressing progenitors contribute to the DMH and VMH.....	53
Shh signaling is required to maintain tuberal hypothalamic progenitors in a proliferative state	54
Cell-autonomous requirement for Smo in promoting tuberal hypothalamic neuron identity.....	55
Non-cell autonomous defects in cSmo embryos alter VMH neuron subtype identity.....	56
Discussion	58
Shh directs dorsoventral patterning and neurogenesis in the hypothalamus.....	58
Shh restricts ventral midline development in the tuberal hypothalamus.....	59
Later Shh signaling- delineating fates.....	61
Later Shh signaling- maintaining proliferation of progenitor pools.....	63
Non-cell autonomous phenotypes in cSmo mutants due to heightened Shh signaling.....	63
Materials and Methods	66
Figures	69
CHAPTER 4: CONCLUSIONS, DISCUSSION, FUTURE DIRECTIONS.....	86
Heterogeneity of hypothalamic neurons:	89
Mosaic nature of Hh deletion:	90
BIBLIOGRAPHY	93

LIST OF ILLUSTRATIONS

Figure 1. Location and organization of the hypothalamus.....	11
Figure 2 Subdivisions of the Ventromedial Hypothalamus (VMH) and associated gene expression.....	12
Figure 3. <i>Cdon</i> mutation and ethanol exposure independently cause optic nerve hypoplasia.....	32
Figure 4. The optic disc is not compromised in <i>Cdon</i> ^{-/-} or ethanol-treated embryos.....	33
Figure 5. Selective reduction of <i>Gli1</i> expression in the eyes of <i>Cdon</i> ^{-/-} and ethanol-treated embryos.....	35
Figure 6. Reduced proliferation of RPCs in <i>Cdon</i> ^{-/-} and ethanol-treated embryos.....	37
Figure 7. Precocious differentiation of RGCs in <i>Cdon</i> ^{-/-} and ethanol-treated embryos.....	39
Figure 8. Model depicting the influence of <i>Cdon</i> mutation and ethanol exposure on <i>Shh</i> signaling activity in the developing eye.....	41
Figure 9. Loss of tuberal hypothalamic neurons in <i>Shh</i> ^{hyp} embryos.....	69
Figure 10. Altered dorsoventral patterning, neurogenesis, and ventral midline development in <i>Shh</i> ^{hyp} embryos.....	71
Figure 11. Persistence of <i>Shh</i> signaling during peak periods of hypothalamic neurogenesis.....	73
Figure 12. <i>Shh</i> and <i>Gli1</i> expressing cells contribute to overlapping and distinct tuberal hypothalamic nuclei.....	74
Figure 13. <i>Shh</i> and <i>Gli1</i> lineages occupy distinct regions of the VMH.....	76

Figure 14. Shh signaling is required for proliferation of tuberal hypothalamic progenitors.	77
Figure 15. No differences in cell death between control and <i>cSmo</i> embryos.	79
Figure 16. Shh signaling is required for subtype identity of VMH and DMH neurons.	80
Figure 17. Non-cell autonomous alterations in hypothalamic progenitors in <i>cSmo</i> embryos.	82
Figure 18. <i>cSmo</i> embryos show ectopic activation of Shh responsive genes in non-recombined (wild type) cells.	84

CHAPTER 1: INTRODUCTION

The Hypothalamus

The hypothalamus is a highly conserved brain region which acts as a critical regulator of several homeostatic processes and animal behaviors. Neurons of the hypothalamus are responsible for controlling diverse functions required for survival of the organism and propagation of the species. Genetic and lesion experiments identified neural circuits mapping to distinct areas of the hypothalamus that are responsible for food intake, energy expenditure, fluid balance, temperature regulation, wakefulness, daily rhythms, as well as social behaviors associated with reproduction, aggression, arousal, and stress (Saper and Lowell, 2014; Zha and Xu, 2015; Hashikawa et al., 2017; Tan and Knight, 2018). In order to perform this range of functions, the hypothalamus is composed of a diverse array of neuronal cell types characterized by their expression of transcription factors, neuropeptides, neurotransmitters, and hormones (Caqueret et al., 2006).

An anatomically complex structure, the hypothalamus is located in the ventral forebrain where it sits above the pituitary gland and ventral to the thalamus (Fig. 1a). The hypothalamus is symmetrical in nature, each aspect duplicated on either side of the ventral midline. These two halves of the hypothalamus are separated by the third ventricle of the brain. Whereas other regions of the central nervous system are typically arranged in cell layers, the hypothalamus is organized into discrete clusters of neurons termed nuclei (Shimada and Nakamura, 1973; Altman and Bayer, 1986). The adult hypothalamus is divided into four principal regions along the rostral to caudal axis:

preoptic, anterior, tuberal, and mammillary with each region containing defined hypothalamic nuclei (Fig. 1B).

The tuberal hypothalamus:

Perhaps the best described region of the hypothalamus is the tuberal territory. Within the tuberal hypothalamus, beginning most ventrally, are the arcuate nucleus (ARC), ventromedial hypothalamic nucleus (VMH), and dorsomedial hypothalamic nucleus (DMH). The positioning of the tuberal hypothalamus offers unique exposure to peripheral cues carried through the bloodstream or cerebrospinal fluid through a specialized structure termed the median eminence (Yin and Gore, 2010). The median eminence sits at the base of the third ventricle in the tuberal hypothalamus and includes a fenestrated capillary bed, allowing for sensing of peripheral signals as well as allowing for parvocellular neurons to release hormones to be transported to the pituitary. Furthermore, the median eminence is derived from a specialized domain containing networks of radial glial cells termed tanycytes (Salvatierra et al., 2014; Rizzoti and Lovell-Badge, 2017). At the median eminence, these unique cell types are integral to the sensing of factors including insulin, leptin, and ghrelin to allow the hypothalamus to maintain homeostatic conditions (reviewed in Rodríguez et al., 2005; Robins et al., 2013; reviewed in Bolborea and Dale, 2013).

The nuclei of the tuberal hypothalamus constitute the hypothalamic circuit that regulates feeding behavior and energy homeostasis (McClellan et al., 2006; Morton et al., 2006). Recent advances have been made in our understanding of the neuronal circuitry and function of the VMH in particular. The VMH is an elliptical shaped nucleus located above the ARC and below the DMH (Fig. 2) and can be subdivided into

ventrolateral (VMH_{vl}), central (VMH_c) and dorsomedial (VMH_{dm}) regions, each with distinguishable gene expression profiles (Segal et al., 2005; McClellan et al., 2006; Kurrasch et al., 2007). Genetic, pharmacogenetic and optogenetic approaches have further delineated VMH neurons into functionally distinct categories. ER α -expressing neurons in the VMH_{vl} regulate sexually dimorphic features related to energy expenditure, reproductive behavior and aggression (Lin et al., 2011; Lee et al., 2014; Correa et al., 2015). Whereas, insulin receptor (IR) expressing neurons in the VMH_c and Leptin Receptor (LEPR) neurons in the VMH_{dm} effect body weight regulation in both males and females (Dhillon et al., 2006; Klöckener et al., 2011). Steroidogenic factor 1 (SF1, officially designated Nr5a1) neurons in the VMH_{dm} also influence behavioral responses to fear and anxiety (Silva et al., 2013; Kunwar et al., 2015).

Sonic Hedgehog

Hedgehog genes:

A major focus of developmental biology is how complex multicellular organisms are generated from a single cell. Early experiments in the field focused on identifying genes involved in establishing the layout or body plan of an organism. One such discovery was that of the Hedgehog (hh) gene, identified in a mutagenesis screen in *Drosophila* larvae for factors that disrupted body plan organization. Larvae mutant for *hh* displayed ectopic bristle-like structures called denticles, causing them to resemble a hedgehog (Nüsslein-Volhard and Wieschaus, 1980). In vertebrates, gene duplication

events have expanded the Hedgehog family such that mammals have Indian hedgehog (Ihh), Desert hedgehog (Dhh) and Sonic hedgehog (Shh).

Though there are three Hedgehog genes in mammals, Shh is perhaps the best studied owing to its integral roles in the development of many tissues. Specifically, Shh acts as a secreted morphogen in numerous organizing centers of the developing embryo to pattern the limbs, central nervous system, inner ear, skin, as well as other tissues. The best studied context is within the central nervous system, where Shh is responsible for the patterning the neural tube along the dorsoventral axis (Echelard et al., 1993).

Hedgehog signaling pathway:

In the Shh expressing cell, Shh protein undergoes a series of post-translational modifications and cleavage events to produce N-terminal and C-terminal fragments (Bumcrot et al., 1995). Cholesterol molecules are then added to the N-terminal fragment of Shh, targeting the ligand for secretion (Kelley et al., 1996; Roessler et al., 1997). Upon release, Shh ligand travels to its cognate receptors on Shh-receiving cells. Cells competent to receive Shh signal will express several factors required for transduction of the signal. The ligand-binding receptor for Shh is the 12-pass transmembrane receptor Patched (*Ptch*). Further, the obligate transducer of Shh signal is the G-protein-coupled receptor-like seven-pass transmembrane protein Smoothed (*Smo*). In certain contexts, additional co-receptors are also required for proper Shh signaling. These include Cell Adhesion Associated, Oncogene Regulated (*Cdon*), Brother of Cdo (*Boc*) and Growth arrest specific 1 (*Gas1*). Downstream, the Glioma-associated transcription factors (*Gli1*, *Gli2*, and *Gli3*) act to activate or repress target gene transcription (Allen et al., 2007; Goodrich et al., 1997; Van den Heuvel and Ingham, 1996; Hui et al., 1994;

Kinzler et al., 1988; Lee et al., 1997; Marigo et al., 1996; Tenzen et al., 2006; Zhang and Jetten, 2001). Though the mechanisms are not fully understood, Shh requires the primary cilium organelle for proper signaling and many components of the Shh pathway undergo localization to the cilium as a result of Shh ligand-binding response, (Huangfu and Anderson, 2005; Huangfu et al., 2003; Liu et al., 2005).

In the absence of ligand, Ptch1 is localized to the cilium, preventing the accumulation of Smo in this compartment. As a result, Ptch1 acts to repress the pathway (Rohatgi et al., 2007; Strutt et al., 2001; Taipale et al., 2002; Fig. 3.1A). Downstream, Gli2 and 3 are bound by Suppressor of fused (*Sufu*). This causes the transcription factors to remain in the cytoplasm where they are phosphorylated (Ding et al., 1999; Kogerman et al., 1999; Liu et al., 2005; Svärd et al., 2006). These phosphorylation events target Gli2/3 for proteolytic processing (Haycraft et al., 2005; Pan et al., 2006; Wang et al., 2000). Cleavage of the transcriptional activator Gli2 targets it for degradation. Meanwhile, cleavage of Gli3 releases an N-terminal repressor domain that translocates to the nucleus and acts to repress gene expression.

Upon Shh ligand binding to Ptch1, the Ptch-mediated repression of Smo is alleviated. Thus, Smo is able to accumulate at the tip of the primary cilium (Chen and Struhl, 1998; Murone et al., 1999; Martín et al., 2001; Corbit et al., 2005; Rohatgi et al., 2007). Smo accumulation at the membrane allows for downstream signaling resulting in the dissociation of Gli proteins from Sufu. Thus, Gli2 and Gli3 are maintained in their full-length forms and are able to translocate to the nucleus to activate transcription of target genes, such as Gli1 (Lee et al., 1997; Wang et al., 2000; Haycraft et al., 2005; Pan et al., 2006).

Shh in the neural tube:

In the developing neural tube, Shh ligand is secreted first from the notochord, a mesendodermal structure residing below the neural tube. This induces a secondary source of Shh expression in the ventral-most cells of the neural tube termed the floor plate. Generation of a transgenic mouse expressing a Shh-GFP fusion protein allowed for *in vivo* imaging of the spread of Shh ligand from the notochord to the apical surface of cells in the ventral neural tube (Chamberlain, 2008).

Shh ligand continues to be secreted in a graded fashion and induces the expression of transcription factors in a concentration dependent manner. In turn, these transcription factors pattern progenitor domains along the dorsoventral axis that will give rise to the neuronal populations of the mature spinal cord. Downstream of ligand binding, Shh signaling cascade results in the specification and formation of distinct domains of progenitor cells marked by differential expression of homeodomain and basic HLH transcription factors, activated in relation to the strength of Shh signaling to which it is exposed (Ericson et al., 1996; Ericson et al., 1997). These transcription factors include those termed Class I proteins, which are repressed by Shh and Class II proteins which are induced by and require a threshold of Shh accumulation. Nkx2.2, Olig2, and Nkx6.1 characterize the three most ventral neural progenitor cell groups: p3, pMN, and p2, respectively. Lower levels of Shh signaling also influence more dorsal p1 and p0 neural progenitor domains (Briscoe et al., 2000; Briscoe and Ericson, 2001).

Shh in the hypothalamus:

As in the spinal cord, Shh acts to pattern ventral cell fates in the developing hypothalamus. However, the temporal and spatial dynamics of Shh signaling in the

hypothalamus differ from those in more posterior regions of the CNS. Beginning at 8.5 days of mouse development (E8.5), Shh is secreted from the prechordal plate, a mesendodermal structure that transiently underlies the anterior neural tube. This source of Shh induces signaling activity in the overlying hypothalamus. Shh signaling is then downregulated in ventral midline cells of the tuberal hypothalamus. This downregulation of Shh signaling is a step which distinguishes hypothalamic development from other regions of the central nervous system. In addition to Shh, additional factors are secreted by prechordal plate. Interestingly, BMP ligands derived from the prechordal plate are required for the rostralization of the neural tube to impart hypothalamic identity. (Dale et al., 1997; Ohyama et al., 2005). This Bmp signaling in the ventral midline upregulates Gli3-R expression, thus downregulating Shh signaling in the midline (Ohyama et al., 2008).

Following the extinguishing of Shh signaling in the hypothalamic midline, a secondary source of *Shh* transcription is induced in the hypothalamus itself between E9.0-E9.5. At this time, Shh is initially broadly expressed in ventral hypothalamic progenitors and then rapidly downregulated in the ventral midline at the level of the tuberal hypothalamus (Manning et al., 2006; Trowe et al., 2013). As a result, Shh is expressed in bilateral stripes adjacent to the ventral midline, unlike in spinal cord and hindbrain regions where Shh is restricted to the floor plate (Echelard et al., 1993). Our lab suggested this process is also mediated by Bmp signaling. Though the exact mechanism is unclear, Bmp signaling induces Tbx3 expression in the ventral midline. Tbx3 binds Sox2, interfering with the ability of Sox2 to activate the expression of Shh (Zhao et al., 2012; Trowe et al., 2013). Moreover, neural progenitors immediately dorsal to the bilateral stripes of Shh are responsive to Shh signaling, indicated by Gli1

expression, whereas progenitors located in the ventral midline remain refractory to Shh signaling (Ohyama et al., 2008).

One additional factor which may serve to distinguish the role of Shh in patterning of the hypothalamus from other areas of the central nervous system is Low-density lipoprotein receptor-related protein 2 (Lrp2). Biochemical and *in vivo* studies of Lrp2 function have revealed Lrp2 is able to bind both Shh (as a co-receptor) and Bmp4 (as a scavenger receptor) (McCarthy et al., 2002; Spoelgen et al., 2005; Christ et al., 2012). Thus, Lrp2 may act to regulate a balance between Shh and Bmp signaling in the ventral midline of the hypothalamus.

Mis-regulation of Shh in the hypothalamus:

The hypothalamus is particularly sensitive to proper levels of Shh signaling during development. A loss of this prechordal source of Shh results in a brain malformation termed Holoprosencephaly (HPE). As shown in Shh null mice, the prechordal source of Shh is necessary to drive the separation of the cerebral hemispheres, eye fields, and craniofacial structures (Chiang et al., 1996). This prechordal source of Shh is further required for the induction of the hypothalamic territory (Chiang et al., 1996; Dale et al., 1997). To circumvent this loss of hypothalamic tissue, conditional approaches were used to target and identify roles for the forebrain source of Shh. Foxb1-mediated recombination ablated Shh expression throughout the ventral forebrain. This model left the prechordal source of Shh intact. The prechordal plate and its source of Shh were sufficient to specify the hypothalamic territory, marked

by Nkx2.1, but not the identity of neuronal progenitors (Szabó et al., 2009) within the tuberal hypothalamus.

However, in these experiments, additional forebrain sources of Shh were also disrupted. Thus, our lab developed an *SBE2-cre* is a transgenic mouse line that uses Shh brain enhancer 2 (SBE2) to activate *cre* transcription in the ventral diencephalon in a similar pattern to the endogenous expression of *Shh*. This model allowed for the selective deletion of *Shh* in the ventral diencephalon of *Shh*^{Δhyp} embryos by E9.0. These *Shh*^{Δhyp} mutants display optic nerve and pituitary defects with similarities to SOD in humans (Zhao et al., 2012). The eye and pituitary develop in close proximity to the source of SHH in the anterior hypothalamus. However, loss-of-function mutations in *SHH* have not been associated with SOD in human patients (Paulo et al., 2015; Gregory et al., 2015). Previous work in our lab thus sought to examine whether SOD may represent a malformation with a later manifestation compared to HPE. Specifically, HPE and SOD may be differentiated by the timing and location of disruption in SHH signaling, with an early loss of SHH from the prechordal plate giving rise to HPE, and a slightly later absence of SHH from the presumptive hypothalamus resulting in SOD.

Furthermore, *Shh* and *Gli1* continue to be expressed beyond the stage when tuberal hypothalamic progenitors first acquire their identity and their expression extends into the peak period of DMH, VMH and ARC neurogenesis between E12.5 and E14.5. The experiments presented in the following chapters sought to further describe roles for the various temporal windows of dynamic Shh expression and signaling in hypothalamic development.

Chapter 1 Figures

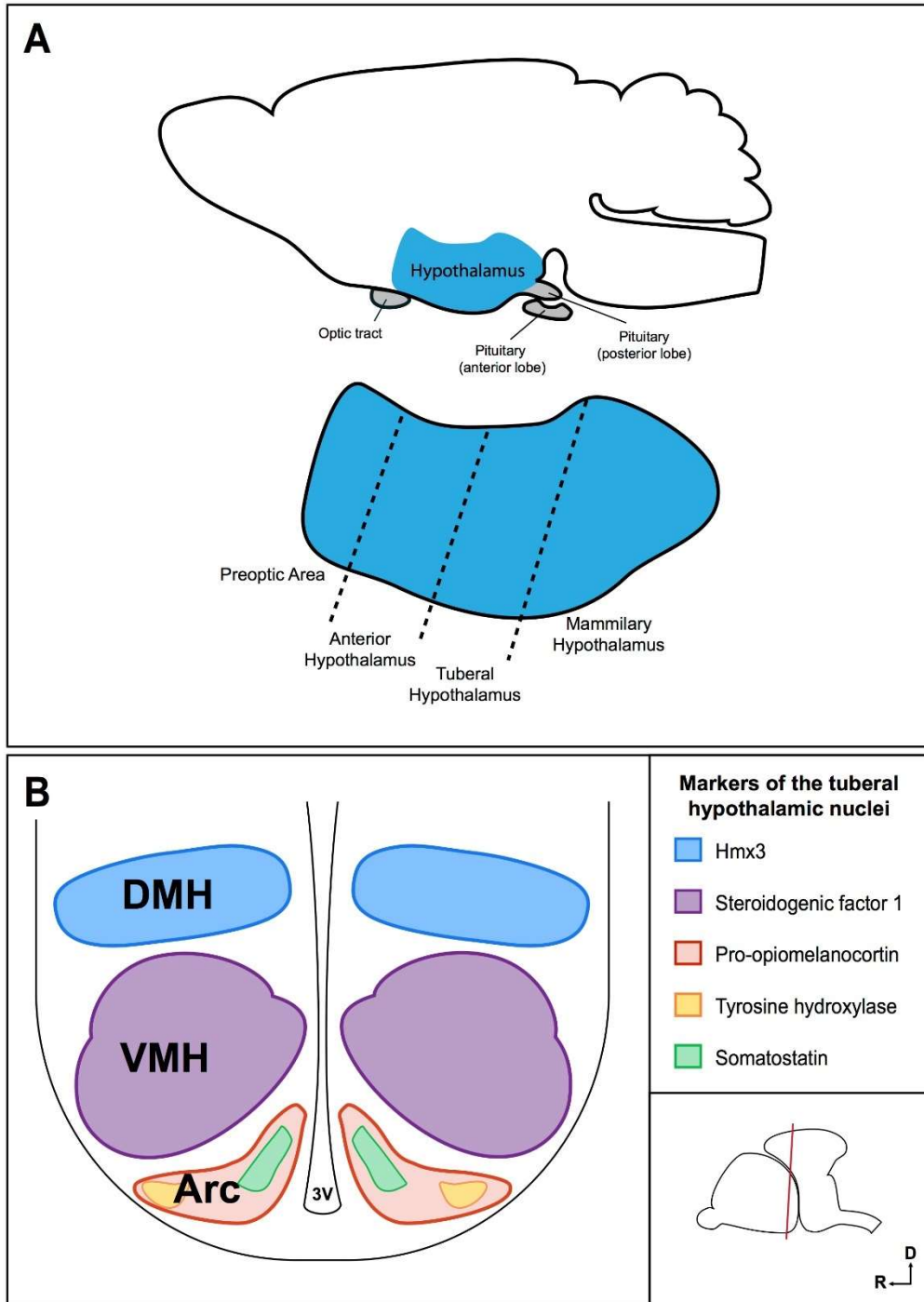


Figure 1. Location and organization of the hypothalamus.

(A) Schematic of the adult mouse brain highlighting the location of the hypothalamus in blue. The four subdivisions of the hypothalamus along the rostrocaudal axis are the preoptic area, the anterior hypothalamus, the tuberal hypothalamus, and the mammillary hypothalamus. (B) Diagram depicting the nuclei in a cross-section through the tuberal hypothalamus. Characteristic gene expression markers of the various nuclei are color coded. From ventral to dorsal- the arcuate nucleus (ARC), ventromedial hypothalamic nucleus (VMH) and the dorsomedial hypothalamic nucleus (DMH).

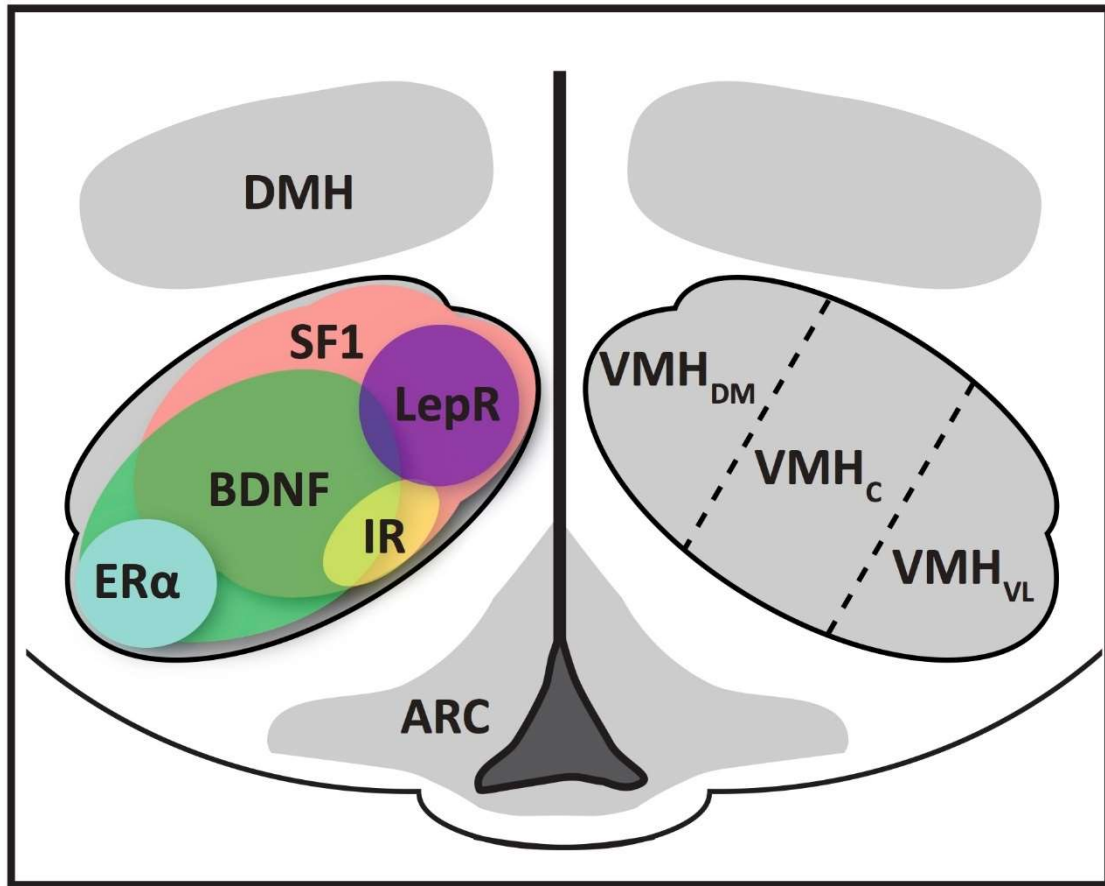


Figure 2. Subdivisions of the Ventromedial Hypothalamus (VMH) and associated gene expression.

The VMH can be subdivided into dorsomedial (DM), central (C), and ventrolateral (VL) compartments. Each compartment is associated with the expression of specific transcription factors or receptors for neuropeptides or hormones including steroidogenic factor-1 (SF-1), brain-derived neurotrophic factor (BDNF), estrogen receptor alpha (ERα), leptin receptor (LepR), or insulin receptor (IR).

CHAPTER 2: Prenatal ethanol exposure in mice phenocopies *Cdon* mutation by impeding Shh function in the etiology of optic nerve hypoplasia

Benjamin M. Kahn, Tanya S. Corman, Korah Lovelace, Mingi Hong, Robert S. Krauss, and Douglas J. Epstein

Abstract

Septo-optic dysplasia (SOD) is a congenital disorder characterized by optic nerve, pituitary and midline brain malformations. The clinical presentation of SOD is highly variable with a poorly understood etiology. The majority of SOD cases are sporadic, but in rare instances inherited mutations have been identified in a small number of transcription factors, some of which regulate the expression of *Sonic hedgehog* (*Shh*) during mouse forebrain development. SOD is also associated with young maternal age, suggesting that environmental factors, including alcohol consumption at early stages of pregnancy, might increase the risk of developing this condition. Here, we address the hypothesis that SOD is a multifactorial disorder stemming from interactions between mutations in Shh pathway genes and prenatal ethanol exposure. Mouse embryos with mutations in the Shh co-receptor, *Cdon*, were treated *in utero* with ethanol or saline at embryonic day 8 (E8.0) and evaluated for optic nerve hypoplasia (ONH), a prominent feature of SOD. We show that both *Cdon*^{-/-} mutation and prenatal ethanol exposure independently cause ONH through a similar pathogenic mechanism that involves selective inhibition of Shh signaling in retinal progenitor cells, resulting in their premature

cell-cycle arrest, precocious differentiation and failure to properly extend axons to the optic nerve. The ONH phenotype was not exacerbated in *Cdon*^{-/-} embryos treated with ethanol, suggesting that an intact Shh signaling pathway is required for ethanol to exert its teratogenic effects. These results support a model whereby mutations in *Cdon* and prenatal ethanol exposure increase SOD risk through spatiotemporal perturbations in Shh signaling activity.

Introduction

Septo-optic dysplasia (SOD) is a clinically heterogeneous disorder that is diagnosed on the presence of at least two of the following conditions: optic nerve hypoplasia (ONH), hypopituitarism and absence of the septum pellucidum (Webb and Dattani, 2010). The severity of these features varies widely in SOD, which has an incidence of 1 in 10,000 live births (Patel et al., 2006). ONH is the most common finding in SOD, and manifests as a thinning of the optic nerve as it exits the eye, resulting in insufficient photo-transduction to the brain and, in many instances, blindness (Morishima and Aranoff, 1986; Cemeroglu et al., 2015). Variable pituitary dysfunction, including isolated growth hormone deficiency, central hypothyroidism, and panhypopituitarism is also observed in individuals with SOD, with decreased levels of one or more pituitary hormones being diagnosed by two years of age (Cemeroglu et al., 2015). Cognitive delay and seizure disorders are also frequently seen in SOD.

The cause of SOD is poorly understood. Most cases are idiopathic, but in rare instances (<1%) inherited mutations have been described in a small number of transcription factors (*SOX2*, *SOX3*, *HESX1*, *OTX2*, *TCF7L1*) expressed during embryonic brain development (McCabe et al., 2011; Gaston-Massuet et al., 2016). The high phenotypic variability, coupled with its sporadic nature, suggest that SOD might be influenced by a combination of environmental and genetic factors.

Insight into the pleiotropic nature of the SOD phenotype was recently realized from the study of a conditional mouse mutant lacking Shh in the developing hypothalamus (*Shh^{Δhyp}*). *Shh^{Δhyp}* mutants display optic nerve and pituitary defects with similarities to SOD in humans (Zhao et al., 2012). The eye and pituitary develop in close

proximity to the source of SHH in the anterior hypothalamus and depend on this signal for formation of the optic disc, from where the optic nerve exits the eye, and for coordinating pituitary morphogenesis. These findings raise the possibility that reduced SHH expression and or signaling activity from the hypothalamus might underlie the pathogenesis of SOD in humans. In support of this hypothesis, *SOX2* and *SOX3* – two SOD-associated genes – were shown to be dose-dependent regulators of *SHH* transcription that directly bind and activate a long-range *SHH* forebrain enhancer (Zhao et al., 2012).

Nonetheless, loss-of-function mutations in *SHH* are not associated with SOD (Paulo et al., 2015; Gregory et al., 2015), but instead are known to cause another brain malformation, holoprosencephaly (HPE), with partially overlapping features to SOD (Roessler et al., 1996). HPE results from imperfect separation of the cerebral hemispheres and craniofacial structures as a result of reduction in SHH signaling from the prechordal plate, a transient embryonic tissue required for early aspects of forebrain development, including the specification of the hypothalamic territory (Chiang et al., 1996). Therefore, HPE and SOD could be distinguished by the timing and location of *SHH* signal disruption, with an early loss of SHH from the prechordal plate giving rise to HPE, and a slightly later absence of SHH from the presumptive hypothalamus resulting in SOD.

The SHH pathway has many roles during eye development. Early functions include separation of the eye fields and patterning of the optic cup (Chiang et al., 1996). At later stages, Shh secreted from retinal ganglion cells (RGCs) controls the proliferation of multipotent retinal progenitor cells (RPCs), the timing of their differentiation, as well as the guidance of RGC axons out of the eye (Wang et al., 2005; Kolpak et al., 2005;

Sanchez-Camacho and Bovolenta, 2008; Stacher Hörndli and Chien, 2012). Mice lacking Shh in RGCs display ONH resulting from a failure in optic disc formation (Dakubo et al., 2003). Thus, ONH can arise by interfering with SHH signaling from two independent sources, anterior hypothalamus and RGCs, at distinct stages of eye development.

Epidemiological studies indicate that SOD associates with young maternal age and primiparity (Haddad and Eugster, 2005; Murray et al., 2005; Garcia-Filion and Borchert, 2013; Cemeroglu et al., 2015). How these risk factors contribute to the etiology of SOD is unknown, but they might be linked to adverse maternal behavior during early stages of pregnancy (Garcia-Filion and Borchert, 2013). For instance, several clinical features of fetal alcohol syndrome overlap with HPE and SOD, suggesting that prenatal ethanol exposure might increase the risk of both conditions, depending on the timing of the insult (Sulik et al., 1981; Strömland, 1987; Coulter et al., 1993; Ashwell and Zhang, 1994; Blader and Strähle, 1998; Hellström, 1999; Ribeiro et al., 2007; Aoto et al., 2008; Loucks and Ahlgren, 2009; Lipinski et al., 2010, 2012; Zhang et al., 2011).

The SHH signaling pathway is a key target of prenatal ethanol exposure and its perturbation explains much of the HPE-like phenotype observed in animal models of this condition (Ahlgren et al., 2002; Li et al., 2007; Higashiyama et al., 2007; Aoto et al., 2008). Interestingly, mouse embryos with mutations in Shh pathway genes that have no, or minimal, phenotypic consequence on their own, show a profound increase in the penetrance and severity of HPE when exposed to sub-teratogenic doses of ethanol (Hong and Krauss, 2012; Kietzman et al., 2014). The synergy between these genetic and environmental risk factors for HPE is dependent on the timing of ethanol administration during pregnancy, with a strong interaction observed at embryonic day 7

(E7.0), coinciding with a disruption in Shh signaling from the prechordal plate (Hong and Krauss, 2012).

On the basis of these studies, we postulate that SOD is a multifactorial condition that results from interactions between genetic and environmental risk factors acting at slightly later stages of forebrain development than those that cause HPE. To test this hypothesis and better define the relationship between ethanol intake, Shh signaling and SOD, we examined eye development in mouse embryos with mutations in the Shh co-receptor, *Cdon*, that were exposed *in utero* to either ethanol or saline at E8.0. Wild--type embryos treated with ethanol phenocopied *Cdon*^{-/-} mutants treated with saline in the manifestation of ONH by selectively impeding Shh signaling activity in RPCs. The combination of *Cdon* mutation and ethanol exposure did not worsen the ONH phenotype, indicating that this gene–environment interaction is not additive or synergistic. These results support a model whereby mutations in *Cdon* and prenatal ethanol exposure are risk factors for SOD and HPE through temporally and spatially distinct perturbations in Shh signaling activity.

Results

We followed a previously validated protocol for prenatal ethanol exposure (see Materials and Methods) to determine whether *Cdon*^{-/-} embryos were sensitive to ethanol-induced ONH, a prominent feature of SOD. All mice described in this study were maintained on a 129S6/SvEvTac genetic background, which is largely impervious to the HPE-associated phenotypes caused by *Cdon* mutation or ethanol exposure observed in other mouse strains (Zhang et al., 2006; Downing et al., 2009; Hong and Krauss, 2012). Pregnant *Cdon*^{+/-} females that were time-bred with *Cdon*^{+/-} males received intraperitoneal injections of ethanol (3.48 g/kg) or saline at E8.0 and again four hours later. This embryonic stage was chosen because it was subsequent to the HPE-critical period at E7.0, allowing us to address the temporal specificity of gene–environment interactions in the etiology of SOD.

***Cdon* mutation and prenatal ethanol exposure independently cause ONH**

Cdon is expressed at early stages of eye development (E9-E11.5), including progenitors of the neural retina and lens vesicle (Zhang et al., 2009). *Cdon*^{-/-} and wild-type embryos were harvested at E14.5, cryo-sectioned along the coronal plane of their heads, and immunostained for neurofilament. No gross abnormalities in the size or structure of the brain were observed between wild-type and *Cdon*^{-/-} embryos in either the ethanol or saline treatment groups. Moreover, none of the prominent eye defects displayed by *Cdon*^{-/-} mutant embryos on the C57BL/6 genetic background, including coloboma, microphthalmia and lens dysmorphology (Zhang et al., 2009) were detected in any of the 129S6 embryos (129S6.*Cdon*^{-/-}), consistent with the strain specificity of these phenotypes.

To assess the embryos for ONH, the diameter of the optic nerve was measured at the level of the optic disc. *Cdon*^{-/-} embryos treated with saline showed a 39% reduction in optic nerve diameter (mean±s.d., 32.26±1.83 μm, n=9, P<0.001) compared with control littermates (52±3.47 μm, n=8) (Fig. 3A,B,E). This difference was significant after normalizing for eye size (Fig. 3F-H). Wild-type embryos exposed to ethanol showed a similar reduction in optic nerve diameter (29.7±2.14 μm, n=9, P<0.001) compared with saline-treated controls (Fig. 3A,C). This result was unexpected given that 129S6 embryos were thought to be resistant to ethanol-mediated teratogenicity (Downing et al., 2009; Hong and Krauss, 2012), although the optic nerve was not examined in these prior studies. The combination of *Cdon* mutation and prenatal ethanol exposure did not exacerbate the ONH phenotype compared with embryos with either condition alone. Ethanol-treated *Cdon*^{-/-} embryos showed a 37% decrease in optic nerve width (33±2.4 μm, n=8, P<0.001) compared with saline--treated controls (Fig. 3A,D), which was a similar reduction to that seen in saline-treated *Cdon*^{-/-} embryos and ethanol-treated wild-type embryos (Fig. 3A-E). These data indicate that *Cdon* mutation and prenatal ethanol exposure both contribute to the etiology of ONH and that additional risk factors, such as genetic background (129S6 versus C57BL/6) and timing of ethanol exposure (E7.0 versus E8.0), influence the phenotypic outcome of ONH versus HPE.

Formation of the optic disc is not disturbed in *Cdon*^{-/-} and ethanol-exposed embryos

The optic nerve exits the eye through the optic disc, which forms at the juncture of the optic stalk and cup. ONH can arise from defects in optic disc formation or from a deficit in the number of RGC axons that make up the optic nerve (Deiner et al., 1997;

Dakubo et al., 2003; Zhao et al., 2012). To distinguish between these two possibilities, we evaluated the expression of Pax2 in the optic disc of *Cdon*^{-/-} and wild-type embryos that were exposed *in utero* to either saline or ethanol at E8.0 of gestation. No significant differences were observed between the number of Pax2⁺ cells in embryos from the experimental and control groups (Fig. 4), thus excluding major defects in optic disc formation as a likely explanation for the ONH phenotype in either of these mouse models.

Shh-dependent proliferation of RPCs is compromised in Cdon^{-/-} and ethanol-treated embryos

The absence of a synergistic interaction between *Cdon*^{-/-} mutation and prenatal ethanol exposure in the manifestation of ONH suggested that both insults might be disrupting a common or parallel signaling pathway(s) important for eye development. Shh is the most likely pathway to be compromised in these mouse models of ONH given the established role of Cdon as a Shh co-receptor, the essential function of Shh in RPC proliferation, and the negative influence of ethanol on Shh pathway activation in a variety of developing tissues (Ahlgren et al., 2002; Wang et al., 2005; Zhang et al., 2006; Tenzen et al., 2006; Li et al., 2007; Aoto et al., 2008; McLellan et al., 2008; Allen et al., 2011; Hong and Krauss, 2013).

To evaluate the integrity of Shh signaling we assessed *Gli1* expression, a reliable readout of Shh pathway activation (Marigo et al., 1996), on sections through the eye at E14.5. Wild-type embryos treated with saline showed robust expression of *Gli1* in the RPC layer of the developing eye at E14.5 (Fig. 5A). In comparison, *Gli1* was markedly reduced in the RPCs of wild-type and *Cdon*^{-/-} embryos exposed to ethanol at E8.0, as

well as *Cdon*^{-/-} embryos treated with saline (Fig. 5A-D). The downregulation of *Gli1* seemed to be specific to the eye as an adjacent domain of expression in the anterior hypothalamus was unaffected across genotypes and treatment groups (Fig. 5E-H). Moreover, *Shh* expression was not compromised in the eye or hypothalamus of any of the embryos (Fig. 5I-P), suggesting that both *Cdon* mutation and prenatal ethanol exposure were acting directly on some aspect of RPC development downstream of *Shh*.

Shh signaling maintains RPCs in a mitotically active state until they are poised to differentiate into RGCs (Zhang and Yang, 2001; Wang et al., 2005). Therefore, we next determined whether the downregulation in *Shh* signaling observed in *Cdon*^{-/-} and ethanol-treated embryos compromised the growth and differentiation properties of RPCs. The proliferation marker Ki67 labeled 670 RPCs per section ($n=3$) in saline--treated wild-type embryos at E14.5 (Fig. 6A,I). By contrast, a drastic reduction in the number of Ki67-positive RPCs was observed in *Cdon*^{-/-} embryos treated with ethanol (88 RPCs/section, $n=3$, $P<0.001$) or saline (117 RPCs/section, $n=3$, $P<0.001$), as well as wild-type embryos exposed to ethanol (113 RPCs/section, $n=3$, $P<0.001$) (Fig. 6A-D,I). Despite the significant reduction in Ki67 staining, trace amounts were still detected in *Cdon*^{-/-} and ethanol-treated embryos upon increased exposure times. Reduced proliferation was also noted in the lens epithelium of *Cdon*^{-/-} and ethanol-treated embryos (Fig. 6J), as described previously (Zhang et al., 2009). The proliferation defects seem to be specific to the eye as no significant differences were detected in the number of Ki67-positive neural progenitors in adjacent brain regions from either genotype or treatment group (Fig. 6E-H,K). These results suggest that the failure of RPCs to respond to *Shh* signaling in both *Cdon*^{-/-} and ethanol-treated embryos at E8.0 compromises their

ability to replicate, in agreement with other studies of Shh signaling in the eye (Wang et al., 2005).

Precocious differentiation of RGCs in $Cdon^{-/-}$ and ethanol-treated embryos

To determine if the differentiation of RPCs was affected by their premature cell-cycle exit we assessed expression of *Math5* (also known as *Atoh7*), a bHLH transcription factor required at the onset of RGC differentiation (Wang et al., 2001). In control embryos, *Math5* expression was confined to postmitotic progenitors in the ventricular zone. By contrast, in $Cdon^{-/-}$ and ethanol-treated embryos, *Math5* expression extended from the ventricular zone into the ganglion cell layer (Fig. 7A-D). This observation is similar to the previous report of expanded *Math5* expression in mouse mutants that lack Shh signaling in the eye (Sakagami et al., 2009), and suggests that loss of Shh-dependent RPC proliferation might be associated with precocious differentiation of RPCs.

RGCs are the earliest born retinal cell type originating from a subset of RPCs expressing *Math5* (Feng et al., 2010; Brzezinski et al., 2012). The LIM homeobox transcription factor *Isl1* functions downstream of *Math5*, and in conjunction with the POU domain protein *Pou4F2* promotes RGC differentiation (Mu et al., 2008; Pan et al., 2008; Prasov and Glaser, 2012; Wu et al., 2015). We evaluated the status of RGC differentiation in $Cdon^{-/-}$ and ethanol-treated embryos by immunostaining for *Isl1*. At E14.5, RGCs are still early in their differentiation as evidenced by the sparse labeling of *Isl1* in saline--treated wild-type embryos (225 cells/section, $n=3$) (Fig. 7E). However, the number of *Isl1*-positive cells was increased by 32% in wild-type (329 cells/section, $n=3$, $P<0.05$) and $Cdon^{-/-}$ (338 cells/section, $n=3$, $P<0.01$) embryos exposed to ethanol at

E8.0, as well as in saline--treated *Cdon*^{-/-} mutants (349 cells/section, $n=3$, $P<0.05$) (Fig. 7E-H,M). Although *Isl1* is not exclusively expressed by RGCs, we did not observe significant differences in the number of other early-born retinal progenitors, such as amacrine cells expressing AP-2 α (also known as *Tfap2a*), between controls and treatment groups, suggesting that the precocious differentiation was limited to RGCs (Fig. 7I-L,N).

These data suggest that the loss of Shh signaling in *Cdon*^{-/-} and ethanol-treated embryos results in the precocious differentiation of RGCs, which would likely deplete the pool of non-proliferating RPCs over time (Wang et al., 2005). The significant thinning of the optic nerve in experimental embryos likely results from the failure of these prematurely differentiating RGCs to properly extend axons to the optic disc, a premise that is supported by a previously characterized role for Shh in regulating the guidance of RGC axons (Sanchez-Camacho and Bovolenta, 2008). Taken together, our results demonstrate that prenatal ethanol exposure at E8.0 phenocopies 129S6.*Cdon*^{-/-} mutant embryos in the manifestation of ONH by selective interference with Shh-dependent expansion and differentiation of RPCs in the eye.

Discussion

Ethanol and Cdon mutation impede Shh signaling in RPCs to cause ONH

The association of SOD with young maternal age led to the hypothesis that adverse behavior, including prenatal alcohol exposure, is a predisposing factor in its etiology (Haddad and Eugster, 2005; Murray et al., 2005; Garcia-Filion and Borchert, 2013; Cemeroglu et al., 2015). Fetal exposure to alcohol causes a spectrum of developmental disorders; however, direct evidence linking ethanol to SOD has been lacking. Here, we used a mouse model to demonstrate that *in utero* exposure to ethanol at E8.0 causes ONH, the most prevalent SOD-associated phenotype. We show that ethanol causes ONH through a similar mechanism to that observed in *Cdon*^{-/-} embryos, involving the inhibition of Shh signaling activity in retinal progenitor cells, which leads to their premature cell-cycle arrest, precocious differentiation, and failure to properly extend axons to the optic nerve (Fig. 8).

These data are consistent with previous studies showing that Shh secreted from RGCs is required to maintain RPCs in a proliferative state, thus preventing their differentiation (Zhang and Yang, 2001; Wang et al., 2005; Sakagami et al., 2009). RGCs also remain dependent on Shh during their maturation, as evidenced by the axonal outgrowth defects that occur upon further inhibition of Shh (Kolpak et al., 2005; Sanchez-Camacho and Bovolenta, 2008). Taken together, our findings implicate the disruption of RGC-derived Shh signaling as the pathogenic mechanism by which *Cdon* mutation and prenatal ethanol exposure cause ONH (Fig. 8D).

Interestingly, *Cdon* has also been reported to antagonize hedgehog (Hh) signaling in the optic vesicle of zebrafish and chick embryos (Cardozo et al., 2014).

However, we did not observe any of the gain of Hh function phenotypes described in *Cdon* morphants, including expansion of Pax2-expressing cells in the ventral retina, or increased Hh signaling in the hypothalamic territory adjacent to the eye. Moreover, the HPE phenotype displayed by *Cdon*^{-/-} mouse embryos exposed to ethanol at E7.0 was rescued by increasing Shh signaling activity (Hong and Krauss, 2013), in contrast to the decrease in Hh that restored eye patterning in *Cdon* morphants (Cardozo et al., 2014). The differences between our findings and those of Cardozo et al. (2014) might be related to the species in which the experiments were performed, or possibly the nature of the genetic manipulations – germline mutation versus morpholino knockdown – that in some cases might result in phenotypic differences resulting from distinct modes of genetic compensation (Rossi et al., 2015).

Strain-dependent modifiers and timing of prenatal ethanol exposure influence

Shh-related phenotypes

A particularly striking feature of our mouse model is the influence that genetic background and timing of prenatal ethanol exposure have on the variable phenotypic severity, in keeping with other studies of ethanol-induced teratogenesis (Downing et al., 2009; Lipinski et al., 2012). When bred on the 129S6/SvEvTac strain, both *Cdon*^{-/-} mutants and wild-type embryos exposed to ethanol at E8.0 presented with ONH. By contrast, when raised on a C57BL/6 (C57BL/6NTac or C57BL/6J) genetic background, both *Cdon*^{-/-} embryos, and wild-type embryos exposed to ethanol one day earlier at E7.0, exhibited HPE (Zhang et al., 2006; Higashiyama et al., 2007; Aoto et al., 2008; Godin et al., 2010). Thus, strain-dependent modifiers of the *Cdon*^{-/-} mutation and timing of prenatal ethanol exposure affect the spatiotemporal dynamics of Shh pathway

disruption in the eye and prechordal plate, which influences the likelihood of developing ONH versus HPE, respectively.

It is intriguing that we did not detect any interaction between *Cdon*^{-/-} mutation and ethanol in the manifestation of ONH, or other SOD-related phenotypes, whereas synergy between the two insults was observed for HPE (Hong and Krauss, 2012). This finding suggests that the eye is especially vulnerable to genetic and environmental perturbations in Shh signaling, at least on the more resistant 129S6 background. Pituitary hypoplasia is another prominent feature of SOD that arises from Shh pathway disruption (Treier et al., 2001; Wang et al., 2010; Zhao et al., 2012). However, *Shh* expression in the anterior hypothalamus, which is required for pituitary morphogenesis, was not affected in the embryos analyzed in our study. Hence, more impactful perturbations in Shh signaling might be needed to compromise pituitary development, as described in other mouse models of SOD (Zhao et al., 2012; Gaston-Massuet et al., 2016).

Effects of ethanol on Shh signaling

Another interpretation for the inability of ethanol to worsen the ONH phenotype in *Cdon*^{-/-} mutants is that an intact Shh signaling pathway is required for ethanol to exert its teratogenic effect. Ethanol treatment reduces Shh signaling through diverse mechanisms, including the activation of Shh pathway antagonists (PKA), repression of Shh pathway modulators (cholesterol), and indirect consequences that decrease the survival of Shh-expressing and/or responsive cells, possibly owing to increased oxidative stress (Ahlgren et al., 2002; Li et al., 2007; Aoto et al., 2008; Zhang et al., 2011). In each of these examples the acute effect of ethanol on Shh signaling is short-lived, occurring

close to the developmental stage when Shh function is required. However, in our study *Shh* is not expressed in the eye until several days after ethanol administration, suggesting that ethanol-induced alterations persist beyond the time of exposure.

One potential mechanism by which ethanol might invoke long-lasting changes in gene expression is through epigenetic modifications of DNA and chromatin structure (Kleiber et al., 2014). Acetyl-CoA is an end product of ethanol metabolism and, among its many cellular functions, serves as a substrate for histone acetylation. Stable alterations in the acetylation and methylation of histone tails at several loci were detected in the cerebral cortex of E17 mouse embryos after *in utero* ethanol exposure at E7.0 (Veazey et al., 2015). Whether these ethanol-induced changes in histone modifications alter gene expression programs that are responsible for specific developmental defects requires further experimentation. Nonetheless, these observations suggest an intriguing model in which prenatal ethanol exposure at E8.0 perturbs the epigenetic landscape leading to alterations in Shh-dependent gene expression in the eye at E14.5 (Fig. 8C).

SOD is a multifactorial disorder

The idiopathic nature of most SOD cases suggests a multifactorial etiology to this debilitating condition, including sporadic mutations and environmental teratogens that impinge on Shh-dependent mechanisms of eye and pituitary development. Exome and whole-genome sequencing of SOD cases should assist in the identification of as-yet undiscovered genetic variants that increase disease risk. Although our study demonstrated the adverse effects of prenatal ethanol exposure on Shh signaling during eye development, other drugs, including cannabinoids and their more potent synthetic

derivatives, might also contribute to disease pathogenesis by interfering with Shh signal transduction at key stages of embryonic development (Khaliullina et al., 2015; Gilbert et al., 2015). The use of drugs and alcohol at early stages of pregnancy is particularly harmful to the embryo because it coincides with a sensitive period of brain development during the first month when young mothers are often unaware of their pregnancy. A better understanding of the gene–environment interactions underlying SOD risk might improve treatment options, time to diagnosis, and public awareness of the importance for early prenatal care, even when pregnancy is inadvertent.

Materials and Methods

Mice

All animal work was approved by the Institutional Animal Care and Use Committee (IACUC) at the Icahn School of Medicine at Mount Sinai and the Perelman School of Medicine, University of Pennsylvania. The animal facilities at both institutions are accredited by the Association for Assessment and Accreditation of Laboratory Animal Care International (AAALAC). Detailed methods for all mouse breeding experiments, *in utero* ethanol administration, measurements of maternal blood alcohol concentration and embryo harvest are described in Hong and Krauss (2012). Briefly, *Cdon*^{+/-} mice on a 129S6/SvEvTac (129S6) background were mated for one hour in the dark and checked for the presence of a vaginal plug. The time of plug detection was designated as embryonic day 0 (E0). Pregnant female mice were injected intraperitoneally with 15 μ l/g body weight of a solution of 30% ethanol in saline (3.48 g/kg) at E8.0, and again 4 h later. Saline injections were used as a control. Generation of mice with a targeted *Cdon* null allele was described previously (Cole and Krauss, 2003).

Immunohistochemistry and *in situ* hybridization

Embryos were harvested at E14.5, fixed overnight in 4% paraformaldehyde at 4°C, washed in PBS, dehydrated through a graded ethanol series, and stored in 100% ethanol at -20°C. Embryos were rehydrated in PBS, cryoprotected in 30% sucrose overnight at 4°C, embedded in Tissue-Tek OCT Compound (Sakura Finetek USA, Inc., Torrance, CA), quick-frozen on dry ice, and cryosectioned at 16 μ m. Primary antibodies used for immunohistochemistry and their dilutions are as follows: mouse anti-

neurofilament (1:250, 2H3), mouse anti-islet1/2 (1:100, 39.4D5), mouse anti AP-2alpha (1:100, 5E4) were obtained from Developmental Studies Hybridoma Bank (University of Iowa, Iowa City, IA); rabbit anti-Pax2 (1:250, 71-6000, Invitrogen); mouse anti-Ki67 (1:1000, ACK02, Leica Biosystems). Detection of primary antibodies was achieved using secondary antibodies conjugated to Cy3 (1:100, 115-106-006, Jackson ImmunoResearch Laboratories) or Alexa 488 (1:100, A32723, Molecular Probes). Section *in situ* hybridization was performed with digoxigenin-UTP-labeled riboprobes essentially as described (Nissim et al., 2007). At least three to five embryos in the experimental and control groups were evaluated for each antibody or *in situ* probe.

Quantification and statistical analysis

All cell counts were performed using the cell counter function in ImageJ (NIH) on tissue sections from at least three embryos of each experimental and control group. The width of the optic nerve was determined at its mid-point using image software in the Leica Application Suite (Leica Microsystems). The axial width and length of each eye was also determined. Eye measurements were taken from at least eight embryos of each experimental and control group that were blind to the observer. Statistical analysis was performed in GraphPad Prism using the Student's *t*-test.

Acknowledgements

We thank members of the Epstein Lab for helpful discussions and comments on the manuscript. We also thank Jeremy Horrell for advice on Ki67 immunostaining. The support of Danielle Marino and the Franklin Institute STEM Scholars Program is greatly appreciated.

Chapter 2 Figures

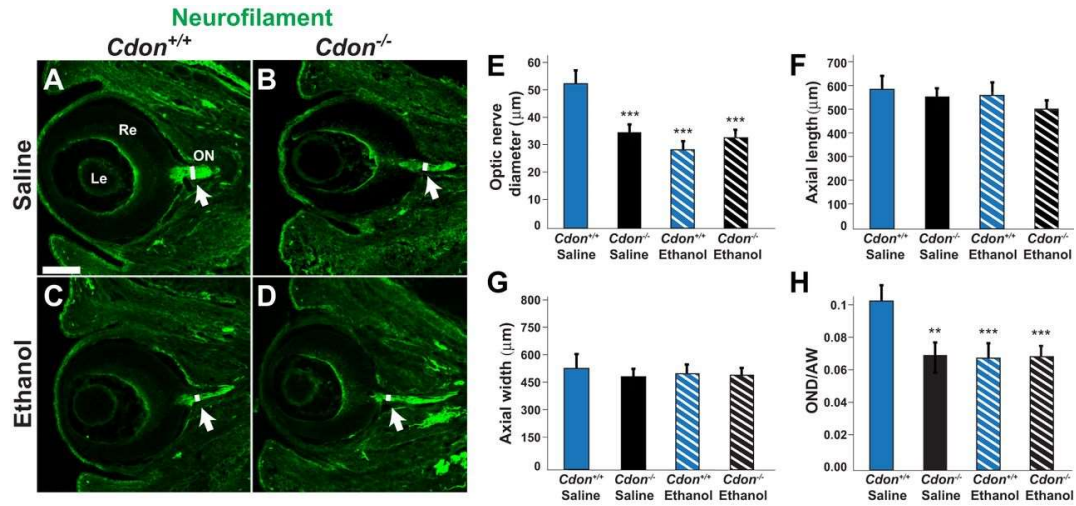


Figure 3. *Cdon* mutation and ethanol exposure independently cause optic nerve hypoplasia.

(A-D) Immunostaining for neurofilament (green) on transverse sections through the eye at E14.5 labels the optic nerve (arrow). Compared with (A) saline-treated wild-type (*Cdon*^{+/+}) embryos (n=9), the diameter of the optic nerve (white line) is significantly reduced in (B) saline-treated *Cdon*^{-/-} mutants (n=8), (C) ethanol-treated wild-type embryos (n=9), and (D) ethanol-treated *Cdon*^{-/-} mutants (n=9). Scale bar: 200 μm. (E-H) Quantification of (E) optic nerve diameter, (F) axial length of eye, (G) axial width of eye, and (H) optic nerve diameter (OND) normalized to axial width (AW) of the eye. Error bars represent s.d. **P<0.01, ***P<0.001 by Student's t-test

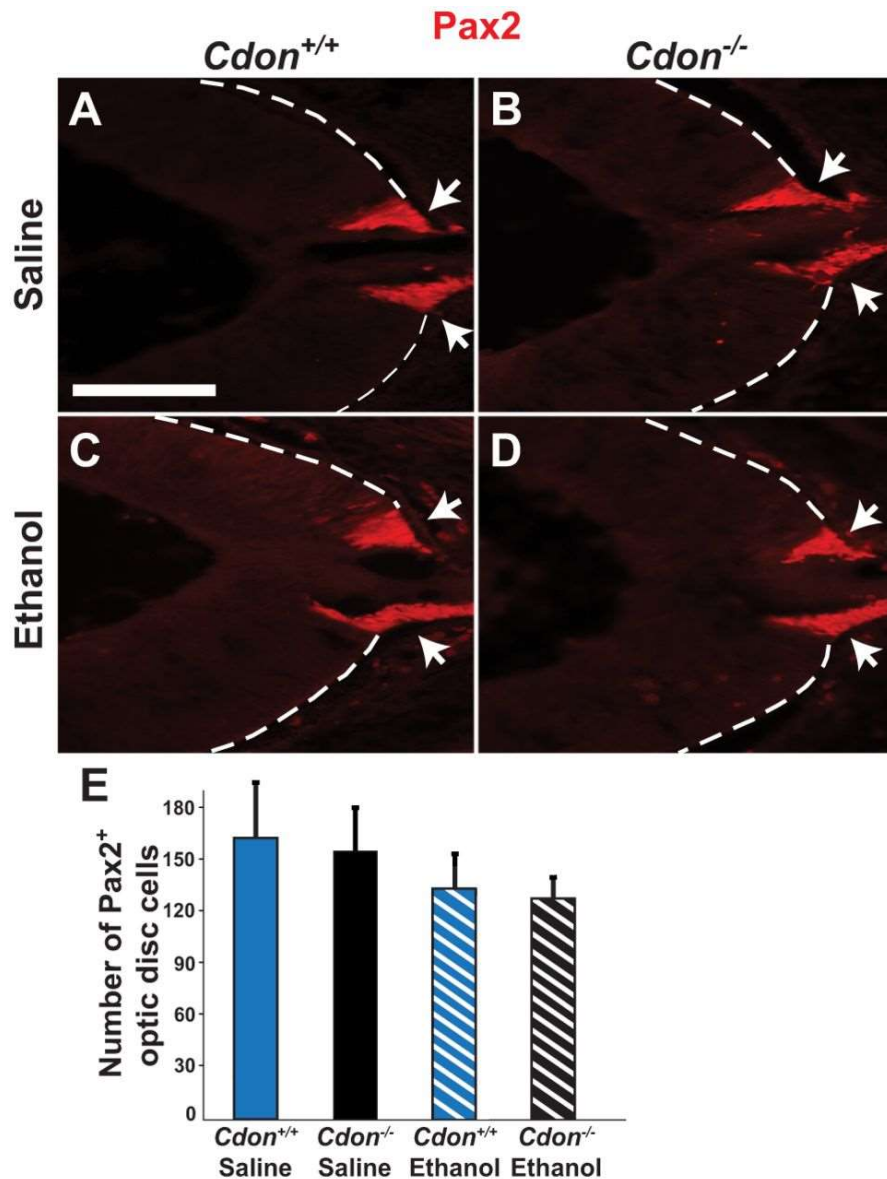


Figure 4. The optic disc is not compromised in *Cdon*^{-/-} or ethanol-treated embryos.

(A-D) Immunostaining for Pax2 on transverse sections through the eye at E14.5 marks the optic disc (arrows). No significant differences were observed in the average number of Pax2⁺ optic disc cells per section from (A) saline-treated wild-type (*Cdon*^{+/+}) embryos

($n=6$), (B) saline-treated $Cdon^{-/-}$ mutants ($n=8$), (C) ethanol-treated wild-type embryos ($n=8$), and (D) ethanol-treated $Cdon^{-/-}$ mutants ($n=8$). Scale bar: 200 μm . (E) Quantification of Pax2⁺ optic disc cells. Error bars represent s.d. Student's *t*-test.

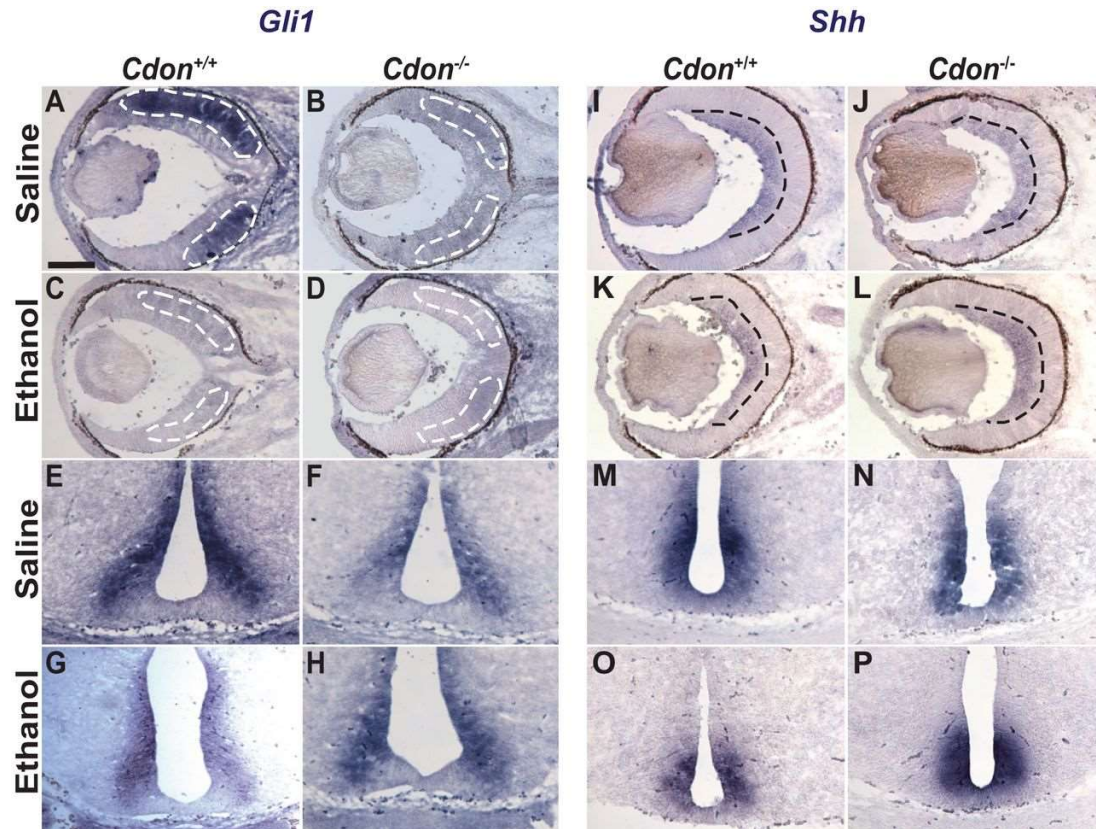


Figure 5. Selective reduction of *Gli1* expression in the eyes of *Cdon*^{-/-} and ethanol-treated embryos.

In situ hybridization for *Gli1* (A-H), and *Shh* (I-P) on transverse sections through the eye (A-D, I-L) and hypothalamus (E-H, M-P) of E14.5 wild-type (*Cdon*^{+/+}) and *Cdon*^{-/-} embryos treated with saline or ethanol at E8.0. *Gli1* expression is detected in retinal progenitor cells (RPCs, area marked by dotted white line) of (A) saline-treated wild-type embryos ($n=5$). *Gli1* expression is markedly reduced in RPCs of (B) saline-treated *Cdon*^{-/-} mutants ($n=5$), (C) ethanol-treated wild-type embryos ($n=9$), and (D) ethanol-treated *Cdon*^{-/-} mutants ($n=5$). No differences were observed in the expression of *Gli1* in the hypothalamus between genotypes or treatment groups (E-H). No differences were observed in the level of *Shh* expression in retinal ganglion cells (RGCs, area marked by

dotted black line, I-L) or the hypothalamus (M-P) between genotypes or treatment groups. Scale bar: 200 μ m.

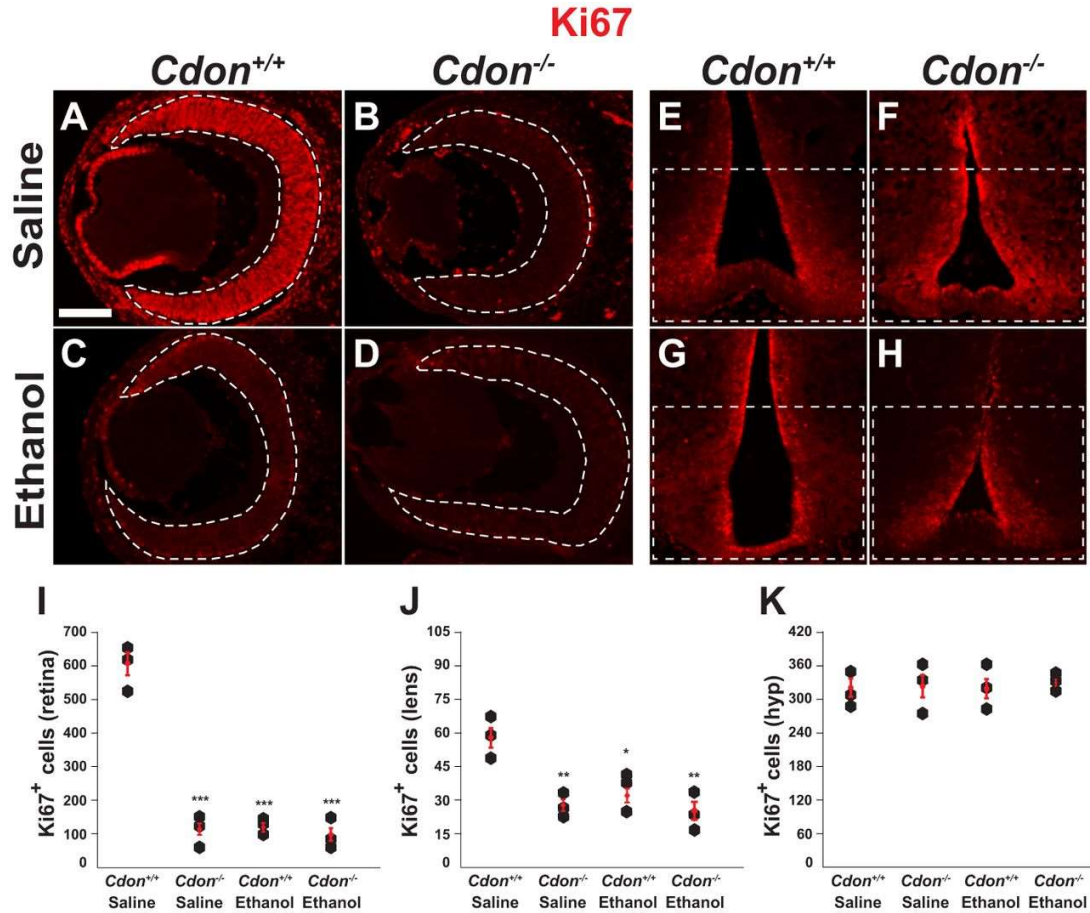


Figure 6. Reduced proliferation of RPCs in $Cdon^{-/-}$ and ethanol-treated embryos.

(A-H) Immunostaining for Ki67 on transverse sections through the eye (A-D) and hypothalamus (E-H) of E14.5 embryos labels proliferating progenitors. (A) The majority of retinal progenitor cells (RPCs, area marked by dotted white line) in saline-treated wild-type ($Cdon^{+/+}$) embryos ($n=3$), are marked by Ki67. The number of Ki67⁺ RPCs is significantly reduced in (B) saline-treated $Cdon^{-/-}$ embryos ($n=3$), (C) ethanol-treated wild-type embryos ($n=3$), and (D) ethanol-treated $Cdon^{-/-}$ embryos ($n=3$). No differences in the number of Ki67⁺ cells in the ventricular layer of the ventral hypothalamus (boxed area) were observed between genotypes or treatment groups (E-H). Scale bar: 200 μ m.

(I-K) Quantification of Ki67⁺ cells in (I) retina, (J) lens and (K) hypothalamus sections across all experimental groups. Error bars represent s.d. * $P < 0.05$, ** $P < 0.01$, *** $P < 0.001$ by Student's *t*-test.

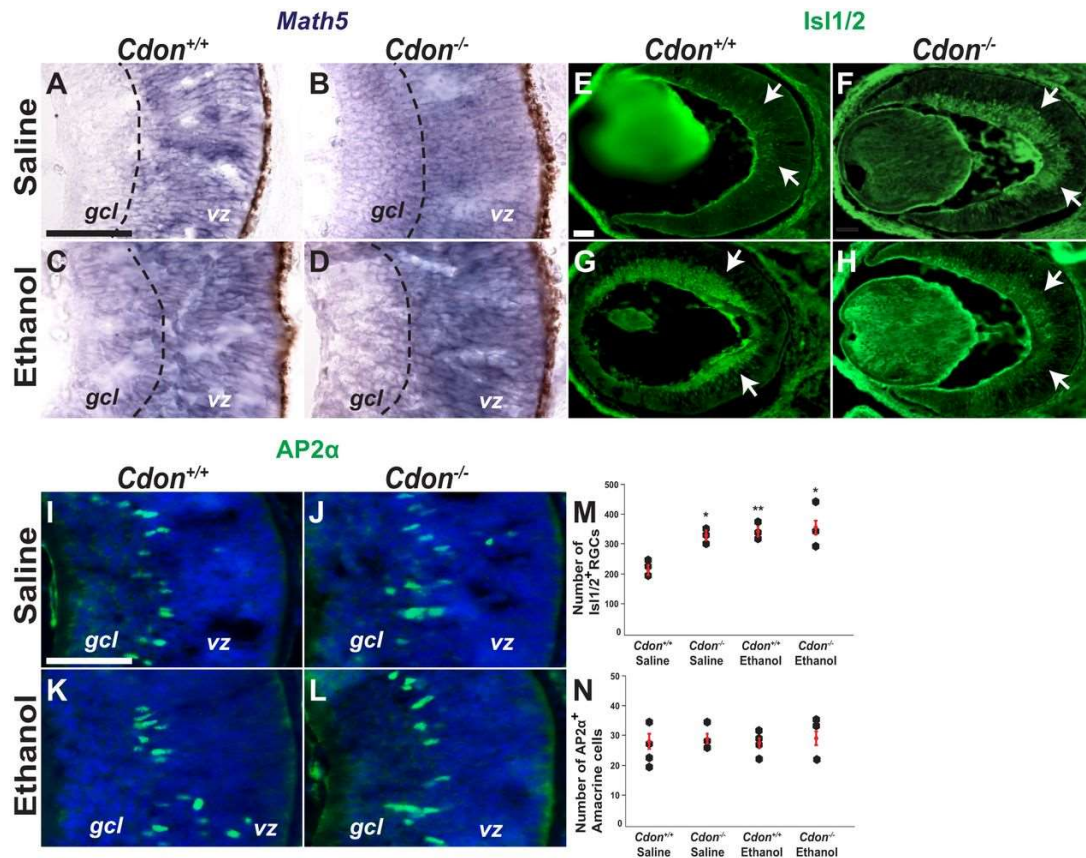


Figure 7. Precocious differentiation of RGCs in $Cdon^{-/-}$ and ethanol-treated embryos.

(A-D) *In situ* hybridization for *Math5* on transverse sections through the eye at E14.5 labels postmitotic progenitors in the ventricular zone (vz) of control embryos ($n=3$) (A). *Math5* expression expands into the ganglion cell layer (gcl) of $Cdon^{-/-}$ and ethanol-treated embryos ($n=3$ for each experimental group) (B-D). Dashed line marks the vz–gcl boundary. (E-H) Immunostaining for Isl1/2 on transverse sections through the eye of E14.5 embryos primarily labels differentiating retinal ganglion cells (RGCs, arrows). Compared with (E) saline-treated wild-type ($Cdon^{+/+}$) embryos ($n=3$), the number of Isl1/2⁺ RGCs is significantly increased in (F) saline-treated $Cdon^{-/-}$ mutants ($n=3$), (G)

ethanol-treated wild-type embryos ($n=3$), and (H) ethanol-treated $Cdon^{-/-}$ mutants ($n=3$). (I-L) Immunostaining for AP-2 α in amacrine cells. No significant differences were observed between the average number of AP-2 α^+ amacrine cells per section from (I) saline-treated wild-type ($Cdon^{+/+}$) embryos ($n=4$), (J) saline-treated $Cdon^{-/-}$ mutants ($n=3$), (K) ethanol-treated wild-type embryos ($n=4$), and (L) ethanol-treated $Cdon^{-/-}$ mutants ($n=3$). Scale bar: 50 μm . (M,N) Quantification of cells expressing Isl1/2 (M) and AP-2 α (N). Error bars represent s.d. * $P<0.05$, ** $P<0.01$ by Student's t -test.

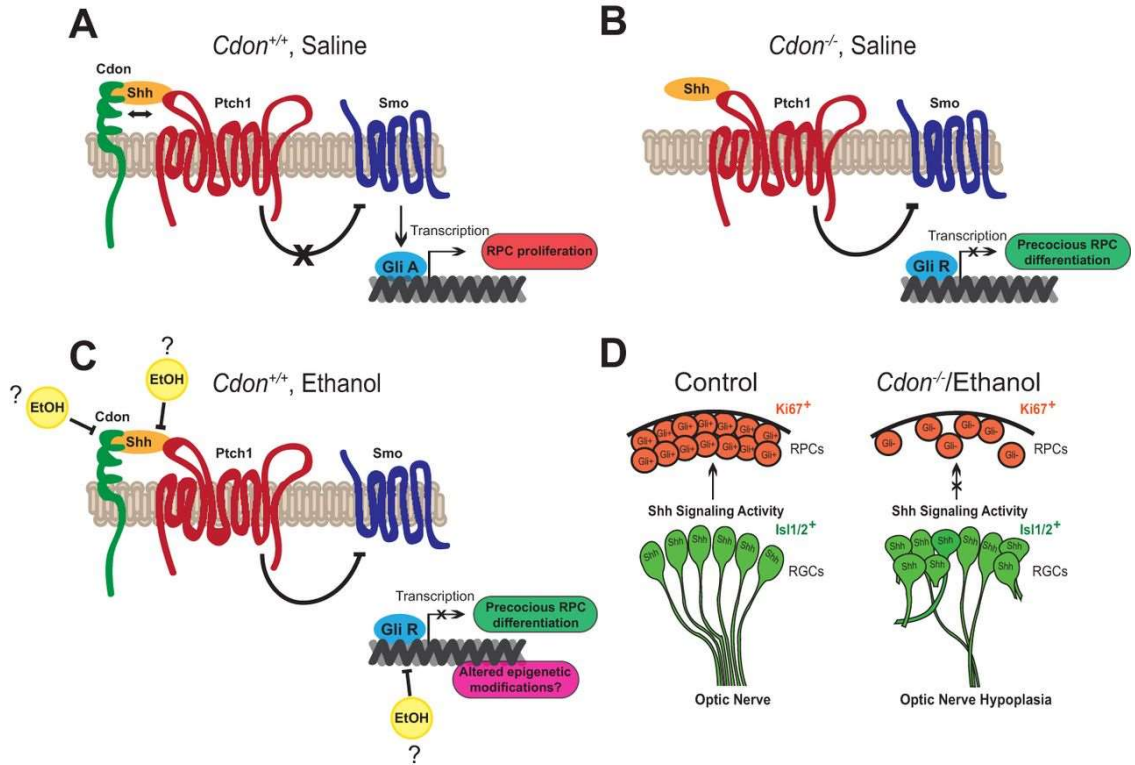


Figure 8. Model depicting the influence of *Cdon* mutation and ethanol exposure on Shh signaling activity in the developing eye.

(A) In wild-type embryos (E14.5), the binding of Shh to Cdon and Ptch1 releases the inhibition on smoothed (Smo), facilitating the transcription by Gli activator (GliA) of target genes involved in RPC proliferation. (B) In the eyes of 129S6. *Cdon*^{-/-} embryos, there is persistent inhibition of Smo by Ptch1, even in the presence of Shh, causing Gli repressor (GliR) to block transcription of genes involved in RPC proliferation, resulting in precocious RPC differentiation. (C) Ethanol exposure at E8.0 interferes with Shh signaling in the eye through a variety of proposed mechanisms. The lengthy delay between ethanol exposure (E8.0) and its negative effects on Shh signaling activity (E14.5), suggests that the epigenetic landscape of Shh target genes might be modified

to suppress RPC proliferation. (D) *Cdon* mutation or ethanol exposure at E8.0 impedes Shh signaling activity in RPCs resulting in optic nerve hypoplasia.

CHAPTER 3: Distinct temporal requirements for Sonic hedgehog signaling development of the tuberal hypothalamus

Tanya S. Corman, Solsire Zevallos, and Douglas J. Epstein

Note: The work in this chapter was submitted to *Development* on May 7, 2018. Reviewer comments were received on May 29, 2018. Revisions are ongoing.

Abstract

Roles for the secreted morphogen, Sonic hedgehog (Shh), have been well characterized in several brain and spinal cord regions. However, the hypothalamus has presented a particular challenge owing to its complex anatomy and neuronal heterogeneity. Here, we utilize fate-mapping and conditional deletion models in mice to define requirements for dynamic Shh activity at distinct stages of tuberal hypothalamic development, a brain region with important homeostatic functions. Tuberal hypothalamic nuclei are dependent on early roles for Shh in dorsoventral patterning, neurogenesis and restricting ventral midline area. Fate mapping experiments demonstrate that Shh expressing and responsive progenitors contribute to distinct neuronal subtypes, accounting for some of the cellular heterogeneity in tuberal hypothalamic nuclei. Conditional deletion of the Hedgehog transducer Smoothed (Smo), after dorsoventral patterning has been established, reveals that Shh signaling is necessary to maintain proliferation and progenitor identity during peak periods of hypothalamic neurogenesis. We also find that mosaic disruption of *Smo* causes a non-cell autonomous gain in Shh signaling activity in

neighboring wild type cells, suggesting a possible mechanism for the growth of hypothalamic hamartomas, a benign tumor that forms at fetal stages of hypothalamic development.

Introduction

The hypothalamus is an ancient brain region with important roles in the regulation of several homeostatic processes and animal behaviors. Neural circuits mapping to distinct areas of the hypothalamus control a variety of essential bodily functions, including food intake, energy expenditure, fluid balance, temperature regulation, wakefulness, daily rhythms, as well as social behaviors associated with reproduction, aggression, arousal, and stress (Saper and Lowell, 2014; Zha and Xu, 2015; Hashikawa et al., 2017; Tan and Knight, 2018). Organized into small clusters of neurons, termed nuclei, the hypothalamus is unlike other regions of the central nervous system (CNS) that are typically arranged in cell layers (Shimada and Nakamura, 1973; Altman and Bayer, 1986). Further adding to this complex architecture, most hypothalamic nuclei are composed of diverse neuronal cell types with opposing or sometimes unrelated functions. The developmental mechanisms regulating neuronal heterogeneity within hypothalamic nuclei are poorly understood compared to other CNS regions (Bedont et al., 2015; Burbridge et al., 2016; Xie and Dorsky, 2017).

The hypothalamus derives from the ventral diencephalon and can be divided into four principal regions from rostral to caudal: preoptic, anterior, tuberal, and mammillary. Within the tuberal hypothalamus, neurons in the arcuate nucleus (ARC), ventromedial hypothalamic nucleus (VMH), dorsomedial hypothalamic nucleus (DMH), and paraventricular nucleus (PVN) integrate sensory information from the environment in order to illicit autonomic, endocrine and behavioral responses that maintain vital set points in the animal or adapt to various stressors (Saper and Lowell, 2014). In addition to receiving inputs from other brain regions, the positioning of the tuberal hypothalamus

offers unique exposure to peripheral cues carried through the bloodstream which are presented to neurons at the median eminence.

Recent advances have been made in our understanding of the neuronal circuitry and function of tuberal hypothalamic nuclei. This is particularly true for the VMH, an elliptical shaped nucleus located above the ARC and below the DMH (Fig. 9). The VMH is subdivided into ventrolateral (VMH_{VL}), central (VMH_C) and dorsomedial (VMH_{DM}) regions, each with distinguishable gene expression profiles (Segal et al., 2005; McClellan et al., 2006; Kurrasch et al., 2007). Genetic, pharmacogenetic and optogenetic approaches have further delineated VMH neurons into functionally distinct categories. ER α -expressing neurons in the VMH_{VL} regulate sexually dimorphic features related to energy expenditure, reproductive behavior and aggression (Lin et al., 2011; Lee et al., 2014; Correa et al., 2015). Whereas, insulin receptor (IR) expressing neurons in the VMH_C and Leptin Receptor (LEPR) neurons in the VMH_{DM} effect body weight regulation in both males and females (Dhillon et al., 2006; Klöckener et al., 2011). Steroidogenic factor 1 (SF1, officially designated Nr5a1) neurons in the VMH_{DM} also influence behavioral responses to fear and anxiety (Silva et al., 2013; Kunwar et al., 2015).

Despite the progress in assigning function to VMH neurons, we still know relatively little about how this nucleus forms and the process by which its subdivisions are established. During hypothalamic development, Nr5a1 is selectively expressed by all VMH neurons soon after they exit the cell cycle and undergo neurogenesis (Tran et al., 2003). Nr5a1 is required for the terminal differentiation of VMH neurons, as well as their coalescence into a nucleus with a distinct cytoarchitecture (Ikeda et al., 1995; Davis et al., 2004; Büdefeld et al., 2011). Consequently, mice lacking Nr5a1 in the VMH are

obese, anxious, and infertile (Majdic et al., 2002; Zhao et al., 2008; Kim et al., 2010). Additional cell type specific factors acting upstream of Nr5a1 remain to be identified.

One signaling molecule that may help bridge the gap in knowledge concerning the ontogeny of VMH neurons is Sonic Hedgehog (Shh). Shh has been studied in several spatial and temporal contexts related to hypothalamic development. Shh signaling from the prechordal plate, which underlies the ventral forebrain at early stages of its development, is required for the induction of the hypothalamic territory (Chiang et al., 1996; Dale et al., 1997). The conditional deletion of Shh in the ventral diencephalon causes defects in the patterning, regionalization and formation of ventral hypothalamic nuclei (Szabó et al., 2009; Shimogori et al., 2010; Zhao et al., 2012; Carreno et al., 2017). Nevertheless, the pathogenic mechanisms underlying these Shh dependent alterations in hypothalamic development have yet to be fully realized. Moreover, since Shh continues to be expressed in VMH progenitors well beyond the initial patterning stage, additional roles for Shh in VMH nucleogenesis and neuronal subtype identity are likely (Alvarez-Bolado et al., 2012).

Here, we use conditional knockout mice to interrogate the functional requirements of Shh signaling at specific periods of hypothalamic development. We show that the pronounced loss of hypothalamic nuclei that manifests from the early deletion of Shh at embryonic day 9 (E9.0) is caused by defects in dorsoventral patterning, neurogenesis and the expansion of ventral midline cells, indicating a novel role for Shh in restricting ventral midline development in the tuberal hypothalamus. Fate mapping experiments reveal that Shh expressing and Shh responsive cell lineages are enriched in distinct domains of the VMH, contributing to the neuronal heterogeneity of this nucleus. The deletion of Smoothed (Smo), an essential transducer of Shh

signaling, at later stages of hypothalamic development (after E10.5), results in a cell autonomous loss of VMH neuronal subtype identity. Remarkably, we also detect a non-cell autonomous expansion and reprogramming of neighboring wild type cells, which likely occurs in response to residual Shh ligand that was not taken up by *Smo* mutant cells. This gain in Shh signaling activity may explain the pathogenesis of hypothalamic hamartomas (HH), a benign tumor caused, in some cases, by somatic gene mutations that block Shh responsiveness (Saito et al. 2016; Hildebrand et al., 2016).

Results

Shh is required for the development of tuberal hypothalamic nuclei

To determine how Shh signaling contributes to the formation of tuberal hypothalamic nuclei we first evaluated the expression of cell type specific markers in *SBE2-cre; Shh^{loxp/-} (Shh^{Δhyp})* embryos. *SBE2-cre* is a transgenic mouse line that uses Shh brain enhancer 2 (SBE2) to activate *cre* transcription in the ventral diencephalon in a similar pattern to the endogenous expression of *Shh*. We previously showed that Shh is selectively deleted in the ventral diencephalon of *Shh^{Δhyp}* embryos by E9.0 (Zhao et al., 2012). The expression of cell type specific markers of the DMH (Hmx3), VMH (Nr5a1) and ARC (Pro-opiomelanocortin, POMC; Tyrosine Hydroxylase, TH; and Somatostatin, Sst) nuclei was either absent or greatly diminished in *Shh^{Δhyp}* embryos at E14.5 (Fig. 9A-K; POMC: control 140.8 ± 52.9 , *Shh^{Δhyp}* 1.0 ± 1.7 , n=5, p=0.0004; TH: control 104.0 ± 13.2 , *Shh^{Δhyp}* 12.3 ± 6.6 , n=4, p<0.0001; Sst: control 63.0 ± 3.0 , *Shh^{Δhyp}* 0.3 ± 0.6 , n=3, p<0.0001). Ectopic expression of *Hmx3* was also detected in the VMH, possibly due to its derepression in the absence of Shh (Fig. 9A, B). These results are consistent with previous findings demonstrating a requirement for Shh in the development of tuberal hypothalamic nuclei (Fig. 9L-N; Szabó et al., 2009; Shimogori et al., 2010; Carreno et al., 2017).

Alterations in dorsoventral patterning, neurogenesis and ventral midline formation explain the absence of tuberal hypothalamic nuclei in Shh^{Δhyp} embryos

Shh signaling is required to establish distinct neuronal identities at ventral positions along the length of the vertebrate neural tube through the activation and

repression of homeodomain and basic helix-loop-helix (bHLH) transcription factors (Ericson et al., 1997; Briscoe et al., 1999; Briscoe et al., 2000; Muhr et al., 2001; Balaskas et al., 2012). However, the temporal and spatial dynamics of Shh signaling in the hypothalamus differ from more posterior regions of the CNS. *Shh* is initially broadly expressed in ventral hypothalamic progenitors and then rapidly downregulated in the ventral midline at the level of the tuberal hypothalamus (Manning et al., 2006; Trowe et al., 2013). Consequently, *Shh* is expressed in bilateral stripes adjacent to the ventral midline, unlike spinal cord and hindbrain regions where *Shh* is restricted to the floor plate (Fig. 10A; and Echelard et al., 1993). Moreover, neural progenitors immediately dorsal to the bilateral stripes of *Shh* are responsive to Shh signaling, indicated by *Gli1* expression, whereas progenitors located in the ventral midline are refractory to Shh signaling (Fig. 10B; and Ohyama et al., 2008).

We evaluated key patterning genes in *Shh*^{Δhyp} mutants at E10.5 to address whether alterations in their expression might explain the loss of tuberal hypothalamic nuclei at later stages. As expected, *Shh* and *Gli1* were absent in *Shh*^{Δhyp} embryos (Fig. 10A,B,H,I). The number of cells expressing Nkx2.1, a broad determinant of ventral hypothalamic progenitor identity (Kimura et al., 1996; Sussel et al., 1999), was reduced by 48% in *Shh*^{Δhyp} embryos compared to control littermates (Fig. 10C,J,O; control: 540.8 ± 56.4, n=5; *Shh*^{Δhyp}: 282.0 ± 22.0, n=6, p<0.0001). In addition, Pax6, a prethalamic marker was expanded ventrally to a position abutting the Nkx2.1 domain (Fig. 10C,J). Nkx2.2 is expressed in Shh responsive progenitors of the DMH that occupy the gap between Pax6 and Nkx2.1 (Fig. 10D). The expression of Nkx2.2 was dramatically reduced in *Shh*^{Δhyp} embryos (Fig. 10D,K,P; control: 221.0 ± 21.2, n=4; *Shh*^{Δhyp}: 1.6 ± 2.1, n=5, p<0.0001), which may explain the ventral expansion of Pax6 due to deficient cross-

repressive interactions between these transcription factors (Ericson et al., 1997; Briscoe et al., 1999; Muhr et al., 2001). These results suggest that alterations in the dorsoventral patterning of tuberal hypothalamic progenitors are responsible, at least in part, for the loss of their identities in *Shh*^{Δhyp} embryos.

The bHLH transcription factor, *Ascl1*, is required for ARC and VMH neurogenesis (McNay et al., 2006). We observed an 81% reduction in the number of *Ascl1* expressing cells in the ventral hypothalamus of *Shh*^{Δhyp} embryos compared to control littermates (Fig. 10E,L,Q; control: 252.7 ± 11.7 , n=3; *Shh*^{Δhyp}: 47.0 ± 18.5 , n=3, p<0.0001). Therefore, the reduction of neuroendocrine neurons in the ARC and VMH nuclei of *Shh*^{Δhyp} embryos may also be explained by the downregulation of *Ascl1*.

Another striking feature of *Shh*^{Δhyp} embryos is the dysmorphic appearance of the ventral midline. Rather than the V-shaped morphology typical of wild type embryos, the ventral midline of *Shh*^{Δhyp} embryos is U-shaped with a flattened appearance (Fig. 10F,M). Ventral midline cells in the tuberal hypothalamus undergo BMP dependent cell-cycle arrest and express the T-box protein, *Tbx3* (Manning et al., 2006; Trowe et al., 2013). We quantified the zone of non-proliferation by counting the number of DAPI positive nuclei in the *Ki67* negative ventral midline territory and observed a significant increase in *Shh*^{Δhyp} embryos (Fig. 10F,M,R; 50.5 ± 3.7 , n=4) compared to control littermates (14.67 ± 1.5 , n=3, p<0.0001). The length of the ventral midline territory marked by *Tbx3* was also significantly increased in *Shh*^{Δhyp} embryos (Fig. 10G,N,S; $239.1 \pm 8.2 \mu\text{m}$, n=3) compared to control littermates ($96.7 \pm 11.6 \mu\text{m}$, n=3, p=0.0001). These results demonstrate that the loss of *Shh* in the tuberal hypothalamus expands the fate of non-dividing ventral midline cells at the expense of proliferating *Nkx2.1* positive neural progenitors. Interestingly, *Bmp4* was previously shown to be upregulated in the

ventral midline of *Shh*^{Δhyp} embryos (Zhao et al., 2012). Hence, our findings highlight a unique role for Shh in restricting the size of the ventral midline in the tuberal hypothalamus by opposing Bmp signaling, in stark contrast to the floor plate promoting activity of Shh in more posterior regions of the CNS (Echelard et al., 1993; Roelink et al., 1994; Roelink et al., 1995; Marti et al., 1995; Ericson et al., 1996; Chiang et al., 1996).

Descendants of Shh expressing progenitors contribute to the VMH

Shh and *Gli1* continue to be expressed beyond the stage when tuberal hypothalamic progenitors first acquire their identity and extend into the peak period of DMH, VMH and ARC neurogenesis between E12.5 and E14.5 (Fig. 11). We next sought to determine the relative contributions of Shh expressing and Shh responsive progenitors to distinct tuberal hypothalamic nuclei. We used a genetic fate mapping strategy to indelibly label Shh expressing (*Shh*^{CreER}) and Shh responsive (*Gli1*^{CreER}) progenitors with an inducible GFP reporter (*Rosa*^{ZsGreen}). Pregnant dams carrying either *Shh*^{CreER/+}; *Rosa*^{ZsGreen/+} or *Gli1*^{CreER/+}; *Rosa*^{ZsGreen/+} embryos were administered tamoxifen at E10.5. The contribution of *Shh* and *Gli1* expressing cells to tuberal hypothalamic nuclei was evaluated by co-labeling with GFP and cell type specific markers at E14.5.

The majority of postmitotic neurons in the VMH express Nr5a1 and Nkx2.1 at E14.5 (Fig. 12A,B; Correa et al., 2015). GFP⁺ cells in *Shh*^{CreER/+}; *Rosa*^{ZsGreen/+} embryos were detected in the ventricular zone adjacent to the VMH as well as 46% of Nr5a1 positive neurons (Fig. 12A,G). This finding suggests that Shh expressing progenitors in the ventricular zone of the tuberal hypothalamus migrate radially to populate the VMH, in agreement with a previous study (Alvarez-Bolado et al., 2012). GFP and Nr5a1 double labeled neurons were enriched in ventral (199.3 ± 11.9 , n=3) compared to dorsal (112.3

± 8.0 , $n=3$, $p=0.0005$) regions of the VMH in *Shh*^{CreER/+}; *Rosa*^{ZsGreen/+} embryos (Figs. 12A and 13). A similar ventral VMH bias was observed for GFP and Nkx2.1 double labeled neurons (Fig. 12B). Nkx2.2 is expressed in a subset of post-mitotic neurons in the dorsal VMH, of which 22% co-label with GFP (Fig. 12C,G). These data reveal that descendants of Shh expressing progenitors marked with GFP at E10.5 are partitioned along the dorsoventral axis of the VMH into primarily ventral and central positions and are largely excluded from the dorsal most region (Figs. 12J and 13).

We also assessed the contribution of Shh expressing progenitors to other tuberal hypothalamic nuclei. The DMH is composed of GABA-ergic neurons that express Gad1 and a subset of neurons that express Isl1. No overlap in GFP and Gad1 or Isl1 was observed in the DMH of *Shh*^{CreER/+}; *Rosa*^{ZsGreen/+} embryos, suggesting that Shh expressing progenitors do not contribute to this nucleus when labeled at E10.5 (Fig. 12H-J). Some overlap between GFP and Isl1 was observed in ventrolateral neurons in the VMH, as well as a small subset of ARC neurons (Fig. 12I,N). In summary, Shh expressing neuronal progenitors in the tuberal hypothalamus predominantly contribute to the VMH when labeled at E10.5.

Descendants of Gli1 expressing progenitors contribute to the DMH and VMH

We next examined the fate of Shh responsive cells in *Gli1*^{CreER/+}; *Rosa*^{ZsGreen/+} embryos administered tamoxifen at E10.5 and collected at E14.5. Given that *Gli1* is expressed dorsal to *Shh*, we expected that GFP⁺ cells would be confined to the DMH. Indeed, GFP⁺ cells were detected in the ventricular zone immediately adjacent to the DMH, as well as in Gad1 and Isl1 expressing neurons that appeared to migrate radially into the DMH (Fig. 12K-N).

Surprisingly, we also identified a small population of Nr5a1 neurons in the VMH of *Gli1^{CreER/+}; Rosa^{ZsGreen/+}* embryos that co-labeled with GFP (Fig. 12D,G; 10.6% ± 1.4%, n=3). These GFP⁺ cells appeared to stream ventrally from a more dorsal progenitor domain to occupy a dorsolateral region of the VMH (Fig. 12D-F). GFP and Nr5a1 double labeled neurons were enriched in dorsal (57.3 ± 13.5, n=3) compared to ventral (5.0 ± 1.7, n=3, p=0.002) regions of the VMH in *Gli1^{CreER/+}; Rosa^{ZsGreen/+}* embryos (Figs. 12D and 13). GFP co-labeling was also observed with Nkx2.1 and Nkx2.2 in primarily dorsal regions of the VMH (Fig. 12E-G). These data suggest that VMH neurons originate from spatially segregated pools of Shh expressing and Shh responsive progenitors that may contribute to the cellular heterogeneity of the VMH (Fig. 12J,M).

Shh signaling is required to maintain tuberal hypothalamic progenitors in a proliferative state

The results of our lineage tracing and gene expression experiments demonstrated that Shh signaling is active in tuberal hypothalamic progenitors after their dorsoventral identity is established. To address whether Shh signaling is also required at later stages of DMH and VMH neurogenesis we generated mice in which *Smoothened* (*Smo*), an essential regulator of Shh signaling, was conditionally deleted in *Gli1* expressing cells after E10.5.

Pregnant dams carrying *Gli1^{CreER/+}; Smo^{lox/-}; Rosa^{ZsGreen/+}* (*cSmo*) and *Gli1^{CreER/+}; Smo^{lox/+}; Rosa^{ZsGreen/+}* (control) embryos were administered tamoxifen at E10.5 and collected at different developmental stages. Strikingly, the number of GFP positive cells in the tuberal hypothalamus was decreased by 43% in *cSmo* embryos (453.8 ± 52.27, n=8) compared to control littermates (800.2 ± 155.3, n=9, p=0.0003) when harvested at

E14.5 (Fig. 14A-C). This reduction in GFP⁺ cells was detected in both mantle and ventricular zones. A significant reduction in the number of GFP⁺ cells was also observed one day earlier at E13.5 (Fig. 14D-F; *cSmo*: 418.1 ± 45.5, n=7, versus control: 603 ± 138.9, n=6, p=0.0066), but not at E12.5 (Fig. 14 G-I; *cSmo*: 512.4 ± 96.1, n=5, versus control: 578.6 ± 96.7, n=5, p>0.05).

The failed expansion of Shh responsive cells in *cSmo* embryos between E12.5 and E14.5 might be explained by increased cell death, decreased proliferation, or both. Immunostaining for activated caspase-3, an indicator of apoptosis, was minimal in *cSmo* and control embryos at E14.5 with no significant differences between genotypes (Fig. 15). On the other hand, fewer GFP positive cells co-labeled with the proliferation marker Ki67 in the ventricular zone of *cSmo* embryos at E12.5 (Fig. 14J-L; 28.5% ± 6.2%, n=3) compared to control littermates (50.1% ± 8.7%, n=9, p=0.0249). From these results, we conclude that Shh signaling is required to maintain tuberal hypothalamic progenitors in a mitotically active state during the peak period of VMH and DMH neurogenesis.

Cell-autonomous requirement for Smo in promoting tuberal hypothalamic neuron identity

Given the contribution of Shh responsive cells to distinct neuronal subtypes in the DMH and VMH, we next assessed whether aspects of their identity were compromised in *cSmo* mutants. We observed a 30% reduction in the number of *Isl1* positive neurons in the DMH of *cSmo* (Fig. 16A-C; 477.6 ± 130.7, n=5) compared to control littermates (678.3 ± 44.6, n=4, p=0.0229). There was also a 30% reduction in the number of neurons expressing *Nkx2.2* in the dorsal VMH of *cSmo* (Fig. 16D-F; 315.2 ± 52.1, n=9) compared to control embryos (451.6 ± 28.2, n=9; p<0.0001). These findings, in

conjunction with the proliferation defects described above, suggest that the conditional loss of Shh signaling after E10.5 causes a cell autonomous reduction of distinct DMH and VMH neuronal subtypes.

Non-cell autonomous defects in cSmo embryos alter VMH neuron subtype identity

Remarkably, despite the reduction of Nkx2.2 staining in *cSmo* embryos, the total number of Nr5a1 expressing neurons in the VMH was unchanged (Fig. 16G-I; *cSmo*: 598.5 ± 100.7 , n=8, versus control: 590.8 ± 196.4 , n=6, p=0.9253). Moreover, fewer Nr5a1 expressing neurons co-labeled with Nkx2.1 in *cSmo* embryos, which was especially notable in ventral regions of the VMH where *Gli1* is not normally expressed (Fig. 16J-L). The presence of defects in regions of the tuberal hypothalamus that are not known to be Shh responsive suggests that some of the phenotypes in *cSmo* embryos may occur through non-cell autonomous mechanisms.

The seemingly incongruous findings that Nkx2.2 neurons are partially reduced in the dorsal VMH of *cSmo* embryos without an effect on the total number of VMH cells prompted us to reassess the specification of tuberal hypothalamic progenitors. Nkx2.1 marks a broad ventral region of the ventricular zone in control embryos at E14.5, from the ventral midline of the hypothalamus to a dorsal limit that approximates the border between the VMH and DMH (Fig. 17A). The expression of Nkx2.2 overlaps with Nkx2.1 at the level of the dorsal VMH and extends dorsally into the ventricular zone of the prethalamus (Fig. 17A). There was a significant reduction in the number of cells expressing Nkx2.1 in the ventricular zone of *cSmo* embryos (Fig. 17A; *cSmo*: 131.0 ± 80.4 , n=5, versus control: 259.4 ± 58.9 , n=5, p=0.0205) and a concomitant ventral

expansion of *Nkx2.2* (Fig. 17A; *cSmo*: 118.2 ± 42.9 , $n=9$, versus control: 58.0 ± 23.2 , $n=9$, $p=0.002$). Given that *Nkx2.2* is a direct transcriptional target of Shh signaling, it was puzzling that its expression was increased in *cSmo* mutants (Lei et al., 2006; Vokes et al., 2007). We evaluated other molecular readouts of Shh signaling and observed a similar ventral expansion of *Olig2* (*cSmo*: 125.8 ± 12.9 , $n=5$, versus control: 73.4 ± 6.5 , $n=5$, $p<0.0001$) and *Ki67* (*cSmo*: 107.0 ± 13.5 , $n=8$, versus control: 81.8 ± 16.4 , $n=9$, $p=0.0037$) in *cSmo* embryos (Fig. 17B,C). Notably, the cells displaying ectopic expression of *Nkx2.2*, *Olig2* and *Ki67* were not GFP positive, suggesting that they were wild type cells that had not undergone *Smo* recombination (Fig. 18). No change in the expression of *Gli1* was observed between *cSmo* and control embryos at E14.5, suggesting that the ectopic response to Shh signaling was transient and/or occurred at an earlier stage (Fig. 17D). The most parsimonious explanation for these results is that the conditional deletion of *Smo* prevented the normal uptake of Shh ligand, causing a non-cell autonomous gain in Shh signaling in neighboring wild type cells (Fig. 17E).

Discussion

Previous studies identified requirements for Shh at distinct spatial and temporal points in hypothalamic development, from induction to nucleogenesis (Chiang et al., 1996; Szabó et al., 2009; Shimogori et al., 2010; Zhao et al., 2012). Here, we further define the phenotypic consequences and pathogenic mechanisms attributed to the loss of Shh signaling at early (E9.0) and late (after E10.5) stages of hypothalamic development. We determine that the loss of hypothalamic nuclei in cases where Shh was deleted at early time points results from requirements for Shh in establishing proper dorsoventral patterning, neurogenesis, and limiting the expansion of the non-proliferative ventral midline. Using an inducible approach, we then characterize requirements for later Shh activity, at time points after dorsoventral patterning has been established. We find that Shh is necessary to maintain proliferation and subtype identity of VMH and DMH progenitors during peak periods of hypothalamic neurogenesis.

Shh directs dorsoventral patterning and neurogenesis in the hypothalamus

Our results confirm that the early source of Shh in the hypothalamus is required to generate the full complement of tuberal hypothalamic neurons (Szabó et al., 2009; Shimogori et al., 2010; Zhao et al., 2012). In order to understand the mechanism underlying the loss of these cell types in *Shh^{Δhyp}* mutants, we evaluated embryos at E10.5 and observed a failure to activate the appropriate patterning, proliferation and neurogenic programs. This result is consistent with the known morphogenetic role of Shh in establishing ventral neuronal identities through the regulation of homeodomain and bHLH transcription factors with some notable differences described below (Ericson

et al., 1997; Briscoe et al., 1999; Briscoe et al., 2000; Muhr et al., 2001; Balaskas et al., 2012).

At spinal cord and hindbrain levels of the CNS, the notochord is the principle source of Shh required to specify ventral neuronal progenitors, whereas, the secondary source of Shh in the floor plate is needed for the formation of later born glial and ependymal cells types (Matise et al., 1998; Yu et al., 2013). In contrast to the notochord, the expression of Shh in the prechordal plate is transient and only present for sufficient time to specify the hypothalamic territory, marked by Nkx2.1, but not the identity of neuronal progenitors (Szabó et al., 2009). Instead, it is the hypothalamic source of Shh that establishes VMH and DMH progenitor domains. Thus, whereas notochord derived Shh activates target genes, such as Nkx2.2 and Olig2, in the overlying neural tube, a similar function is fulfilled by the hypothalamic source of Shh. Given that hypothalamic neurons develop over a protracted period compared to most spinal cord neurons, it makes sense that they rely on an enduring source of Shh within the hypothalamus for their development (Davis et al., 2004; Altman and Bayer, 2006; Ishii and Bouret, 2012).

Shh restricts ventral midline development in the tuberal hypothalamus

In addition to the dorsoventral patterning and neurogenic defects, our analysis of *Shh*^{Δhyp} mutants revealed an unexpected expansion of ventral midline identity. It is likely that the increased number of ventral midline cells in *Shh*^{Δhyp} embryos is a consequence of heightened Bmp signaling as evidenced by the expanded zone of non-proliferation and *Tbx3* expression, two molecular readouts of this pathway (Manning et al., 2006). Indeed, the loss of Shh signaling in the anterior hypothalamus of *Shh*^{Δhyp} embryos was previously shown to cause a rostral shift in *Bmp4* expression as early as E9.5 (Zhao, et

al., 2012). Interestingly, a similar phenotype was also observed in *Lrp2*^{-/-} mutant embryos, including a downregulation in Shh signaling, flattened and expanded ventral midline, and a rostral shift in *Bmp4* expression (Christ et al., 2012). *Lrp2* belongs to the LDL receptor gene family and binds both Shh (as a co-receptor) and *Bmp4* (as a scavenger receptor) (McCarthy et al., 2002; Spoelgen et al., 2005; Christ et al., 2012). Therefore, a disruption in the balance of Shh and *Bmp* signaling, loss and gain respectively, is responsible for the ventral midline defects in *Lrp2*^{-/-} and *Shh*^{Δhyp} mutants.

A role for Shh in restricting ventral midline development in the tuberal hypothalamus is intriguing given the opposite function it plays in promoting floor plate induction in posterior regions of the CNS (Echelard et al., 1993; Roelink et al., 1995; Martí et al., 1995; Ericson et al., 1996; Chiang et al., 1996). Why might Shh have contrasting roles in the development of ventral midline cells at different levels of the neural tube? Firstly, the cells at the ventral midline of the tuberal hypothalamus, known as the median eminence, differ from floor plate cells in the spinal cord in that they are comprised of tanycytes, a specialized form of radial glia with neurogenic and gliogenic properties (Rizzoti and Lovell-Badge, 2017). In mammals, floor plate cells of the spinal cord are considered glial-like but do not give rise to neurons or glia. Tanycytes are an integral component of the hypophyseal portal system that connects the hypothalamus to the pituitary gland and regulate a variety of homeostatic processes given their access to blood borne signals (Rodríguez et al., 2005; Robins et al., 2013; Bolborea and Dale, 2013). Secondly, the hypothalamic ventral midline is a site of integration for multiple signaling pathways, including Shh, *Bmp*, Wnt and Fgf that help facilitate the unique organization of the hypothalamic-pituitary axis (Manning et al., 2006; Davis and Camper., 2007; Zhu et al., 2007; Potok et al., 2008; Zhao et al., 2012; Carreno et al.,

2017; Fu et al., 2017). At the level of the spinal cord, Shh is the primary regulator of ventral neuronal identities, with additional signals serving to modulate Shh responsiveness (Gouti et al., 2015; Kong et al., 2015). Thirdly, Shh expressing cells in the hypothalamus are different from elsewhere in the neural tube in that they constitute actively dividing neuronal progenitors (Szabó et al., 2009; this study). Within the spinal cord, Shh expressing floor plate cells lack neurogenic properties. Given the clear differences in ventral development between the hypothalamus and spinal cord, it is not altogether surprising that Shh exhibits unique and overlapping functions at each of these CNS regions.

Later Shh signaling- delineating fates

We sought to investigate roles and requirements for the enduring source of Shh in the tuberal hypothalamus. Our lineage tracing experiments revealed biased contributions of Shh expressing and Shh responding lineages to the VMH and DMH. On the basis of this observation, we wondered whether integration of progenitors may serve as a potential means by which neuronal heterogeneity is achieved within these hypothalamic nuclei.

Shh expressing and Shh responsive populations mix to give rise to the large domain of Nr5a1 cells in the VMH, though their contributions remain somewhat spatially discrete. Initially found broadly in the VMH, Nr5a1 expression becomes restricted to the VMH_{DM} by P0 (Cheung et al., 2013; Correa et al., 2015). Transcriptome analysis of the VMH in both neonatal and adult mice has revealed enrichment of 200 genes relative to expression in neighboring nuclei (Segal et al., 2005; Kurrasch et al., 2007). Examining the patterns of these markers revealed distinct spatial domains and biases, some

overlapping with Nr5a1 and some mutually exclusive. Thus, it is clear that VMH neurons are diverse in nature. Molecular characterization of VMH neuronal subclasses has largely been performed in postnatal animals. Specifically, Islet1 and ER α are restricted to the VMH_{VL} (Davis et al., 2004), BDNF to the VMH_{DM} and VMH_C (McClellan et al., 2006), and leptin receptor to the VMH_{DM} (Balthasar et al., 2004; Dhillon et al., 2006). However, little is known regarding the processes through which these diverse populations are specified. Thus, within the VMH, the ventral bias of cells derived from Shh expressing progenitors and the dorsal bias of Gli1 expressing descendants may be indicative of a role for Shh signaling as a means of delineating distinct fates within a single nucleus.

The migration of a small number of Shh responsive progenitors into the VMH bears similarity to other hypothalamic cell types that originate from outside of their local progenitor territory. Most neuronal populations in the ARC are generated from multipotent progenitors that migrate radially from the adjacent ventricular zone (Li et al., 1996; McNay et al., 2006; Yee et al., 2009; Pelling et al., 2011; Lu et al., 2013; Lee et al., 2016), however some cells migrate tangentially from distal locations. For instance, GnRH neurons originate in the olfactory bulb and cross substantial distance to arrive at their final location within the ARC (Wray et al., 1989; Wray, 2002). Moreover, gene expression studies suggest that some Sst neurons migrate to the ARC from an anterior hypothalamic birthplace (Morales-Delgado et al., 2011). We propose that the migration of a Shh responsive cell population into the VMH, albeit from a nearby location, may further explain how cellular diversity is achieved in this nucleus.

Later Shh signaling- maintaining proliferation of progenitor pools

In assessing the requirements of Shh at later stages of hypothalamic development, we observed a dependency on Shh for maintaining tuberal hypothalamic progenitors in a mitotically active state. When Shh signaling was disrupted after E10.5, there were fewer *cSmo* mutant cells in the VMH and DMH due to reduced cell division. Thus, Shh signaling is required to maintain hypothalamic progenitors in a mitotically active state during peak periods of VMH and DMH neurogenesis. These results are consistent with previous findings demonstrating a mitogenic role for Shh in other neurodevelopmental contexts (Rowitch et al., 1999; Wallace, 1999; Wechsler-Reya and Scott, 1999; Fuccillo et al., 2006; Komada et al., 2008).

Non-cell autonomous phenotypes in cSmo mutants due to heightened Shh signaling

Our analysis of *cSmo* embryos also revealed that Shh is required to maintain the subtype identity of postmitotic VMH neurons. Despite the reduced number of Nkx2.2⁺, GFP⁺ neurons in the dorsal VMH of *cSmo* embryos, the total number of VMH neurons was unchanged. Moreover, fewer VMH neurons expressed Nkx2.1, especially in ventral regions where *Smo* was not deleted. We propose a non-cell autonomous mechanism to account for some of these differences in VMH neuron identity, whereby residual Shh ligand that was not taken up by *cSmo* mutant cells signaled to adjacent wild type progenitors, altering their patterns of gene expression and proliferation. In further support of this claim, a similar non-cell autonomous upregulation of Shh signaling was previously described upon the mosaic deletion of *Smo* in the ventral telencephalon (Xu et al., 2010).

Our observation of increased Shh signaling in non-recombined cells from *cSmo* mutant embryos is provocative in light of the association of somatic mutations in regulators of Shh signaling with hypothalamic hamartomas (Craig et al., 2008; Wallace et al., 2008; Hildebrand et al., 2016; Saitsu et al., 2016). Hypothalamic hamartomas are benign tumors that form during fetal brain development and, depending on their size and location, may disrupt endocrine function and cause seizures. Dominant mutations in *GLI3* that produce a truncated protein with constitutive repressor activity were identified in hypothalamic hamartomas (Craig et al., 2008; Wallace et al., 2008; Hildebrand et al., 2016; Saitsu et al., 2016). Individuals with Pallister Hall syndrome possess similar germline truncating mutations in *GLI3* and also develop hypothalamic hamartomas (Kang et al., 1997). Mutations in other components of the SHH signaling pathway, *OFD1* and *PRKRAC* (encoding the catalytic subunit α of PKA), have also been described in resected hamartoma tissue (Hildebrand et al., 2016; Saitsu et al., 2016).

The mechanism of hypothalamic hamartoma formation is unknown. Paradoxically, the mutations that have been described in SHH pathway components are generally thought to inhibit SHH signaling, which, given its mitogenic activity, would be expected to suppress rather than promote the growth of this ectopic mass. Interestingly, the allele rate for somatic mutations in *GLI3* and *OFD1* ranged from 7-54%, suggesting that in some instances only a fraction of the cells in a given hypothalamic hamartoma may actually contain mutations (Saitsu et al., 2016). As with the *cSmo* mutants described in our study, somatic mosaicism in hypothalamic hamartomas may provide wild type cells with a temporary boost in SHH signaling and transient growth advantage, due to reduced ligand uptake by mutant cells that have lost their responsiveness to SHH. While experiments in our study did not extend into postnatal life and may not have

targeted enough cells to induce hypothalamic hamartomas, they do nevertheless offer a compelling explanation for how these ectopic growths might form during brain development.

Materials and Methods

Mice

All animal work was approved by the Institutional Animal Care and Use Committee (IACUC) at the Perelman School of Medicine, University of Pennsylvania. The *SBE2-cre* mouse line was previously described (Zhao, et al., 2012). *Gli1^{CreER}* (*Gli1^{tm3(cre/ERT2)Alj}*), *Gli1^{lacZ}* (*Gli1^{tm2Alj}*), *Rosa^{ZsGreen}* (*Gt(ROSA)26Sor^{tm6(CAG-ZsGreen1)Hze}*), *Shh^{+/-}*, *Shh^{loxp/loxp}* (*Shh^{tm2Amc}*), *Shh^{CreER}* (*Shh^{tm2(cre/ERT2)Cjt}*), *Smo^{+/-}* (*Smo^{tm1Amc}*), and *Smo^{loxp/loxp}* (*Smo^{tm2Amc}*) mouse strains were procured from the Jackson labs (Bar Harbor, ME). Tamoxifen dissolved in corn oil was orally gavaged at 0.15 mg/g body weight to pregnant dams at appropriate developmental time points.

Tissue dissection

Embryos were collected at the stated developmental age, with noon of plug day designated E0.5. Heads were dissected in cold PBS and fixed in 4% paraformaldehyde (PFA) for 90 minutes to overnight at 4°C. Heads were then cryoprotected in 30% sucrose and embedded in Tissue-Tek OCT Compound. Frozen tissue was cryosectioned at 16 µm (for E12.5 and E13.5 embryos), 18 µm (for E14.5 embryos), or 20 µm (for E10.5 and E18.5 embryos).

Immunohistochemistry and section in situ hybridization

Immunohistochemistry was performed with the following antibodies: mouse anti-Ascl1 (1:100 BD Pharmingen, 556604), mouse anti-Gad1 (1:500, EMD Millipore, MAB5406), mouse anti-Isl1 (1:100, Developmental Studies Hybridoma Bank, 39.4D5), rabbit anti-

Ki67 (1:1000, Novocastra. NCL-Ki67p), rabbit anti-Nkx2.1 (1:1000, Abcam, AB76013), mouse anti-Nkx2.2 (1:1000, DSHB, 74.5A5), rabbit anti-Olig2 (1:500, Millipore, AB9610), mouse anti-Pax6 (1:1000, Developmental Studies Hybridoma Bank, Pax6), rabbit anti-POMC (1:500, Phoenix Pharmaceuticals Inc., H-029-30), mouse anti-Nr5a1 (1:200, R&D Systems, PP-N1665), rat anti-Somatostatin (1:200, Millipore, MAB354) rabbit anti-Tyrosine Hydroxylase (1:1000, Pel-Freez, P40101-0). Somatostatin, Pax6, Nkx2.2, Nr5a1, Gad1, and Isl1 antibodies required antigen retrieval in 10mM citric acid buffer pH 6.0 at 90° C. Mouse on Mouse detection kit (Vector Laboratories BMK-2202) was used for blocking and primary antibody dilution of Nkx2.2, Gad1, and Isl1 antibodies. Detection of primary antibodies was achieved using secondary antibodies conjugated to Cy3 anti-rabbit (1:200, 111-165-003, Jackson ImmunoResearch Laboratories), Cy3 anti-mouse (1:200, 115-166-006, Jackson ImmunoResearch Laboratories), Cy3 anti-rat (1:200, 112-166-003, Jackson ImmunoResearch Laboratories) or AlexaFluor 633 anti-rabbit (1:100, Invitrogen, A21070).

Section *in situ* hybridization with digoxigenin-UTP-labeled riboprobes was performed as described (Nissim et al., 2007). A minimum of three each of control and mutant embryos were evaluated for each antibody or *in situ* probe.

β-galactosidase staining

Heads from *Gli1^{lacZ/+}* embryos were dissected in cold PBS and fixed in 4% paraformaldehyde (PFA) for 90 minutes at 4°C. Heads were then cryoprotected in 30% sucrose and embedded in Tissue-Tek OCT Compound. Frozen tissue was cryosectioned at 20 μm. Slides were then stained in a solution containing 1 mg/ml X-gal

at 37°C overnight. Following staining, slides were post-fixed in 4% PFA and washed in PBS.

Quantification and statistical analysis

All cell counts were performed using the cell counter function in ImageJ (NIH) on tissue sections from at least three control and mutant embryos. In cases where double labeling was examined for GFP and another cell specific marker, the tissue was imaged at a single Z-plane. Each channel (green for GFP, red for the marker) was first examined independently, assigning a positive count for a given marker to the DAPI stained nucleus most closely associated with the staining. A cell was only counted as double labeled if a single nucleus marked by DAPI had been assigned to the cell labeled by GFP and the cell specific marker. Statistical analysis of all cell counts was performed in GraphPad Prism using the Student's *t*-test.

Chapter 3 Figures

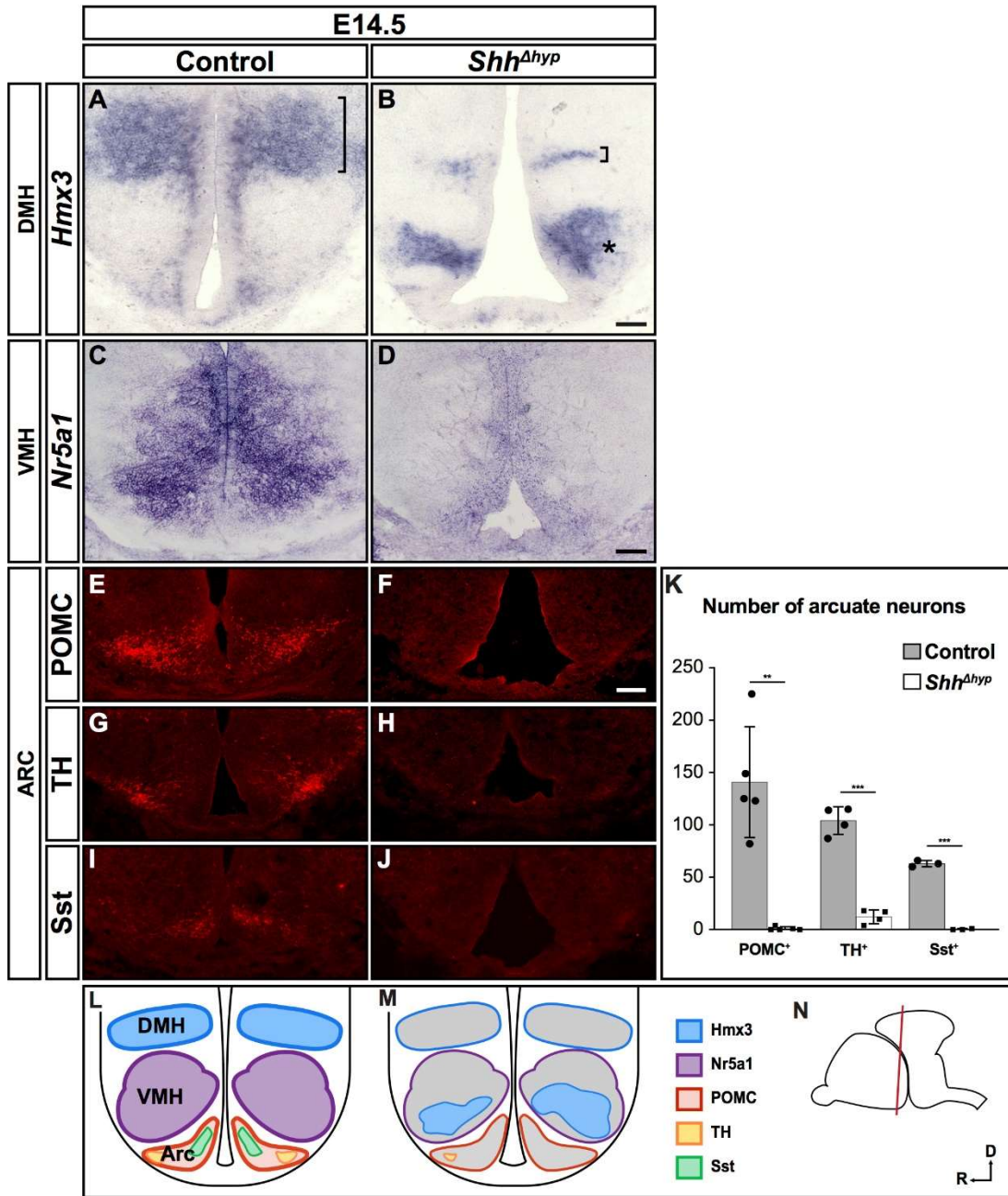


Figure 9. Loss of tuberal hypothalamic neurons in *Shh^{Ahyp}* embryos.

Coronal sections through the tuberal hypothalamus of control and *Shh*^{Δhyp} embryos stained by RNA *in situ* hybridization (A-D) or immunofluorescence (E-J) at E14.5 for neuronal markers. (A,B) *Hmx3* is expressed in the DMH of control embryos, and shows reduced (bracket) and ectopic (asterisk) expression in *Shh*^{Δhyp} mutants (n=3). (C,D) *Nr5a1* marks the VMH in control embryos and is absent in *Shh*^{Δhyp} mutants (n=4). (E-K) Markers of distinct neuronal subtypes in the ARC (POMC, TH, and Sst) are reduced or absent in *Shh*^{Δhyp} mutants (n=5 for POMC, **p=0.0004; n=4 for TH, ***p<0.0001; n= 3 for Sst, ***p<0.0001). (L,M) Schematic of coronal sections through the tuberal hypothalamus of control and *Shh*^{Δhyp} embryos showing nuclei and cell type specific markers. (N) Sagittal view of brain showing plane of section (red line) in (L-M). Scale bars: 100 μm. Error bars indicate S.D. Statistical analysis was performed using a two-tailed unpaired *t*-test.

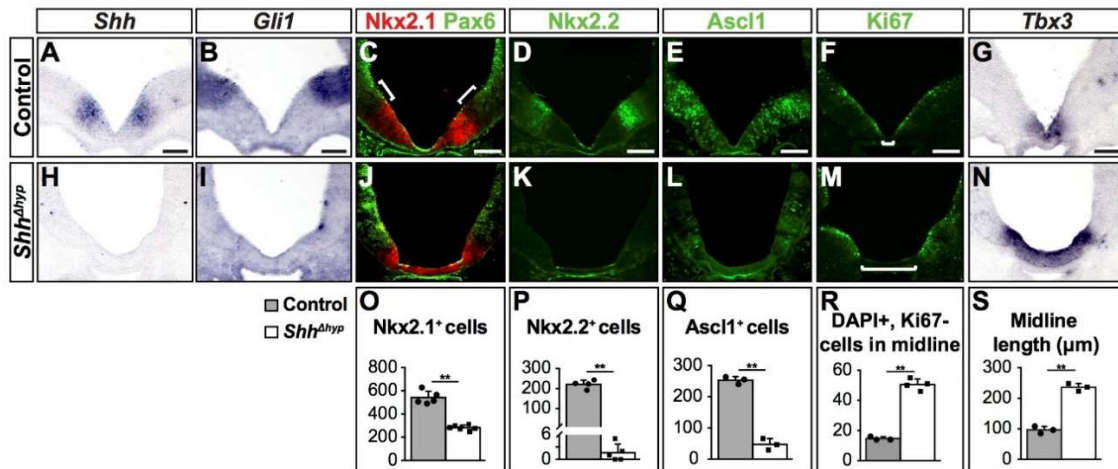


Figure 10. Altered dorsoventral patterning, neurogenesis, and ventral midline development in *Shh*^{Δhyp} embryos.

Coronal sections through control and *Shh*^{Δhyp} embryos stained by RNA *in situ* hybridization (A,B,G-I,N) or immunofluorescence (C-F,J-M) at E10.5. (A,H) *Shh* expression in the prospective tuberal hypothalamus is lost in *Shh*^{Δhyp} mutants (n=3). (B,I) *Gli1* expression in neuronal progenitors immediately dorsal to *Shh* is absent in *Shh*^{Δhyp} mutants (n=3). (C,J,O) Ventral hypothalamic expression of *Nkx2.1* is reduced in *Shh*^{Δhyp} mutants (n=5 for controls, n=6 for *Shh*^{Δhyp}), whereas *Pax6* is expanded ventrally. Note the gap between *Nkx2.1* and *Pax6* (white bracket) in control embryos is missing in *Shh*^{Δhyp} mutants. (D,K,P) *Nkx2.2* expression in *Shh* responsive tuberal hypothalamic progenitors is greatly reduced in *Shh*^{Δhyp} mutants (n=4 for controls, n=5 for *Shh*^{Δhyp}). (E,L,Q) *Ascl1* expression in neurogenic progenitors is reduced in *Shh*^{Δhyp} mutants (n=3). (F,M,R) The number of non-proliferating ventral midline cells identified by the absence of *Ki67* staining is expanded in *Shh*^{Δhyp} mutants (n=4). (G,N,S) The expression of *Tbx3* in the ventral midline is expanded in *Shh*^{Δhyp} mutants (n=3). Scale bars: 100 μm. Error

bars indicate S.D. Statistical analysis was performed using a two-tailed unpaired *t*-test (** $p < 0.0001$).

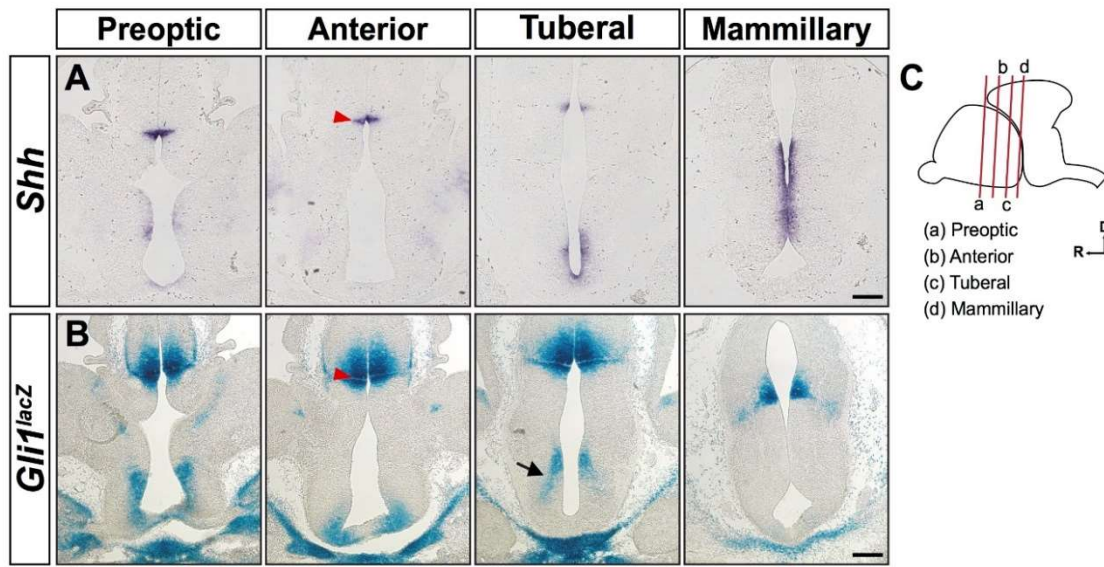
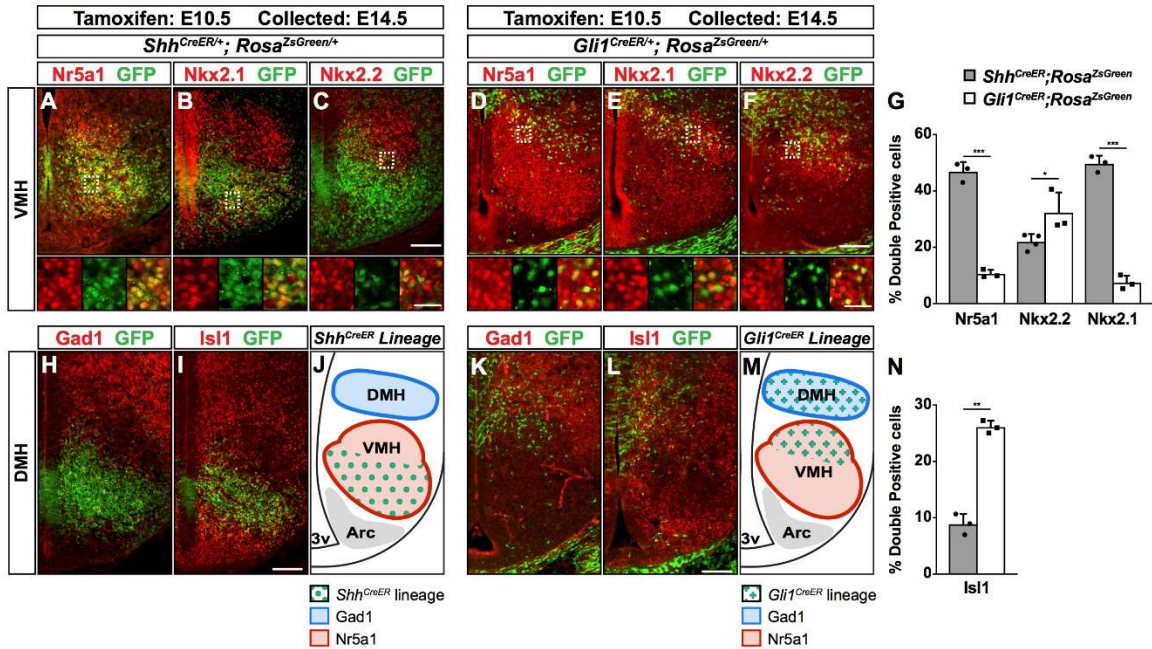


Figure 11. Persistence of *Shh* signaling during peak periods of hypothalamic neurogenesis.

Coronal sections through the hypothalamus of (A) wild type and (B) *Gli1^{lacZ/+}* embryos at E12.5. (A) RNA *in situ* hybridization detects *Shh* expression along the rostrocaudal axis of the hypothalamus. Weak *Shh* expression is detected in the ventral midline at preoptic and anterior hypothalamic regions. *Shh* expression is maintained in hypothalamic progenitors adjacent to the ventral midline in tuberal and mammillary regions. *Shh* is also observed in the zona limitans intrathalamica (red arrowhead) in the caudal diencephalon. (B) X-gal staining of *Gli1^{lacZ}* embryos along the rostrocaudal axis of the hypothalamus. X-gal staining is detected adjacent to *Shh* expressing domains throughout the hypothalamus. At the level of the tuberal hypothalamus, X-gal staining marks progenitors of the DMH and a population of cells that stream ventrally towards the VMH (arrows). Scale bars: 200 μ m.



S.D. Statistical analysis was performed using a two-tailed unpaired *t*-test on arcsin-transformed data.

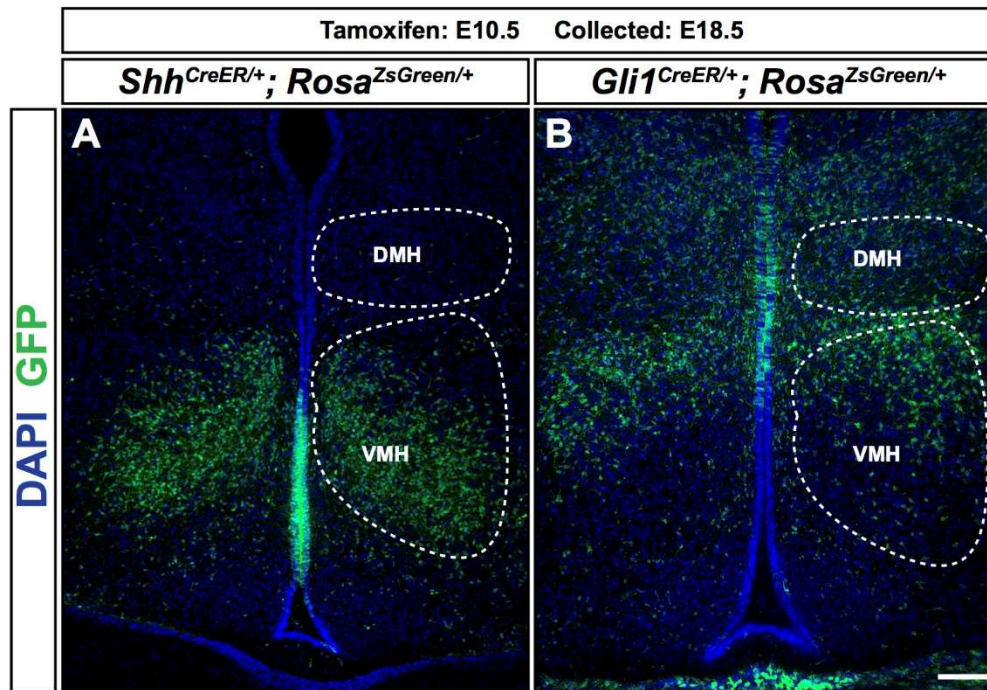


Figure 13. *Shh* and *Gli1* lineages occupy distinct regions of the VMH.

Coronal sections through the tuberal hypothalamus of (A) *Shh*^{CreER/+}; *Rosa*^{ZsGreen/+} and (B) *Gli1*^{CreER/+}; *Rosa*^{ZsGreen/+} embryos at E18.5 that received tamoxifen at E10.5. GFP (ZsGreen) fluorescence is shown on sections counterstained with DAPI. (A) Cells that expressed *Shh* at E10.5, contribute to the ventral and central regions of the VMH at E18.5. (B) Cells that expressed *Gli1* at E10.5, contribute to the DMH and dorsal region of the VMH at E18.5. Scale bar: 100 μ m. White dashed lines outline tuberal hypothalamic nuclei.

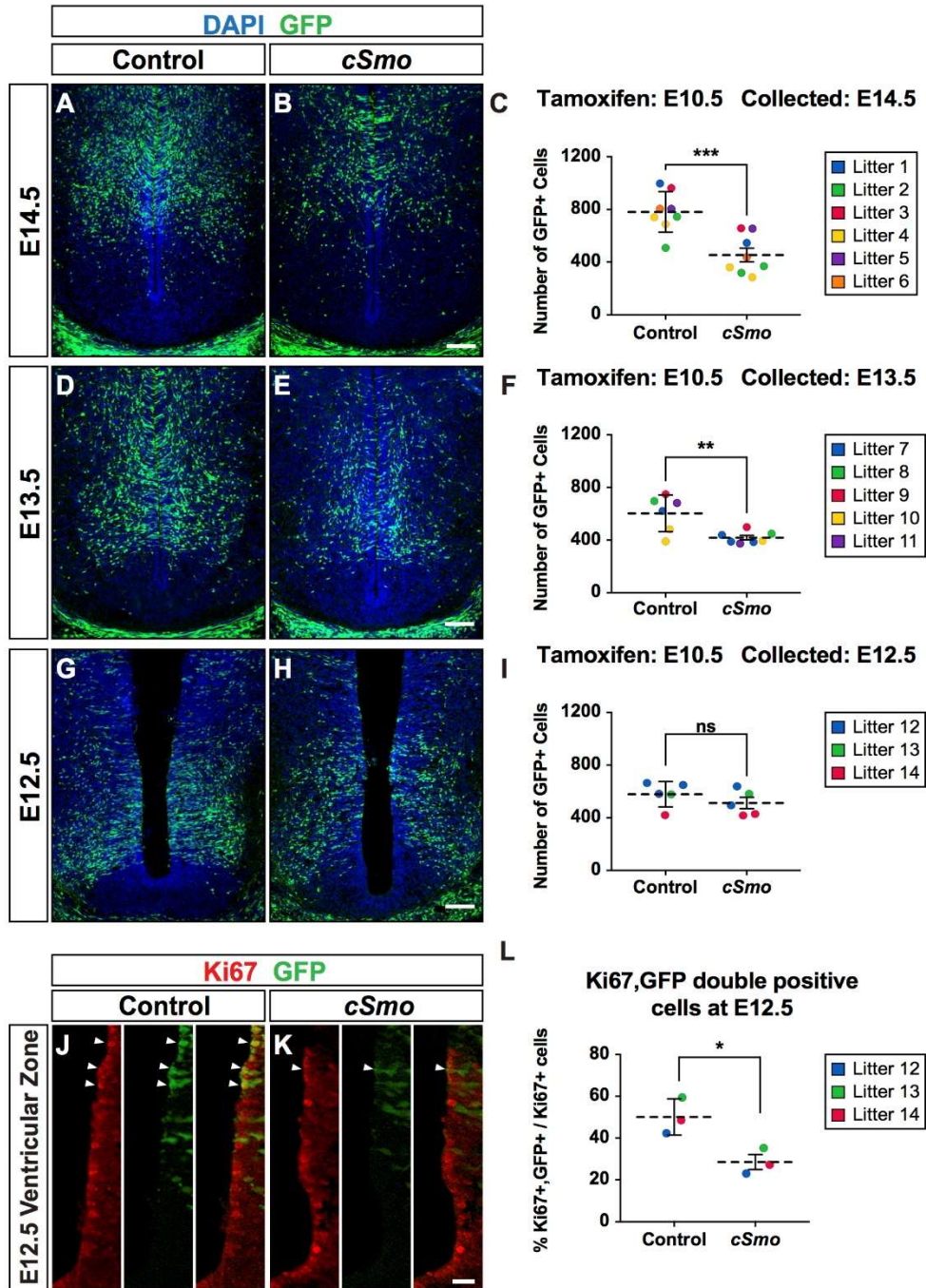


Figure 14. Shh signaling is required for proliferation of tuberal hypothalamic progenitors.

Coronal sections through the tuberal hypothalamus of control and *cSmo* embryos at E14.5 (A,B), E13.5 (D,E), and E12.5 (G,H,J,K) that received tamoxifen at E10.5. (A-H) GFP (ZsGreen) fluorescence is shown on sections counterstained with DAPI. (C,F,I) Quantification of GFP positive cells from *cSmo* and control embryos tracked by litter. (J-K) Co-labeling of GFP and Ki67 expressing cells (arrowhead) in the ventricular zone reveals less proliferation in *cSmo* embryos at E12.5, as quantified in (L). Scale bars: (A-H) 100 μm (J-K) 25 μm . For all graphs, horizontal dotted line represents the mean and error bars indicate S.D. Each data point represents a single embryo that is color-coded by litter. Statistical analysis was performed using a two-tailed unpaired *t*-test (** $p=0.0003$, ** $p=0.0066$, * $p=0.0249$).

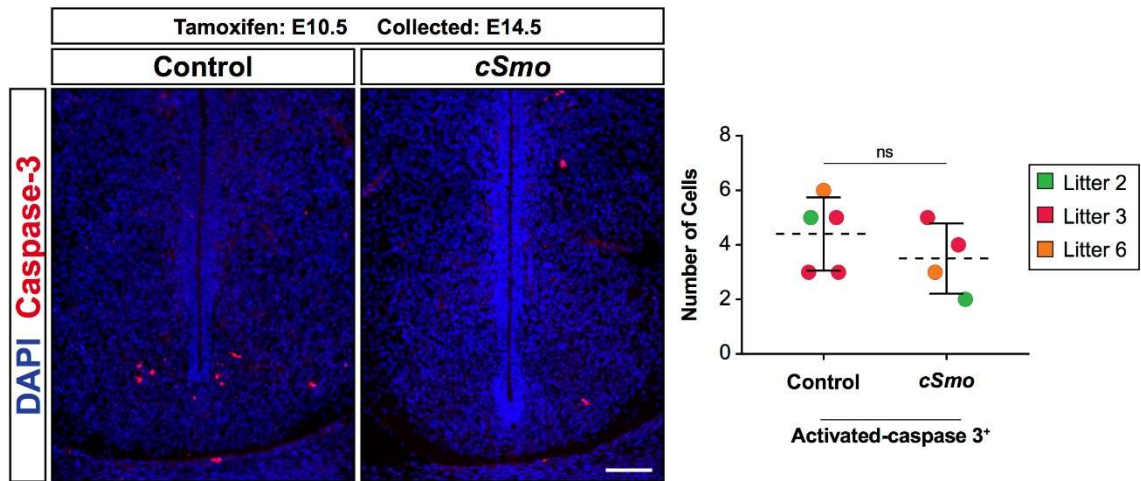


Figure 15. No differences in cell death between control and *cSmo* embryos.

Coronal sections of control and *cSmo* embryos at E14.5 that received tamoxifen at E10.5. Immunostaining for activated caspase-3 counterstained with DAPI reveals no differences in apoptosis between control and *cSmo* embryos (control $n=5$, 4.4 ± 1.3 ; *cSmo* $n=4$, 3.5 ± 1.3 ; $p>0.05$). Each data point represents a single embryo color-coded by litter. Scale bars: 100 μm . Statistical analysis was performed using a two-tailed unpaired *t*-test.

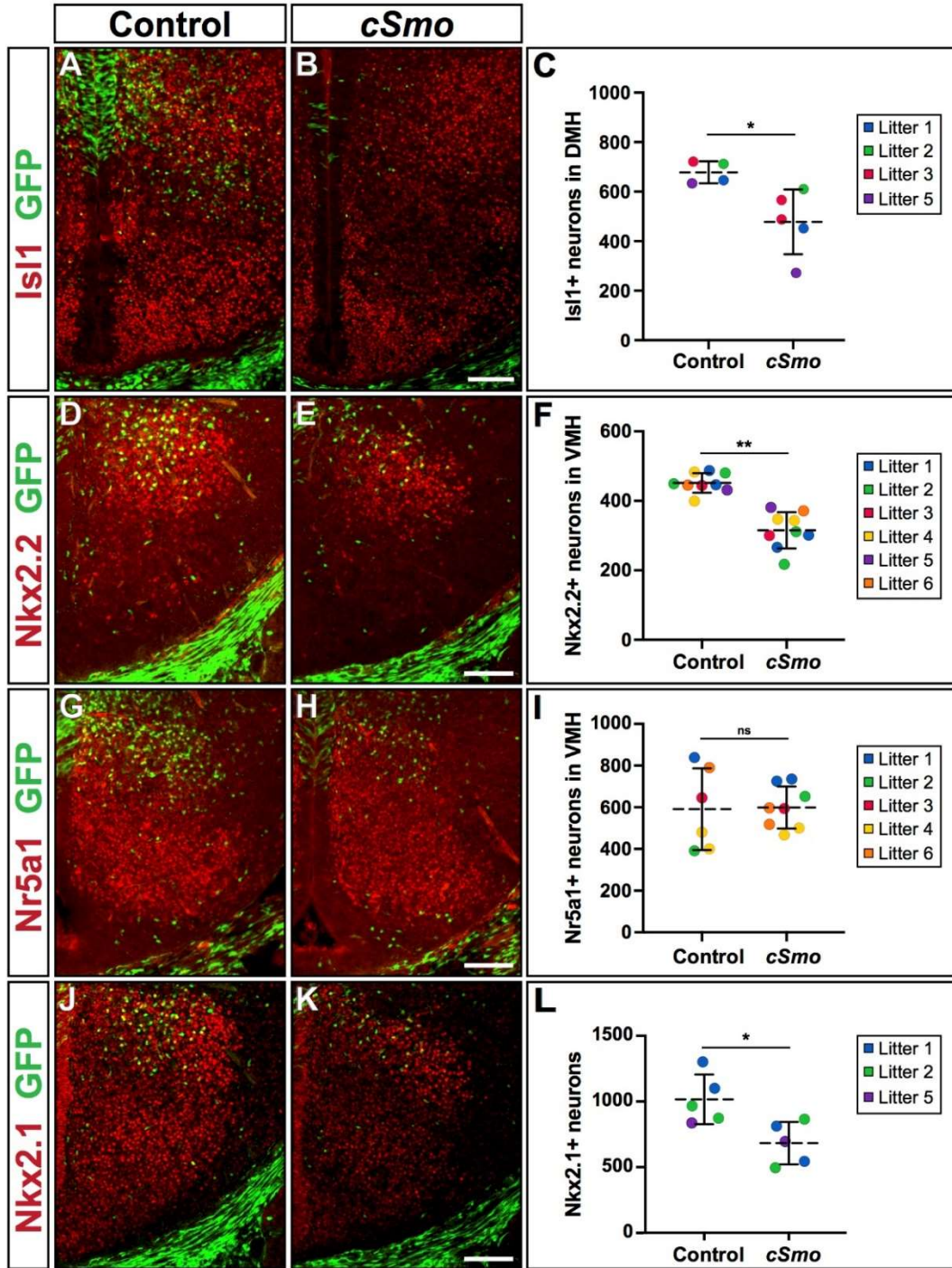


Figure 16. Shh signaling is required for subtype identity of VMH and DMH neurons.

Coronal sections through the tuberal hypothalamus of control and *cSmo* embryos at E14.5 that received tamoxifen at E10.5. (A-C) The number of cells expressing *Isl1* in the DMH is reduced in *cSmo* embryos (control n=4, *cSmo* n= 5, *p=0.0229). (D-F) The number of post mitotic neurons expressing *Nkx2.2* in the dorsal VMH is reduced in *cSmo* embryos compared to control littermates (n=9, **p<0.0001). (G-I) The number of VMH neurons expressing *Nr5a1* is equivalent between control and *cSmo* embryos (control n=6, *cSmo* n= 8, ns p>0.05). (J-L) The number of post-mitotic neurons expressing *Nkx2.1* in the tuberal hypothalamus is reduced in *cSmo* embryos (n=5, *p=0.0174). For all graphs, horizontal dotted line represents the mean and error bars indicate S.D. Each data point represents a single embryo that is color-coded by litter. Statistical analysis was performed using a two-tailed unpaired *t*-test.

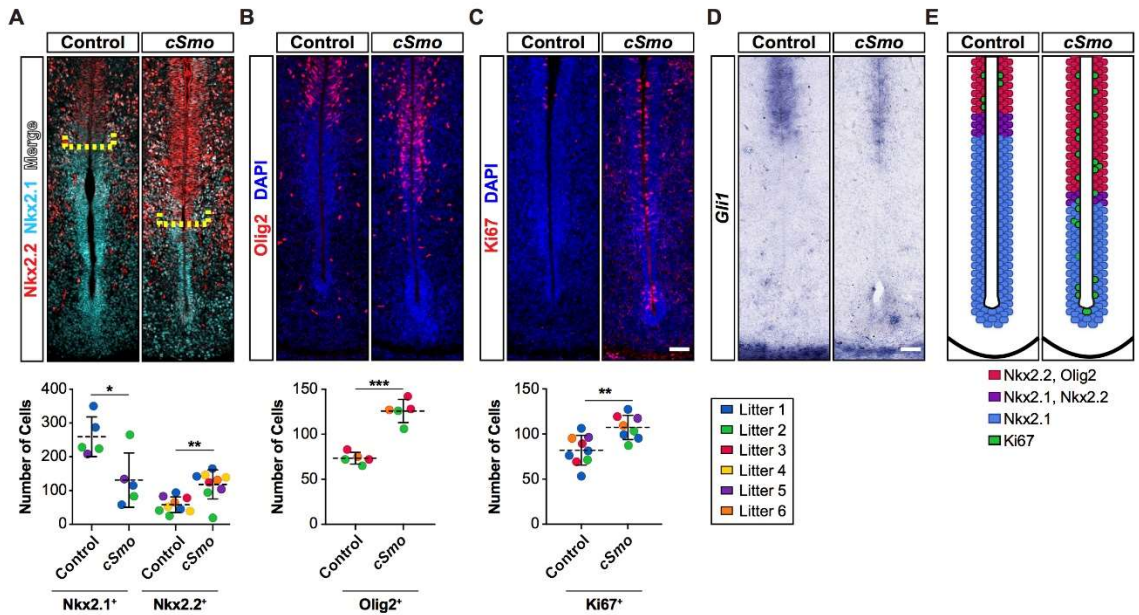


Figure 17. Non-cell autonomous alterations in hypothalamic progenitors in *cSmo* embryos.

Coronal sections through the tuberal hypothalamus of control and *cSmo* embryos at E14.5 (tamoxifen administered at E10.5). (A) The boundary between Nkx2.1 and Nkx2.2 expressing progenitors (yellow bracket) is shifted ventrally in the ventricular zone of *cSmo* embryos compared to control littermates. The ventral expansion of Nkx2.2 expressing progenitors (n=9, **p=0.002) is concomitant with a reduction in the number of cells expressing Nkx2.1 (n=5, *p=0.0205). (B) Olig2 is ectopically expressed in ventral tuberal hypothalamic progenitors in *cSmo* embryos compared to control littermates (n=5, ***p<0.0001). (C) Ki67 is ectopically expressed in ventral tuberal hypothalamic progenitors in *cSmo* embryos compared to control littermates (control n=9, *cSmo* n=8, **p=0.0037). (D) *Gli1* expression is unchanged between control and *cSmo* embryos (n=3). (E) Schematic model depicting the non-cell autonomous gain in Shh

responsiveness by ventral tuberal hypothalamic progenitors in *cSmo* mutant embryos compared to control littermates. For all graphs, horizontal dotted line represents the mean and error bars indicate S.D. Each data point represents a single embryo that is color-coded by litter. Statistical analysis was performed using a two-tailed unpaired *t*-test. Scale bars: 50 μ m.

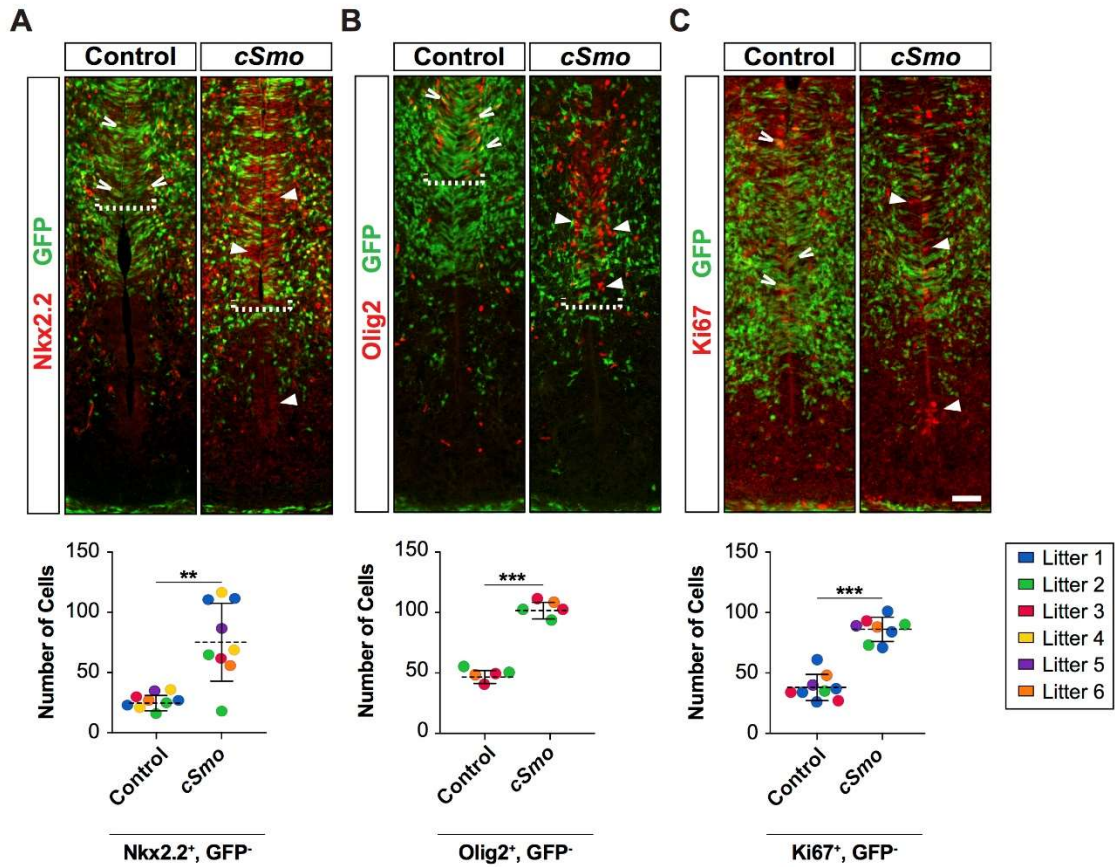


Figure 18. *cSmo* embryos show ectopic activation of Shh responsive genes in non-recombined (wild type) cells.

Coronal sections through the tuberal hypothalamus of control and *cSmo* embryos at E14.5 (tamoxifen administered at E10.5). Shh responsive progenitors in control embryos frequently co-label with GFP and Nkx2.2, Olig2, or Ki67 (open arrowhead). The majority of progenitors in *cSmo* embryos showing ectopic expression of Nkx2.2, Olig2, or Ki67 do not co-label with GFP (closed arrowheads), suggesting that they derive from non-recombined (wild type) cells. (A,B) The ventral boundary of Nkx2.2 and Olig2 expression (white dotted bracket) is shifted ventrally in *cSmo* embryos. The same images are shown

in Figure 6 without the GFP overlay. For all graphs, horizontal dotted line represents the mean and error bars indicate S.D. Each data point represents a single embryo that is color-coded by litter. Statistical analysis was performed using a two-tailed unpaired *t*-test (** $p=0.0003$, *** $p<0.0001$). Scale bar: 50 μm .

CHAPTER 4: Conclusions and Future Directions

One of the foremost questions in the field of developmental biology is how the limited molecular toolkit encoded in the genome is used iteratively to give rise to complex structures composed of heterogeneous cell types. The hypothalamus has been extensively studied for that very reason. Though it is derived from the neural tube in the same manner as other structures of the central nervous system, the hypothalamus requires precise temporal regulation of Shh expression and signaling domains for proper development.

Distinct roles for Shh in the hypothalamus:

Previous studies have identified requirements for Shh at distinct spatial and temporal points in hypothalamic development, from early induction to nucleogenesis (Chiang et al., 1996; Szabó et al., 2009; Shimogori et al., 2010; Zhao et al., 2012). In addition to providing an atlas of hypothalamic gene expression, Shimogori and colleagues also hinted at requirements for the hypothalamic source of Shh. Using an *Nkx2.1-Cre* line to delete Shh, they found a profound disruption of hypothalamic nuclei and loss of gene expression along the rostrocaudal axis (Shimogori et al., 2010). However, this work was descriptive in nature and any mechanism underlying the loss of hypothalamic populations was not suggested. Further studies of roles for Shh and its corresponding signaling activity in the hypothalamus soon followed. In 2012, Alvarez-Bolado and colleagues further described the dynamic pattern of Shh expression in the developing hypothalamus (Alvarez-Bolado, et al., 2012). Using genetic inducible fate mapping techniques driven by the *Shh^{CreER}* mouse line, they uncovered the contribution

of Shh expressing cells and their progeny to the hypothalamic territories. They found cells expressing Shh before E9.5 give rise to neurons and astrocytes populating the preoptic, tuberal, and mammillary hypothalamus. Later induction time points, in contrast, resulted in progressively smaller contributions to the preoptic and mammillary hypothalamus. The tuberal hypothalamus saw a steady contribution of Shh-expressing cells at the level of the VMH during the remainder of neurogenesis (Alvarez-Bolado, et al., 2012). Previous work from our lab described a requirement for early Shh in establishing proper patterning of the hypothalamus along the anteroposterior axis and for proper placement and specification of the pituitary (Zhao, et al., 2012).

The work presented in the preceding chapters serves to further characterize the phenotypic consequences and pathogenic mechanisms attributed to the loss of Shh signaling at early (E9.0) and late (after E10.5) stages of hypothalamic development. We determine that the loss of hypothalamic nuclei in cases where Shh is deleted at early time points results from additional requirements for Shh in establishing proper dorsoventral patterning, neurogenesis, and limiting the expansion of the non-proliferative ventral midline. Using an inducible and conditional approach, we then characterize requirements for later Shh activity, at time points after dorsoventral patterning has been established. We find that Shh is necessary to maintain proliferation and subtype identity of VMH and DMH progenitors during peak periods of hypothalamic neurogenesis. Later, Shh acts as a mitogen to ensure proper proliferation and expansion of progenitors to give rise to the full complement of tuberal hypothalamic neurons.

Shh-expressing cells in the hypothalamus are unique:

Our analysis of *Shh*^{Δhyp} mutants revealed an unexpected phenotype within the ventral midline of the hypothalamus. In *Shh*^{Δhyp} mutants, we observed an expansion of midline identity. This potential role for Shh in restricting ventral midline development in the tuberal hypothalamus is intriguing given the function associated with Shh in more posterior regions of the CNS where Shh promotes floor plate identity in the (Echelard et al., 1993; Roelink et al., 1995; Martí et al., 1995; Ericson et al., 1996; Chiang et al., 1996). We hypothesized that this distinct role of Shh in limiting the ventral midline may be in part due to the different nature of midline cells at this level. At more posterior levels of the central nervous system in mammals, floor plate cells of the spinal cord are considered glial-like but do not give rise to neurons or glia. However, the specialized tanycyte glial cells in the hypothalamic midline connects the hypothalamus to the pituitary gland and regulate a variety of homeostatic processes given their access to blood borne signals (Rodríguez et al., 2005; Robins et al., 2013; Bolborea and Dale, 2013). Additionally, the fact that the hypothalamic ventral midline is a site of integration for multiple signaling pathways, including Shh, Bmp, Wnt and Fgf may explain a different role for Shh in the midline cells at this level (Gouti et al., 2015; Kong et al., 2015).

Perhaps the most striking difference of the hypothalamus is that the Shh expressing cells in the hypothalamus are different from elsewhere in the neural tube in that they constitute actively dividing neuronal progenitors (Szabó et al., 2009). Within the spinal cord, Shh expressing floor plate cells lack neurogenic properties. Further highlighting this unique feature of neurogenic progenitors expressing Shh is that in the neurogenic midline of the midbrain, progenitors must extinguish Shh expression (Bayly

et al., 2007; Joksimovic et al., 2009; Joksimovic et al., 2009b; Perez-Balaguer et al., 2009).

Heterogeneity of hypothalamic neurons:

The developmental mechanisms regulating the vast neuronal heterogeneity within the hypothalamus remains poorly understood compared to other regions of the central nervous system (Bedont et al., 2015; Burbridge et al., 2016; Xie and Dorsky, 2017). In fact, the extent of that heterogeneity is still being realized. In a seminal paper, Shimogori and colleagues used high throughput techniques to catalog gene expression of the developing hypothalamus (Shimogori, et al., 2010). Hypothalamic tissue was collected from brains at each day of development beginning in mid-gestation (E10.5) as well as early postnatal and adult stages. Microarray experiments on this panel of tissue highlighted subsets of genes expressed during development as well as those that became markers of mature neuron populations. Further, these authors went on to perform large-scale *in situ* hybridization analysis to describe the general and/or region-specific expression patterns of transcription factors and neuropeptides at different time points of hypothalamic development. The advent of single-cell techniques including Drop-Seq have also proved useful in further characterizing the diversity of cell types in the tuberal hypothalamus (Campbell et al., 2017).

The work presented in Chapter 3 of this work serves to uncover some of the factors that may act along the differentiation pathways of subpopulations within the VMH. Of note we find the dorsomedial VMH population of neurons which are marked by post-mitotic expression of Nkx2.2 are likely derived from a Shh-responsive population. Gene expression analysis of adult hypothalamic tissue suggests these dorsomedial VMH

neurons include a leptin receptor expressing population implicated in mediating effects on body weight (Dhillon et al., 2006; Kurrasch et al., 2007) However, this population of Nkx2.2 expressing cells has been minimally described in the literature. Additional experiments are necessary to identify requirements for Shh signaling within these compartments as well as other factors that may further define them.

Furthermore, experiments beyond the scope of the work presented here could address the lineage of adult neuronal populations in the tuberal hypothalamus. As fate mapping experiments using the *Gli1^{CreER}* and *Shh^{CreER}* mouse lines were carried out as late as E18.5, we have yet to track the fate of these lineages in the adult hypothalamus. The expression of numerous markers of mature hypothalamic cell types and active neurons are difficult to assess at embryonic time points. Thus, carrying these experiments into early and later postnatal life would allow for the examination of a larger set of gene expression markers.

Mosaic nature of Hh deletion:

The experiments presented in Chapter 3 made use of inducible and conditional approaches to attenuate Hh signaling in mice. These approaches targeted the obligate transducer of the Hh pathway, Smo in a Hh-signaling dependent manner. Thus, our approach allowed for the disruption of further Hh signaling only in those cells which were already Hh responsive. Ideally, additional experiments would be performed using complementary approach in which the ligand of the pathway is deleted. However, because we took this experimental approach, we were able to take advantage of the mosaic nature of conditional *Smo* deletion. This allowed for the unique opportunity to

observe both recombined and non-recombined cells within the context of a single animal.

In fact, we observed hyperproliferation of non-recombined cells in a tamoxifen-treated animal. Furthermore, we saw increased Nkx2.2 and Olig2 expression in the ventricular zone of *cSmo* animals. This is of interest for two reasons. First, Nkx2.2 is a direct transcriptional target of Shh signaling while Olig2 is known to be induced following high levels of Shh signaling. Second, the cells which ectopically expressed Nkx2.2 and Olig2 were large, negative for our marker of recombination (ZsGreen). This is indicative of wild type cells experiencing higher levels of Shh signaling in *cSmo* mutant embryos.

It is possible that the lack of ligand uptake by *cSmo* cells allows for inappropriate spreading of ligand to cells that would normally not respond to Shh. This is not the first example of a mosaic deletion of *Smo* resulting in ectopic activation of the Shh signaling pathway in normally non-responsive cells. In one such example, neighbors of MGE cells which have been made refractory to Shh signaling through *Six3-Cre* mediated deletion of *Smo* exhibited surprising upregulation of Shh pathway targets and compensated for a loss of mutant-derived somatostatin expressing neurons (Xu et al., 2010). An additional explanation for the ectopic Hh signaling observed in *cSmo* animals is that targeted cells may fail to properly express secreted inhibitors of the Shh signaling pathway. At present, we can not rule out the possibility that *cSmo* cells may fail to express secreted inhibitors that would normally limit signaling. In this

As stated in Chapter 3, the observed phenotype of our *cSmo* mice which may display an increase of Shh signaling output in non-recombined cells was reminiscent of a human condition in which patients harbor mutations in regulators of the Hedgehog

pathway. In sporadic cases of Pallister Hall Syndrome with hypothalamic hamartomas (HH), truncating mutations in or loss of heterozygosity at the genomic region surrounding *Gli3* are often seen as the causative genetic factors. Known mutations cluster near the DNA-binding and transactivation domains of Gli3 to produce a truncated protein, which acts as a constitutive repressor of Hh signaling (Craig et al., 2008; Démurger et al., 2015; Saitsu et al., 2016). Mutations in additional negative regulators of the Hh signaling pathway, *OFD1* and *PRKRAC* (encoding the catalytic subunit α of PKA), have also been described in resected HH tissue (Hildebrand et al., 2016; Saitsu et al., 2016).

One of the prevailing models in the study of HH is that neighboring cells not harboring the mutations are exposed to higher levels of Shh signaling due to a lack of ligand uptake. While the experiments within the scope of our study did not extend into postnatal life and may not have targeted enough cells sufficient to induce HH, the similarity of non-cell autonomous phenotypes observed here in cases of mosaic recombination of *Smo* and those present in HH is intriguing. Though HH can be comprised of predominantly neurons or glia, our observation of ectopic *Olig2* expression in *cSmo* mutants may indicate bias towards giving rise to a glial HH (Coons et al., 2007). Previous attempts to establish mouse models of HH have not been fruitful. Future study using this particular genetic model may prove useful as a mouse model of HH.

BIBLIOGRAPHY

- Ahlgren S. C., Thakur V. and Bronner-Fraser M.** (2002). Sonic hedgehog rescues cranial neural crest from cell death induced by ethanol exposure. *Proc. Natl. Acad. Sci. USA* 99, 10476-10481.
- Allen, B.L., Tenzen, T., and McMahon, A.P.** (2007). The Hedgehog-binding proteins Gas1 and Cdo cooperate to positively regulate Shh signaling during mouse development. *Genes Dev.* 21, 1244–1257.
- Allen B. L., Song J. Y., Izzi L., Althaus I. W., Kang J.-S., Charron F., Krauss R. S. and McMahon A. P.** (2011). Overlapping roles and collective requirement for the coreceptors GAS1, CDO, and BOC in SHH pathway function. *Dev. Cell* 20, 775-787.
- Altman, J. and Bayer, S. A.** (1986). The development of the rat hypothalamus. *Adv Anat Embryol Cell Biol* 100, 1–178.
- Alvarez-Bolado, G., Paul, F. A. and Blaess, S.** (2012). Sonic hedgehog lineage in the mouse hypothalamus: from progenitor domains to hypothalamic regions. *Neural Dev* 7, 4.
- Aoto K., Shikata Y., Higashiyama D., Shiota K. and Motoyama J.** (2008). Fetal ethanol exposure activates protein kinase A and impairs Shh expression in prechordal mesendoderm cells in the pathogenesis of holoprosencephaly. *Birth Defects Res. A Clin. Mol. Teratol.* 82, 224-231.
- Ashwell K. W. S. and Zhang L.-L.** (1994). Optic nerve hypoplasia in an acute exposure model of the fetal alcohol syndrome. *Neurotoxicol. Teratol.* 16, 161-167.
- Balaskas, N., Ribeiro, A., Panovska, J., Dessaud, E., Sasai, N., Page, K. M., Briscoe, J. and Ribes, V.** (2012). Gene regulatory logic for reading the Sonic Hedgehog signaling gradient in the vertebrate neural tube. *Cell* 148, 273–284.
- Balthasar, N., Coppari, R., McMinn, J., Liu, S. M., Lee, C. E., Tang, V., Kenny, C. D., McGovern, R. A., Chua, S. C., Elmquist, J. K., et al.** (2004). Leptin receptor signaling in POMC neurons is required for normal body weight homeostasis. *Neuron* 42, 983–991.
- Bedont, J. L., Newman, E. A. and Blackshaw, S.** (2015). Patterning, specification, and differentiation in the developing hypothalamus. *Wiley Interdiscip Rev Dev Biol* 4, 445–468.
- Blader P. and Strähle U.** (1998). Ethanol impairs migration of the prechordal plate in the zebrafish embryo. *Dev. Biol.* 201, 185-201.
- Bolborea, M. and Dale, N.** (2013). Hypothalamic tanycytes: potential roles in the control of feeding and energy balance. *Trends in Neurosciences* 36, 91–100.

- Briscoe, J. and Ericson, J.** (1999). The specification of neuronal identity by graded Sonic Hedgehog signalling. *Semin Cell Dev Biol* 10, 353–62.
- Briscoe, J., Pierani, A., Jessell, T. M. and Ericson, J.** (2000). A homeodomain protein code specifies progenitor cell identity and neuronal fate in the ventral neural tube. *Cell* 101, 435–445.
- Briscoe, J. and Ericson, J.** (2001). Specification of neuronal fates in the ventral neural tube. *Curr. Opin. Neurobiol.* 11, 43–49.
- Brzezinski J. A. IV, Prasov L. and Glaser T.** (2012). Math5 defines the ganglion cell competence state in a subpopulation of retinal progenitor cells exiting the cell cycle. *Dev. Biol.* 365, 395-413.
- Büdefeld, T., Tobet, S. A. and Majdic, G.** (2011). Altered position of cell bodies and fibers in the ventromedial region in SF-1 knockout mice. *Experimental Neurology* 232, 176–184.
- Bumcrot, D.A., Takada, R., and McMahon, A.P.** (1995). Proteolytic processing yields two secreted forms of sonic hedgehog. *Mol. Cell. Biol.* 15, 2294–2303.
- Burbridge, S., Stewart, I. and Placzek, M.** (2016). Development of the Neuroendocrine Hypothalamus. *Compr Physiol* 6, 623–643.
- Campbell, J. N., Macosko, E. Z., Fenselau, H., Pers, T. H., Lyubetskaya, A., Tenen, D., Goldman, M., Verstegen, A. M. J., Resch, J. M., McCarroll, S. A., et al.** (2017). A molecular census of arcuate hypothalamus and median eminence cell types. *Nature Neuroscience* 20, 484.
- Caqueret, A., Boucher, F. and Michaud, J. L.** (2006). Laminar organization of the early developing anterior hypothalamus. *Dev. Biol.* 298, 95–106.
- Cardozo M. J., Sánchez-Arrones L., Sandonis A., Sánchez-Camacho C., Gestri G., Wilson S. W., Guerrero I. and Bovolenta P.** (2014). Cdon acts as a Hedgehog decoy receptor during proximal-distal patterning of the optic vesicle. *Nat. Commun.* 5, 4272
- Carreno, G., Apps, J. R., Lodge, E. J., Panousopoulos, L., Haston, S., Gonzalez-Meljem, J. M., Hahn, H., Andoniadou, C. L. and Martinez-Barbera, J. P.** (2017). Hypothalamic sonic hedgehog is required for cell specification and proliferation of LHX3/LHX4 pituitary embryonic precursors. *Development* 144, 3289–3302.
- Cemeroglu A. P., Coulas T. and Kleis L.** (2015). Spectrum of clinical presentations and endocrinological findings of patients with septo-optic dysplasia: a retrospective study. *J. Pediatr. Endocrinol. Metab.* 28, 1057-1063.
- Cheung, C. C., Kurrasch, D. M., Liang, J. K. and Ingraham, H. A.** (2013). Genetic labeling of steroidogenic factor-1 (SF-1) neurons in mice reveals ventromedial nucleus of

the hypothalamus (VMH) circuitry beginning at neurogenesis and development of a separate non-SF-1 neuronal cluster in the ventrolateral VMH. *J. Comp. Neurol.* 521, 1268–1288.

Chiang, C., Litingtung, Y., Lee, E., Young, K., Corden, J., Westphal, H. and Beachy, P. (1996). Cyclopia and defective axial patterning in mice lacking Sonic hedgehog gene function. *Nature* 383, 407–13.

Christ, A., Christa, A., Kur, E., Lioubinski, O., Bachmann, S., Willnow, T. E. and Hammes, A. (2012). LRP2 is an auxiliary SHH receptor required to condition the forebrain ventral midline for inductive signals. *Dev. Cell* 22, 268–278.

Cole F. and Krauss R. S. (2003). Microform holoprosencephaly in mice that lack the Ig superfamily member Cdon. *Curr. Biol.* 13, 411-415.

Correa, S. M., Newstrom, D. W., Warne, J. P., Flandin, P., Cheung, C. C., Lin-Moore, A. T., Pierce, A. A., Xu, A. W., Rubenstein, J. L. and Ingraham, H. A. (2015). An Estrogen-Responsive Module in the Ventromedial Hypothalamus Selectively Drives Sex-Specific Activity in Females. *Cell Reports* 10, 62–74.

Coulter C. L., Leech R. W., Schaefer G. B., Scheithauer B. W. and Brumback R. A. (1993). Midline cerebral dysgenesis, dysfunction of the hypothalamic-pituitary axis, and fetal alcohol effects. *Arch. Neurol.* 50, 771-775.

Craig, D. W., Itty, A., Panganiban, C., Szelinger, S., Kruer, M. C., Sekar, A., Reiman, D., Narayanan, V., Stephan, D. A. and Kerrigan, J. F. (2008). Identification of somatic chromosomal abnormalities in hypothalamic hamartoma tissue at the GLI3 locus. *Am. J. Hum. Genet.* 82, 366–374.

Dale, J. K., Vesque, C., Lints, T. J., Sampath, T. K., Furley, A., Dodd, J. and Placzek, M. (1997). Cooperation of BMP7 and SHH in the induction of forebrain ventral midline cells by prechordal mesoderm. *Cell* 90, 257–269.

Dakubo G. D., Wang Y. P., Mazerolle C., Campsall K., McMahon A. P. and Wallace V. A. (2003). Retinal ganglion cell-derived sonic hedgehog signaling is required for optic disc and stalk neuroepithelial cell development. *Development* 130, 2967-2980.

Davis, A. M., Seney, M. L., Stallings, N. R., Zhao, L., Parker, K. L. and Tobet, S. A. (2004). Loss of steroidogenic factor 1 alters cellular topography in the mouse ventromedial nucleus of the hypothalamus. *J. Neurobiol.* 60, 424–436.

Davis, S. W. and Camper, S. A. (2007). Noggin regulates Bmp4 activity during pituitary induction. *Dev. Biol.* 305, 145–160.

Deiner M. S., Kennedy T. E., Fazeli A., Serafini T., Tessier-Lavigne M. and Sretavan D. W. (1997). Netrin-1 and DCC mediate axon guidance locally at the optic disc: loss of function leads to optic nerve hypoplasia. *Neuron* 19, 575-589.

Dhillon, H., Zigman, J. M., Ye, C., Lee, C. E., McGovern, R. A., Tang, V., Kenny, C. D., Christiansen, L. M., White, R. D., Edelman, E. A., et al. (2006). Leptin directly activates SF1 neurons in the VMH, and this action by leptin is required for normal body-weight homeostasis. *Neuron* 49, 191–203.

Downing C., Balderrama-Durbin C., Broncucia H., Gilliam D. and Johnson T. E. (2009). Ethanol teratogenesis in five inbred strains of mice. *Alcohol. Clin. Exp. Res.* 33, 1238-1245.

Echelard, Y., Epstein, D. J., St-Jacques, B., Shen, L., Mohler, J., McMahon, J. A. and McMahon, A. P. (1993). Sonic hedgehog, a member of a family of putative signaling molecules, is implicated in the regulation of CNS polarity. *Cell* 75, 1417–1430.

Ericson, J., Morton, S., Kawakami, A., Roelink, H. and Jessell, T. M. (1996). Two critical periods of Sonic Hedgehog signaling required for the specification of motor neuron identity. *Cell* 87, 661–673.

Ericson, J., Rashbass, P., Schedl, A., Brenner-Morton, S., Kawakami, A., van Heyningen, V., Jessell, T. M. and Briscoe, J. (1997). Pax6 controls progenitor cell identity and neuronal fate in response to graded Shh signaling. *Cell* 90, 169–180.

Feng L., Xie Z. H., Ding Q., Xie X., Libby R. T. and Gan L. (2010). MATH5 controls the acquisition of multiple retinal cell fates. *Mol. Brain* 3, 36.

Fu, T., Towers, M. and Placzek, M. A. (2017). Fgf10+ progenitors give rise to the chick hypothalamus by rostral and caudal growth and differentiation. *Development* 144, 3278–3288.

Fuccillo, M., Joyner, A. L. and Fishell, G. (2006). Morphogen to mitogen: the multiple roles of hedgehog signalling in vertebrate neural development. *Nat. Rev. Neurosci.* 7, 772–783.

Garcia-Filion P. and Borchert M. (2013). Prenatal determinants of optic nerve hypoplasia: review of suggested correlates and future focus. *Surv. Ophthalmol.* 58, 610-619.

Gaston-Massuet C., McCabe M. J., Scagliotti V., Young R. M., Carreno G., Gregory L. C., Jayakody S. A., Pozzi S., Gualtieri A., Basu B. et al. (2016). Transcription factor 7-like 1 is involved in hypothalamo–pituitary axis development in mice and humans. *Proc. Natl. Acad. Sci. USA* 113, E548-E557

Gilbert M. T., Sulik K. K., Fish E. W., Baker L. K., Dehart D. B. and Parnell S. E. (2016). Dose-dependent teratogenicity of the synthetic cannabinoid CP-55,940 in mice. *Neurotoxicol. Teratol.* 58:15-2.

Godin E. A., O'Leary-Moore S. K., Khan A. A., Parnell S. E., Ament J. J., Dehart D. B., Johnson B. W., Allan Johnson G., Styner M. A. and Sulik K. K. (2010). Magnetic

- resonance microscopy defines ethanol-induced brain abnormalities in prenatal mice: effects of acute insult on gestational day 7. *Alcohol. Clin. Exp. Res.* 34, 98-111.
- Goodrich, L.V., Milenković, L., Higgins, K.M., and Scott, M.P.** (1997). Altered neural cell fates and medulloblastoma in mouse patched mutants. *Science* 277, 1109–1113.
- Gouti, M., Metzis, V. and Briscoe, J.** (2015). The route to spinal cord cell types: a tale of signals and switches. *Trends Genet.* 31, 282–289.
- Gregory L. C., Gaston-Massuet C., Andoniadou C. L., Carreno G., Webb E. A., Kelberman D., McCabe M. J., Panagiotakopoulos L., Saldanha J. W., Spoudeas H. A. et al.** (2015). The role of the sonic hedgehog signalling pathway in patients with midline defects and congenital hypopituitarism. *Clin. Endocrinol. (Oxf.)* 82, 728-738.
- Haddad N. G. and Eugster E. A.** (2005). Hypopituitarism and neurodevelopmental abnormalities in relation to central nervous system structural defects in children with optic nerve hypoplasia. *J. Pediatr. Endocrinol. Metab.* 18, 853-858.
- Hashikawa, Y., Hashikawa, K., Falkner, A. L. and Lin, D.** (2017). Ventromedial Hypothalamus and the Generation of Aggression. *Front Syst Neurosci* 11.
- Hellström A.** (1999). Optic nerve morphology may reveal adverse events during prenatal and perinatal life—digital image analysis. *Surv. Ophthalmol.* 44 Suppl. 1, S63-S73.
- Higashiyama D., Saitsu H., Komada M., Takigawa T., Ishibashi M. and Shiota K.** (2007). Sequential developmental changes in holoprosencephalic mouse embryos exposed to ethanol during the gastrulation period. *Birth Defects Res. A Clin. Mol. Teratol.* 79, 513-523.
- Hildebrand, M. S., Griffin, N. G., Damiano, J. A., Cops, E. J., Burgess, R., Ozturk, E., Jones, N. C., Leventer, R. J., Freeman, J. L., Harvey, A. S., et al.** (2016). Mutations of the Sonic Hedgehog Pathway Underlie Hypothalamic Hamartoma with Gelastic Epilepsy. *Am. J. Hum. Genet.* 99, 423–429.
- Hong M. and Krauss R. S.** (2012). Cdon mutation and fetal ethanol exposure synergize to produce midline signaling defects and holoprosencephaly spectrum disorders in mice. *PLoS Genet.* 8, e1002999
- Hong M. and Krauss R. S.** (2013). Rescue of holoprosencephaly in fetal alcohol-exposed Cdon mutant mice by reduced gene dosage of Ptch1. *PLoS ONE* 8, e79269
- Hui, C.C., Slusarski, D., Platt, K.A., Holmgren, R., and Joyner, A.L.** (1994). Expression of three mouse homologs of the Drosophila segment polarity gene cubitus interruptus, Gli, Gli-2, and Gli-3, in ectoderm- and mesoderm-derived tissues suggests multiple roles during postimplantation development. *Dev. Biol.* 162, 402–413.
- Ingham, P. W. and McMahon, A. P.** (2001). Hedgehog signaling in animal development: paradigms and principles. *Genes Dev.* 15, 3059–3087.

Ishii, Y. and Bouret, S. G. (2012). Embryonic birthdate of hypothalamic leptin-activated neurons in mice. *Endocrinology* **153**, 3657–3667.

Ikeda, Y., Luo, X., Abbud, R., Nilson, J. H. and Parker, K. L. (1995). The nuclear receptor steroidogenic factor 1 is essential for the formation of the ventromedial hypothalamic nucleus. *Mol. Endocrinol.* **9**, 478–486.

Jessell, T. M. (2000). Neuronal specification in the spinal cord: inductive signals and transcriptional codes. *Nature Reviews Genetics* **1**, 20–29.

Kang, S., Graham, J.M. Jr, Olney, A.H. and Biesecker, L.G. (1997). GLI3 frameshift mutations cause autosomal dominant Pallister-Hall syndrome. *Nat Genet.* **15**, 266-8.

Khaliullina H., Bilgin M., Sampaio J. L., Shevchenko A. and Eaton S. (2015). Endocannabinoids are conserved inhibitors of the Hedgehog pathway. *Proc. Natl. Acad. Sci. USA* **112**, 3415-3420.

Kietzman H. W., Everson J. L., Sulik K. K. and Lipinski R. J. (2014). The teratogenic effects of prenatal ethanol exposure are exacerbated by Sonic Hedgehog or GLI2 haploinsufficiency in the mouse. *PLoS ONE* **9**, e89448

Kim, K. W., Li, S., Zhao, H., Peng, B., Tobet, S. A., Elmquist, J. K., Parker, K. L. and Zhao, L. (2010). CNS-specific ablation of steroidogenic factor 1 results in impaired female reproductive function. *Mol. Endocrinol.* **24**, 1240–1250.

Kimura, S., Hara, Y., Pineau, T., Fernandez-Salguero, P., Fox, C. H., Ward, J. M. and Gonzalez, F. J. (1996). The T/ebp null mouse: thyroid-specific enhancer-binding protein is essential for the organogenesis of the thyroid, lung, ventral forebrain, and pituitary. *Genes Dev.* **10**, 60–69.

Kinzler, K.W., Ruppert, J.M., Bigner, S.H., and Vogelstein, B. (1988). The GLI gene is a member of the Kruppel family of zinc finger proteins. *Nature* **332**, 371–374.

Kleiber M. L., Diehl E. J., Laufer B. I., Mantha K., Chokroborty-Hoque A., Alberry B. and Singh S. M. (2014). Long-term genomic and epigenomic dysregulation as a consequence of prenatal alcohol exposure: a model for fetal alcohol spectrum disorders. *Front. Genet.* **5**, 161.

Klößener, T., Hess, S., Belgardt, B. F., Paeger, L., Verhagen, L. A. W., Husch, A., Sohn, J.-W., Hampel, B., Dhillon, H., Zigman, J. M., et al. (2011). High-fat feeding promotes obesity via insulin receptor/PI3K-dependent inhibition of SF-1 VMH neurons. *Nat. Neurosci.* **14**, 911–918.

Kolpak A., Zhang J. and Bao Z.-Z. (2005). Sonic hedgehog has a dual effect on the growth of retinal ganglion axons depending on its concentration. *J. Neurosci.* **25**, 3432-3441.

Komada, M., Saitsu, H., Kinboshi, M., Miura, T., Shiota, K. and Ishibashi, M. (2008).

Hedgehog signaling is involved in development of the neocortex. *Development* 135, 2717–2727.

Kong, J. H., Yang, L., Dessaud, E., Chuang, K., Moore, D. M., Rohatgi, R., Briscoe, J. and Novitsch, B. G. (2015). Notch activity modulates the responsiveness of neural progenitors to sonic hedgehog signaling. *Dev. Cell* 33, 373–387.

Kunwar, P. S., Zelikowsky, M., Remedios, R., Cai, H., Yilmaz, M., Meister, M. and Anderson, D. J. (2015). Ventromedial hypothalamic neurons control a defensive emotion state. *Elife* 4,.

Kurrasch, D., Cheung, C., Lee, F., Tran, P., Hata, K. and Ingraham, H. (2007). The Neonatal Ventromedial Hypothalamus Transcriptome Reveals Novel Markers with Spatially Distinct Patterning. *Journal of Neuroscience* 27, 13624–13634.

Lee, H., Kim, D.-W., Remedios, R., Anthony, T. E., Chang, A., Madisen, L., Zeng, H. and Anderson, D. J. (2014). Scalable control of mounting and attack by *Esr1+* neurons in the ventromedial hypothalamus. *Nature* 509, 627–632.

Lee, B., Lee, S., Lee, S.-K. and Lee, J. W. (2016). The LIM-homeobox transcription factor *Isl1* plays crucial roles in the development of multiple arcuate nucleus neurons. *Development* 143, 3763–3773.

Lei, Q., Jeong, Y., Misra, K., Li, S., Zelman, A.K., Epstein, D.J. and Matise, M.P. (2006). Wnt signaling inhibitors regulate the transcriptional response to morphogenetic Shh–Gli signaling in the neural tube. *Dev. Cell* 11, 325–337.

Li, H., Zeitler, P. S., Valerius, M. T., Small, K. and Potter, S. S. (1996). *Gsh-1*, an orphan Hox gene, is required for normal pituitary development. *EMBO J.* 15, 714–724.

Li Y.-X., Yang H.-T., Zdanowicz M., Sicklick J. K., Qi Y., Camp T. J. and Diehl A. M. (2007). Fetal alcohol exposure impairs Hedgehog cholesterol modification and signaling. *Lab. Invest.* 87, 231-240.

Lipinski R. J., Godin E. A., O'leary-Moore S. K., Parnell S. E. and Sulik K. K. (2010). Genesis of teratogen-induced holoprosencephaly in mice. *Am. J. Med. Genet. C Semin. Med. Genet.* 154C, 29-42.

Lipinski R. J., Hammond P., O'Leary-Moore S. K., Ament J. J., Pecevich S. J., Jiang Y., Budin F., Parnell S. E., Suttie M., Godin E. A. et al. (2012). Ethanol-induced face-brain dysmorphology patterns are correlative and exposure-stage dependent. *PLoS ONE* 7, e43067.

Lin, D., Boyle, M. P., Dollar, P., Lee, H., Lein, E. S., Perona, P. and Anderson, D. J. (2011). Functional identification of an aggression locus in the mouse hypothalamus. *Nature* 470, 221–226.

Loucks E. J. and Ahlgren S. C. (2009). Deciphering the role of Shh signaling in axial defects produced by ethanol exposure. *Birth Defects Res. A Clin. Mol. Teratol.* 85, 556-567.

Lu, F., Kar, D., Gruenig, N., Zhang, Z. W., Cousins, N., Rodgers, H. M., Swindell, E. C., Jamrich, M., Schuurmans, C., Mathers, P. H., et al. (2013). Rax is a selector gene for mediobasal hypothalamic cell types. *J. Neurosci.* 33, 259–272.

Majdic, G., Young, M., Gomez-Sanchez, E., Anderson, P., Szczepaniak, L. S., Dobbins, R. L., McGarry, J. D. and Parker, K. L. (2002). Knockout Mice Lacking Steroidogenic Factor 1 Are a Novel Genetic Model of Hypothalamic Obesity. *Endocrinology* 143, 607–614.

Manning, L., Ohyama, K., Saeger, B., Hatano, O., Wilson, S. A., Logan, M. and Placzek, M. (2006). Regional Morphogenesis in the Hypothalamus: A BMP-Tbx2 Pathway Coordinates Fate and Proliferation through Shh Downregulation. *Developmental Cell* 11, 873–885.

Marigo V., Johnson R. L., Vortkamp A. and Tabin C. J. (1996). Sonic hedgehog differentially regulates expression of GLI and GLI3 during limb development. *Dev. Biol.* 180, 273-283.

Martí, E., Bumcrot, D. A., Takada, R. and McMahon, A. P. (1995). Requirement of 19K form of Sonic hedgehog for induction of distinct ventral cell types in CNS explants. *Nature* 375, 322–325.

Matise, M. P., Epstein, D. J., Park, H. L., Platt, K. A. and Joyner, A. L. (1998). Gli2 is required for induction of floor plate and adjacent cells, but not most ventral neurons in the mouse central nervous system. *Development* 125, 2759–2770.

McCabe M. J., Alatzoglou K. S. and Dattani M. T. (2011). Septo-optic dysplasia and other midline defects: the role of transcription factors: HESX1 and beyond. *Best Pract. Res. Clin. Endocrinol. Metab.* 25, 115-124.

McCarthy, R. A., Barth, J. L., Chintalapudi, M. R., Knaak, C. and Argraves, W. S. (2002). Megalin functions as an endocytic sonic hedgehog receptor. *J. Biol. Chem.* 277, 25660–25667.

McClellan, K., Parker, K. and Tobet, S. (2006). Development of the ventromedial nucleus of the hypothalamus. *Frontiers in Neuroendocrinology* 27, 193–209.

McLellan J. S., Zheng X., Hauk G., Ghirlando R., Beachy P. A. and Leahy D. J. (2008). The mode of Hedgehog binding to Ihog homologues is not conserved across different phyla. *Nature* 455, 979-983.

McNay, D. E. G., Pelling, M., Claxton, S., Guillemot, F. and Ang, S.-L. (2006). Mash1 is required for generic and subtype differentiation of hypothalamic neuroendocrine cells. *Mol. Endocrinol.* 20, 1623–1632.

- Morales-Delgado, N., Merchan, P., Bardet, S. M., Ferrán, J. L., Puelles, L. and Díaz, C.** (2011). Topography of Somatostatin Gene Expression Relative to Molecular Progenitor Domains during Ontogeny of the Mouse Hypothalamus. *Front Neuroanat* 5.
- Morishima A. and Aranoff G. S.** (1986). Syndrome of septo-optic-pituitary dysplasia: the clinical spectrum. *Brain Dev.* 8, 233-239.
- Muhr, J., Andersson, E., Persson, M., Jessell, T. M. and Ericson, J.** (2001). Groucho-mediated transcriptional repression establishes progenitor cell pattern and neuronal fate in the ventral neural tube. *Cell* 104, 861–873.
- Mu X., Fu X., Beremand P. D., Thomas T. L. and Klein W. H.** (2008). Gene regulation logic in retinal ganglion cell development: *Isl1* defines a critical branch distinct from but overlapping with *Pou4f2*. *Proc. Natl. Acad. Sci USA* 105, 6942-7.
- Murray P. G., Paterson W. F. and Donaldson M. D. C.** (2005). Maternal age in patients with septo-optic dysplasia. *J. Pediatr. Endocrinol. Metab.* 18, 471-476.
- Nissim, S., Allard, P., Bandyopadhyay, A., Harfe, B. D. and Tabin, C. J.** (2007). Characterization of a novel ectodermal signaling center regulating *Tbx2* and *Shh* in the vertebrate limb. *Dev. Biol.* 304, 9–21.
- Nüsslein-Volhard, C. and Wieschaus, E.** (1980). Mutations affecting segment number and polarity in *Drosophila*. *Nature* **287**, 795–801.
- Ohyama, K., Das, R. and Placzek, M.** (2008). Temporal progression of hypothalamic patterning by a dual action of BMP. *Development* 135, 3325–3331.
- Pan L., Deng M., Xie X. and Gan L.** (2008). *ISL1* and *BRN3B* co-regulate the differentiation of murine retinal ganglion cells. *Development* 135, 1981-1990.
- Patel L., McNally R. J. Q., Harrison E., Lloyd I. C. and Clayton P. E.** (2006). Geographical distribution of optic nerve hypoplasia and septo-optic dysplasia in Northwest England. *J. Pediatr.* 148, 85-88.
- Paulo S. S., Fernandes-Rosa F. L., Turatti W., Coeli-Lacchini F. B., Martinelli C. E. Jr., Nakiri G. S., Moreira A. C., Santos A. C., de Castro M. and Antonini S. R.** (2015). Sonic Hedgehog mutations are not a common cause of congenital hypopituitarism in the absence of complex midline cerebral defects. *Clin. Endocrinol. (Oxf)*. 82, 562-569.
- Pelling, M., Anthwal, N., McNay, D., Gradwohl, G., Leiter, A. B., Guillemot, F. and Ang, S.-L.** (2011). Differential requirements for neurogenin 3 in the development of POMC and NPY neurons in the hypothalamus. *Dev. Biol.* 349, 406–416.

Potok, M. A., Cha, K. B., Hunt, A., Brinkmeier, M. L., Leitges, M., Kispert, A. and Camper, S. A. (2008). WNT signaling affects gene expression in the ventral diencephalon and pituitary gland growth. *Dev. Dyn.* 237, 1006–1020.

Prasov L. and Glaser T. (2012). Dynamic expression of ganglion cell markers in retinal progenitors during the terminal cell cycle. *Mol. Cell. Neurosci.* 50, 160-168.

Ribeiro I. M., Vale P. J., Tenedorio P. A., Rodrigues P. A., Bilhoto M. A. and Pereira H. C. (2007). Ocular manifestations in fetal alcohol syndrome. *Eur. J. Ophthalmol.* 17, 104-109.

Rizzoti, K. and Lovell-Badge, R. (2017). Pivotal role of median eminence tanycytes for hypothalamic function and neurogenesis. *Molecular and Cellular Endocrinology* 445, 7–13.

Robins, S. C., Stewart, I., McNay, D. E., Taylor, V., Giachino, C., Goetz, M., Ninkovic, J., Briancon, N., Maratos-Flier, E., Flier, J. S., et al. (2013). α -Tanycytes of the adult hypothalamic third ventricle include distinct populations of FGF-responsive neural progenitors. *Nat Commun* 4, 2049.

Rodríguez, E. M., Blázquez, J. L., Pastor, F. E., Peláez, B., Peña, P., Peruzzo, B. and Amat, P. (2005). Hypothalamic tanycytes: a key component of brain-endocrine interaction. *Int. Rev. Cytol.* 247, 89–164.

Roelink, H., Augsburger, A., Heemskerk, J., Korzh, V., Norlin, S., Ruiz i Altaba, A., Tanabe, Y., Placzek, M., Edlund, T. and Jessell, T. M. (1994). Floor plate and motor neuron induction by vhh-1, a vertebrate homolog of hedgehog expressed by the notochord. *Cell* 76, 761–775.

Roelink, H., Porter, J. A., Chiang, C., Tanabe, Y., Chang, D. T., Beachy, P. A. and Jessell, T. M. (1995). Floor plate and motor neuron induction by different concentrations of the amino-terminal cleavage product of sonic hedgehog autoproteolysis. *Cell* 81, 445–455.

Roessler E., Belloni E., Gaudenz K., Jay P., Berta P., Scherer S. W., Tsui L.-C. and Muenke M. (1996). Mutations in the human Sonic Hedgehog gene cause holoprosencephaly. *Nat. Genet.* 14, 357-360.

Rossi A., Kontarakis Z., Gerri C., Nolte H., Hölper S., Krüger M. and Stainier D. Y. R. (2015). Genetic compensation induced by deleterious mutations but not gene knockdowns. *Nature* 524, 230-233.

Rowitch, D. H., S-Jacques, B., Lee, S. M., Flax, J. D., Snyder, E. Y. and McMahon, A. P. (1999). Sonic hedgehog regulates proliferation and inhibits differentiation of CNS precursor cells. *J. Neurosci.* 19, 8954–8965.

Saitsu, H., Sonoda, M., Higashijima, T., Shirozu, H., Masuda, H., Tohyama, J., Kato, M., Nakashima, M., Tsurusaki, Y., Mizuguchi, T., et al. (2016). Somatic mutations in *GLI3* and *OFD1* involved in sonic hedgehog signaling cause hypothalamic hamartoma. *Ann Clin Transl Neurol* 3, 356–365.

Sakagami K., Gan L. and Yang X.-J. (2009). Distinct effects of Hedgehog signaling on neuronal fate specification and cell cycle progression in the embryonic mouse retina. *J. Neurosci.* 29, 6932-6944.

Sanchez-Camacho C. and Bovolenta P. (2008). Autonomous and non-autonomous Shh signalling mediate the in vivo growth and guidance of mouse retinal ganglion cell axons. *Development* 135, 3531-3541

Saper, C. B. and Lowell, B. B. (2014). The hypothalamus. *Curr. Biol.* 24, R1111-1116.
Segal, J. P., Stallings, N. R., Lee, C. E., Zhao, L., Socci, N., Viale, A., Harris, T. M., Soares, M. B., Childs, G., Elmquist, J. K., et al. (2005). Use of Laser-Capture Microdissection for the Identification of Marker Genes for the Ventromedial Hypothalamic Nucleus. *J. Neurosci.* 25, 4181–4188.

Shimada, M. and Nakamura, T. (1973). Time of neuron origin in mouse hypothalamic nuclei. *Exp. Neurol.* 41, 163–173.

Shimogori, T., Lee, D. A., Miranda-Angulo, A., Yang, Y., Wang, H., Jiang, L., Yoshida, A. C., Kataoka, A., Mashiko, H., Avetisyan, M., et al. (2010). A genomic atlas of mouse hypothalamic development. *Nat. Neurosci.* 13, 767–775.
Silva, B. A., Mattucci, C., Krzywkowski, P., Murana, E., Illarionova, A., Grinevich, V., Canteras, N. S., Ragozzino, D. and Gross, C. T. (2013). Independent hypothalamic circuits for social and predator fear. *Nat. Neurosci.* 16, 1731–1733.

Spoelgen, R., Hammes, A., Anzenberger, U., Zechner, D., Andersen, O. M., Jerchow, B. and Willnow, T. E. (2005). LRP2/megalin is required for patterning of the ventral telencephalon. *Development* 132, 405–414.

Stacher Hörndli C. and Chien C.-B. (2012). Sonic hedgehog is indirectly required for intraretinal axon pathfinding by regulating chemokine expression in the optic stalk. *Development* 139, 2604-2613.

Strömland K. (1987). Ocular involvement in the fetal alcohol syndrome. *Surv. Ophthalmol.* 31, 277-284.

Sulik K. K., Johnston M. C. and Webb M. A. (1981). Fetal alcohol syndrome: embryogenesis in a mouse model. *Science* 214, 936-938.

Sussel, L., Marin, O., Kimura, S. and Rubenstein, J. L. (1999). Loss of *Nkx2.1* homeobox gene function results in a ventral to dorsal molecular respecification within the basal telencephalon: evidence for a transformation of the pallidum into the striatum. *Development* 126, 3359–3370.

Szabó, N.-E., Zhao, T., Çankaya, M., Theil, T., Zhou, X. and Alvarez-Bolado, G. (2009). Role of neuroepithelial Sonic hedgehog in hypothalamic patterning. *J. Neurosci.* 29, 6989.

Tan, C. L. and Knight, Z. A. (2018). Regulation of Body Temperature by the Nervous System. *Neuron* 98, 31–48.

Tenzen T., Allen B. L., Cole F., Kang J.-S., Krauss R. S. and McMahon A. P. (2006). The cell surface membrane proteins Cdo and Boc are components and targets of the Hedgehog signaling pathway and feedback network in mice. *Dev. Cell* 10, 647-656.

Tran, P. V., Lee, M. B., Marín, O., Xu, B., Jones, K. R., Reichardt, L. F., Rubenstein, J. R. and Ingraham, H. A. (2003). Requirement of the orphan nuclear receptor SF-1 in terminal differentiation of ventromedial hypothalamic neurons. *Molecular and Cellular Neuroscience* 22, 441–453.

Treier M., O'Connell S., Gleiberman A., Price J., Szeto D. P., Burgess R., Chuang P. T., McMahon A. P. and Rosenfeld M. G. (2001). Hedgehog signaling is required for pituitary gland development. *Development* 128, 377-386.

Trowe, M.-O., Zhao, L., Weiss, A.-C., Christoffels, V., Epstein, D. J. and Kispert, A. (2013). Inhibition of Sox2-dependent activation of Shh in the ventral diencephalon by Tbx3 is required for formation of the neurohypophysis. *Development* 140, 2299–2309.

Van den Heuvel, M., and Ingham, P.W. (1996). *smoothed* encodes a receptor-like serpentine protein required for hedgehog signalling. *Nature* 382, 547–551.

Veazey K. J., Parnell S. E., Miranda R. C. and Golding M. C. (2015). Dose-dependent alcohol-induced alterations in chromatin structure persist beyond the window of exposure and correlate with fetal alcohol syndrome birth defects. *Epigenetics Chromatin* 8, 39.

Vokes, S.A., Ji, H., McCuine, S., Tenzen, T., Giles, S., Zhong, S., Longabaugh, W.J., Davidson, E.H., Wong, W.H., McMahon, A.P. (2007). Genomic characterization of Gli-activator targets in sonic hedgehog-mediated neural patterning. *Development* 134, 1977–1989.

Wallace, V. A. (1999). Purkinje-cell-derived Sonic hedgehog regulates granule neuron precursor cell proliferation in the developing mouse cerebellum. *Curr. Biol.* 9, 445–448.

Wallace, R. H., Freeman, J. L., Shouri, M. R., Izzillo, P. A., Rosenfeld, J. V., Mulley, J. C., Harvey, A. S. and Berkovic, S. F. (2008). Somatic mutations in GLI3 can cause hypothalamic hamartoma and gelastic seizures. *Neurology* 70, 653–655.

Wang S. W., Kim B. S., Ding K., Wang H., Sun D., Johnson R. L., Klein W. H. and Gan L. (2001). Requirement for *math5* in the development of retinal ganglion cells. *Genes Dev.* 15, 24-29.

Wang Y., Dakubo G. D., Thurig S., Mazerolle C. J. and Wallace V. A. (2005). Retinal ganglion cell-derived sonic hedgehog locally controls proliferation and the timing of RGC development in the embryonic mouse retina. *Development* 132, 5103-5113.

Wang Y., Martin J. F. and Bai C. B. (2010). Direct and indirect requirements of Shh/Gli signaling in early pituitary development. *Dev. Biol.* 348, 199-209.

Webb E. A. and Dattani M. T. (2010). Septo-optic dysplasia. *Eur. J. Hum. Genet.* 18, 393-397.

Wechsler-Reya, R. J. and Scott, M. P. (1999). Control of neuronal precursor proliferation in the cerebellum by Sonic Hedgehog. *Neuron* 22, 103–114.

Wray, S., Grant, P. and Gainer, H. (1989). Evidence that cells expressing luteinizing hormone-releasing hormone mRNA in the mouse are derived from progenitor cells in the olfactory placode. *Proc. Natl. Acad. Sci. U.S.A.* 86, 8132–8136.

Wray, S. (2002). Development of gonadotropin-releasing hormone-1 neurons. *Front Neuroendocrinol* 23, 292–316.

Wu F., Kaczynski T. J., Sethuramanujam S., Li R., Jain V., Slaughter M. and Mu X. (2015). Two transcription factors, Pou4f2 and Isl1, are sufficient to specify the retinal ganglion cell fate. *Proc. Natl. Acad. Sci. USA* 112, E1559-E1568.

Xie, Y. and Dorsky, R. I. (2017). Development of the hypothalamus: conservation, modification and innovation. *Development* 144, 1588–1599.

Xu, Q., Guo, L., Moore, H., Waclaw, R. R., Campbell, K. and Anderson, S. A. (2010). Sonic Hedgehog Signaling Confers Ventral Telencephalic Progenitors with Distinct Cortical Interneuron Fates. *Neuron* 65, 328–340.

Yee, C. L., Wang, Y., Anderson, S., Ekker, M. and Rubenstein, J. L. R. (2009). Arcuate nucleus expression of NKX2.1 and DLX and lineages expressing these transcription factors in neuropeptide Y(+), proopiomelanocortin(+), and tyrosine hydroxylase(+) neurons in neonatal and adult mice. *J. Comp. Neurol.* 517, 37–50.

Yin, W. and Gore, A. C. (2010). The Hypothalamic Median Eminence and its Role in Reproductive Aging. *Ann N Y Acad Sci* 1204, 113–122.

Yu, K., McGlynn, S. and Matise, M. P. (2013). Floor plate-derived sonic hedgehog regulates glial and ependymal cell fates in the developing spinal cord. *Development* 140, 1594–1604

Zha, X. and Xu, X. (2015). Dissecting the hypothalamic pathways that underlie innate behaviors. *Neurosci. Bull.* 31, 629–648.

Zhang, F., and Jetten, A.M. (2001). Genomic structure of the gene encoding GLI-related, Krüppel-like zinc finger protein GLIS2. *Gene* 280, 49–57

Zhang X. M. and Yang X. J. (2001). Regulation of retinal ganglion cell production by Sonic hedgehog. *Development* 128, 943-957.

Zhang W., Kang J.-S., Cole F., Yi M.-J. and Krauss R. S. (2006). Cdo functions at multiple points in the Sonic Hedgehog pathway, and Cdo-deficient mice accurately model human holoprosencephaly. *Dev. Cell* 10, 657-665.

Zhang W., Mulieri P. J., Gaio U., Bae G.-U., Krauss R. S. and Kang J.-S. (2009). Ocular abnormalities in mice lacking the immunoglobulin superfamily member Cdo. *FEBS J.* 276, 5998-6010.

Zhang C., Turton Q. M., Mackinnon S., Sulik K. K. and Cole G. J. (2011). Agrin function associated with ocular development is a target of ethanol exposure in embryonic zebrafish. *Birth Defects Res. A Clin. Mol. Teratol.* 91, 129-141.

Zhao, L., Kim, K. W., Ikeda, Y., Anderson, K. K., Beck, L., Chase, S., Tobet, S. A. and Parker, K. L. (2008). Central nervous system-specific knockout of steroidogenic factor 1 results in increased anxiety-like behavior. *Mol. Endocrinol.* 22, 1403–1415.

Zhao, L., Zevallos, S. E., Rizzoti, K., Jeong, Y., Lovell-Badge, R. and Epstein, D. J. (2012). Disruption of SoxB1-dependent Sonic hedgehog expression in the hypothalamus causes Septo-optic Dysplasia. *Developmental Cell* 22, 585–596.

Zhu, X., Gleiberman, A. S. and Rosenfeld, M. G. (2007). Molecular Physiology of Pituitary Development: Signaling and Transcriptional Networks. *Physiological Reviews* 87, 933–963.